Title	Study on advanced storm model for fatigue assessment of ship structural member
Author(s)	Prasetyo, Fredhi Agung
Citation	大阪大学, 2013, 博士論文
Version Type	VoR
URL	https://doi.org/10.18910/26178
rights	
Note	

Doctoral Dissertation

Study on advanced storm model for fatigue assessment of ship structural member

（船体構造部材の疲労強度評価のための

”嵐”荷重モデルの高度化に関する研究）

Fredhi Agung Prasetyo

July 2013

Graduate School of Engineering

Osaka University

ACKNOWLEDGEMENT

Osaka, July 2013

Fredhi Agung Prasetyo

ABSTRACT

For fatigue assessment of ships and offshore structures, load sequence should be generated so that it can emulate the changing nature of sea state in real oceans. Storm model developed by Tomita et al. (1995) (the 1st generation, 1G model) and its refinement proposed by Kawabe (2002) and Osawa et al. (2006) (the 2nd generation, 2G model) can emulate ocean wave sequences, but these models have many drawbacks: storm profiles cannot be determined automatically; 1G model cannot be coupled with seakeeping analysis; they cannot simulate the variation of storm duration; storm profile configurations were determined only for North Pacific Ocean's GWS data with 2 hours observation period. In order to overcome these drawbacks, a new generation (the 3rd generation, 3G) storm model is developed so that: 1) storm profile is fully-automatically configured; 2) it can simulate the variation of storm duration; 3) it generates the equivalent sea state history from data with different observation period. The effectiveness of the proposed model is demonstrated by comparing the changing nature and the statistical characteristics of simulated sea state histories with those of the source oceanographic data**.** The 3G and 2G storm models, developed in this thesis, posses following capabilities: (i) Storm profiles can be determined fully automatically, and it is easy to prepare storm profile database for numerous seas areas and seasons. (ii) It can be coupled with seakeeping theory. (iii) Long-term joint probability density of H_W and T_W of the source data can be reproduced. (iv) Stochastic characteristic of storm duration can be emulated (the mean value only for 2G, both the mean and the variance for 3G). (v) The relation between, $H_{W,max|storm}$ and the storm's occurrence probability (frequent

distribution of storm class) recorded in the source data can be emulated and (vi) long-term probability of wave-induced stress, which is experienced by a ship on the given route, can be emulated.

LIST OF SYMBOLS

h_W = individual wave height

H_W = significant wave height

T_W = mean wave period

H_{w_mean} = the overall mean of H_W

$p(H_W, T_W)$ = joint probability density of H_W and T_W

$p(H_W)$ = marginal probability density of H_W

$p(T_W|H_W)$ = conditional probability density for T_W given H_W

$F(H_W)$ = cumulative probability density of H_W

$P_{ex}(H_W)$ = long-term exceedance probability of H_W

I_{OB} = observation interval of sea state data

I_{SM} = short sea duration (the period in which H_w remains unchanged)

λ = scale parameter of Weibull distribution

k = shape parameter of Weibull distribution

d = duration of a storm (rough sea state)

$H_{W,max(j)}$ = local maximum of H_W in the j-th ETS

$t_{B,j}$ = time at which H_W's local minimum of appears just before the j-th ETS occurs

$t_{E,j}$ = time at which H_W's local minimum of appears just after the j-th ETS occurs

$d_{(j)}$ = duration of j-th ETS ($d_{(j)} = t_{E,j} - t_{B,j}$)

μ = mean value of the numbers of data

σ^2 = variance of the numbers of data

$H_{W,max}|_{storm}$ = maximum H_W in each storm waveform

L_D = ship's design life

N_{total} = total number of short seas in entire ship's life

N_{SS} = number of short seas in each calm or storm sea

$H_{W,ext}$ = H_W of the once-in-a-lifetime extreme short-sea

$N(H_W)$ = number of short seas with H_W in ship's life

j_{end} = maximum number of H_W levels in a storm

$N_{j,i}$ = number of short-seas of i-th class storm with $H_W = H_{W,max} - j + 1 = H_{W,ext} - i - j + 2$

$p'(H_W)$ = relative frequency distribution of H_W

$R_{tail}(H_W)$ = ratio of $p'(H_W)$ to $P_{ex}(H_W)$ ($R_{tail}(H_W) = \dfrac{p'(H_W)}{P_{ex}(H_W)}$)

$p_{calm}(H_W)$ = frequent distribution of H_W in a calm sea

$n^{(i)}$ = number of occurrence of the i-th class storm in the ship's life

i_{end} = index i of the lowest $H_{W,max|storm}$ ($i_{end} = \mathrm{Int}(H_{W,ext} - 2H_{W,mean})$)

$n^{(storm)}$ = total number of storms in a lifetime ($n^{(storm)} = \displaystyle\sum_{i=1}^{i_{end}} n^{(i)}$)

$n^{(calm)}$ = number of calm seas in a lifetime ($n^{(calm)} = \dfrac{N_{total}}{N_{SS}} - n^{(storm)}$)

d_{var} = variable storm duration

$N_{j,i}{}^{3G}$ = $N_{j,i}$ of the storm with d_{var}

P_{storm} = occurrence probability of a storm seas ($P_{storm} = \dfrac{n^{(storm)}}{n^{(storm)} + n^{(calm)}}$)

P_{calm} = occurrence probability of a calm seas ($P_{calm} = \dfrac{n^{(calm)}}{n^{(storm)} + n^{(calm)}}$)

ω = wave's angular frequency

$S(\omega)$ = specified wave spectrum

$P_{ex}(S_a)$ = long-term exceedance probability of stress range

$\bar{h}_W$ = normalized individual wave height

a = crack's depth

c = crack's length

t = plate's thickness

C and m = material parameters of crack growth rate

S = applied stress load

S_{max} = maximum applied stress load

S_{min} = minimum applied stress load

SIF = Stress intensity factor

K_{max} = maximum SIF at maximum applied stress load

K_{op} = SIF at stress of crack opening level

K_s = stress concentration factor of structural detail

ΔK_{eff} = the effective stress intensity factor range

$\left(\Delta K_{eff}\right)_{th}$ = the threshold of ΔK_{eff}

M_k = SIF's correction factor for weld bead

F_b and F_m = SIF's correction factor for finite plate size

S_a = stress range (S_{max} - S_{min})

$C4$ = the threshold constant of the effective SIF

C5 = cyclic fracture toughness or limiting value of maximum SIF

$K(S_x)$ = SIF at applied load S_x;

S_0' = crack opening stress.

$\bar{s}_a$ = normalized S_a

Abbreviations

CFD = cumulative fatigue damage

FCP = fatigue crack propagation

GWS = Global Wave Statistics

JWA = Japan Weather Association

ETS = Equivalent Triangular Storm

RAO = response amplitude operator

IMO = International Maritime organization

CS = Classification society

WMO = World Maritime Organization

LIST OF FIGURES

LIST OF TABLES

CONTENTS

1   INTRODUCTION

1.1   Background to research

The ship's size has been rapidly increased in recent years. Consequently, many aspects of ship structural safety assessment have been concerned in design stage. In order to enhance the structural safety of ships and reduce the risk of environment pollution, the International Maritime Organization (IMO) has required in Goal Based Standard (GBS) to consider the fatigue strength as one of the functional requirements (IMO resolution 287(87), 2010[15]). Improper fatigue assessment may cause fatigue crack initiation in early of design life resulting in serious troubles, such as oil leakage and brittle fracture. Generally, fatigue assessment in maritime industry is conducted by using a simplified method, in which Palmgreen-Miner formula of cumulative fatigue damage (CFD) and S-N curves are used. In this method, the assessment procedure and calculation conditions are determined by classification societies (CS)'s rules. It is well known that there are times when fatigue cracks are observed in early stage of a ship's service life even though the ship passed the fatigue assessment in design approval (SR219 1996[29], Storhaug et al, 2007[33]).

Figure 1-1 shows an example of the observed crack on the 2800TEU Container Ship (Storhaug et al, 2007[33]). Fricke et al (2002)[11] conducted a comparative study on CS's rules, and they found that predicted fatigue lives varied widely. This indicates that the accuracy of CS's fatigue assessment procedure based on CFD approach might be

inadequate for cases where structural member is subjected to complicated random loadings such as ocean wave-induced load.

(a) a crack on upper inner side longitudinal   (b) a crack in deck longitudinal

Figure 1-1 Cracks were observed in 2800TEU's Container Ship, which sailed on North Atlantic route (Storhaug et al, 2007[33]).

1.1.1   Fatigue crack propagation analysis

In recent years, fatigue life prediction based on fatigue crack propagation (FCP) analysis is applied in fatigue assessment of ship structural members. Crack growth law is one of the most significant research topics in this analysis. Crack growth laws widely used in FCP analysis includes Paris-Elber's rule (Radaj et al, 2006[31], Suresh 1998[34]). The crack growth under constant amplitude loading condition can be predicted accurately by using this rule. However, it causes significant fatigue life estimation errors under random loading conditions. This error results from Paris-Elber's rule's shortage of ability to simulate retardation and acceleration of crack propagation due to load amplitude variation.

Many researchers tried to develop crack growth laws which can simulate retardation and acceleration behavior. Huang et al (2008)[14] proposed an engineering

formula for crack growth under variable amplitude loading by modifying Wheeler's model (Wheeler, 1972[47]) so that the effect of stress ratio on the plastic zone size can be evaluated. Cui et al (2011)[4] proposed a unified fatigue life concept. However, effectiveness of these engineering formulas are verified in limited conditions, and they cannot be applied for real random loading which is experienced by ocean-going ships.

Newman Jr (1981)[25] introduced crack closure concept in FCP analysis. In his method, crack closure level is calculated by analyzing non-uniform plastic deformation in the advanced crack's wake by using modified Dugdale model. This model was developed for a center cracked plate under uniform remote stress. Lately, this model was applied to various cracks subjected to variable amplitude loadings. Newman's crack closure model was implemented in computer program FASTRAN and FASTRAN II[25-26]. Toyosada (1994, 1997, and 2004[40-43]) proposed a crack growth model based on the residual plastic wake model with the re-tensile plastic zone generated (RPG) load criterion. The applicability of Toyosada's model was demonstrated by comparing simulated and measured propagation behaviors of fatigue cracks in weld under variable amplitude loading conditions. RPG load criterion was implemented in computer program FLARP.

Sumi et al (2008, 2011[27, 35]) developed a FCP analysis program CP-system in which Toyosada's RPG load criterion is implemented. They demonstrated the effectiveness of CP-system by calculating fatigue crack propagation under random sequence of clustered loading. They also reported that crack propagation life strongly depends on load sequence.

Earlier studies mentioned above show that the accuracy of FCP analysis hinges on the appropriateness of loading sequence used in the simulation. For fatigue assessment

of ship structural members, the loading sequence should be generated so that it can emulate the changing nature of short-seas (significant wave height, H_W and mean periods, T_W) in real Oceans.

1.1.2 Ocean wave modeling

Short-sea sequence and its modeling have been studied by many researchers. Those studies are based on various wave data, such as buoy data, hind-cast and onboard observation. Tromans et al (1995)[44] proposed a prediction technique of rough wave and load experienced by offshore structures. Tromans's method was derived from statistical characteristics of individual wave in North Sea. He proposed a complete long-term probability distribution of storms from the convolution of the 'sort-time' scale statistics and that of 'long-time'. Short-time scale statistics is a uncertainty model of the extreme wave within a storm, and long-term one is a probability distribution to which the most probable extreme wave in a whole data is fitted. Forristall et al (2008)[10] presented the Borgman integral method for the maximum wave height's long term distribution which is combined with short-term distribution. He showed that the result derived from his method exactly matched with that obtained by Tromans's model. Soares et al (2004)[12] proposed a long-term prediction technique of the extreme wave height.

Baxevani et al (2008, 2009)[2-3] proposed a stochastic model called Spatio-temporal wave model. This model can simulate significant wave height sequence by using satellite wave data. This model was adopted to calculate fatigue damage prediction of ship structure (Mao 2010)[19-20]. In order to determine wave spectrum in certain wave period, Mao used approximation formula to derive mean period of simulated significant wave height. This means that the arbitrary mean period may not be consistent with that of

the wave scatter diagram. Minoura et al (2004, 2006)[22-23], showed yet another stochastic model which can simulate sea state (significant wave height, mean period, wave direction) sequence.

It is necessary to generate load sequence consists of both rough and calm seas in order to simulate retardation and acceleration of crack propagation accurately. Such sequence cannot be generated by using sea state models proposed by Tromans, Forristall and Soares because they were developed for the extreme wave estimation alone. Stochastic models proposed by Baxevani and Minoura can generate sea state sequences which can be used for FCP analysis. In Baxevani's and Minoura's models, the stochastic nature of storms (ie. Storm duration and various maximum wave height of storm) are not clearly distinguishable. Thus, complicated cross-correlation analysis at numerous oceanography data point is required in the application of these models. Such analyses require unacceptable man-hours for practical ship design. It is needed to develop a simple load sequence generation method, which does not need statistical processing at each data point.

Tomita et al (1992, 1995)[37-39] proposed 'storm model' in order to simulate load sequences in the real oceans. In this model, the ocean conditions are classified into either calm-sea or storm. Storms are modeled as crescendo-de crescendo amplitude waveform, while calm-seas are modeled as time-independent random waveform. Hereafter, 'storm profile' is the sea state information consisting of the (individual or significant) wave height sequence in a storm and the occurrence probability of storms with various maximum wave heights. The wave height sequence is determined uniquely by using following parameters: number of individual waves or short-seas in a storm; the frequency distribution of wave height in each storm. Tomita's storm profiles are configured based

on the long-term distribution of individual wave height in North Pacific Ocean, and statistical processing at each data is not required. Tomita's model does not take into account the correlation between significant wave height H_W and mean period T_W, consequently, this model can not be coupled with sea keeping analysis (e.g. Fatilsen, 1990[9]). In order to take into account the correlation between H_W and T_W, Kawabe (2002, 2003)[17-18] proposed a modified storm model by using wave scatter diagram (joint probability of H_W and T_W). Kawabe's storm profiles were configured by using a single (average) wave scatter diagram. Osawa (2006)[28] reported that calculated crack propagation lives might become shorter than those derived from a single averaged scatter diagram when the scatter diagram was changed in each GWS sea area. It is preferable that crack propagation analysis is performed by switching the storm profiles in response to the change of sea area and season. In Kawabe's model, storm profiles were configured by using trial and error manner, and it was difficult to configure storms for numerous sea areas. Tomita's, Kawabe's and Osawa's model assumed that storm duration remains unchanged (3.5 days for North Pacific Ocean) and storm profiles were configured from oceanographic data with 2 hours observation period. In fact that, the storm duration always fluctuate, the assumption may undermine the accuracy of estimation. The oceanographic data, which is used to assembly wave scatter diagram, is available with various observation periods. It is preferable to develop a storm profile configuration technique, which is effective for arbitrary observation period.

1.2   Scope of Work

The goal of this work is to develop a practical load sequence generation method for fatigue assessment of ship structural member. This objective is accomplished by

developing an advanced storm model, which overcome the drawbacks of the existing (Tomita's, Kawabe's and Osawa's) storm models. This advanced model is developed so that: 1) storm profile is fully-automatically configured; 2) it can simulate the variation of storm duration; 3) it generates the equivalent sea state history from data with different observation period.

The present work is structured as follows. Chapter 2 discusses about oceanography data sources. The brief review of oceanography data available (buoy data, onboard measurement, hind-cast, etc.) is presented. Wave sequences of various data are examined, and JWA (Japan Weather Association)'s hind-cast data is chosen as the source data. From this data, wave histories (significant wave height H_W and mean period T_W) are generated, and wave scatter diagrams are determined. The long-term exceedance probability of significant wave height $p(H_W)$ is determined from this diagram by performing Weibull fitting using mid-to-high wave data.

Chapter 3 describes the development of fully-automated 2G storm (constant storm duration) profile configuration system. Only discrete values of H_W in 1m steps are considered. It is assumed that waves twice higher than overall mean ($H_{W,mean}$) does not occurs in calm seas. Storms are classified according to the maximum H_W in it. The crescendo-decrescendo amplitude H_W waveform of storm is determined so that the frequent distribution of H_W in each storm is similar to the tail of $p(H_W)$. A formula, which can resolve the incompatibility in short sea numbers caused by round-off error, is developed. This makes it possible to develop a fully automated storm profile determination system. The effectiveness of the developed system is demonstrated by comparing H_W sequence emulated by the automatically configured 2G storm model and those of the source data.

Chapter 4 describes the development of a storm model, which can emulate the variation of storm duration (the 3rd generation, 3G storm model). The statistical nature of storm duration in is examined by analyzing wave sequence of the source hind-cast data. It is found that there is not much correlation between storm duration and the maximum H_W in each storm, and the duration obeys normal distributions. The storm profiles of a 3G model is determined by expanding or contracting the time axis of 2G storm's waveforms. The applicability of the developed storm profile determination method for various observation periods is examined. It is found that the storm wave sequences for different observation period have about the same waveforms while the maximum H_W becomes higher with the decrease in the observation period. This means that the proposed method can generate almost equivalent wave histories from data with different observation period.

Chapter 5 describes numerical examples of FCP analyses based on the developed storm models. FCP analyses of a surface crack in a weld of a bulk carrier are carried out by using 2G and 3G storm models and two propagation laws: modified Paris-Elber rule and FASTRAN II program. As results, followings are found: the stochastic characteristics of wave induced load which is experienced by a ship sails on North Pacific and North Atlantic Oceans can be emulated by the developed storm models; b) fatigue crack propagation lives estimated by using 2G and 3G storm models have almost the same accuracy under the condition chosen; c) the fatigue crack propagation lives estimated by using the developed storm models becomes shorter with the decrease in the observation period of the source oceanography data.

In Chapter 6, conclusions with a summary of the main findings and an outlook on possible improvements and future tasks are proposed.

In Appendix 1, 2 and 3, the stress RAO, the formulas of stress intensity factors and the classification society rule used in the numerical examples are presented.

In Appendix 4, the load sequence experienced by a 2,800TEU's Containership, which sails in North Atlantic route is simulated by using the developed advanced storm model. The simulated sequence and the calculated fatigue damage are compared with those derived from Baxevani's stochastic model. As results, it is found that the statistical characteristics of the wave and/or load sequence generated the proposed storm model almost agrees with those derived from Baxevani's model, and the fatigue damages calculated using two wave models agree very well. This also demonstrates the effectiveness of the developed storm model.

2   OCEANOGRAPHY DATA ANALYSIS

The success of sea state sequence simulation depends on the applicability of oceanography data source. Actual Ocean condition can be specified accurately from oceanography data source. In this chapter, various kinds of oceanography data are examined and the numerical modeling for long-term prediction is discussed.

2.1   Environment Data Sources

In the marine structure's (ship, offshore platform, etc) design stage, it is needed to prepare an appropriate environmental (oceanography) data for a specific sea area. These data, for ship's design, can be provided from the classification society rules. Because the scope of these rules is marine structures all over the world, the assumed statistical nature of the environmental data may differ from that of the target area.

Various kinds of oceanography data, e.g., visual observation, instrumental observation, hind-cast data, are available. Visual observations are performed onboard or from coastal station in onshore. The procedure and reports of onboard observations are under supervision of World Maritime Organization (WMO)[48]. Some of these data are available to the public. The most well known onboard observation data in maritime industry is 'Global Wave Statistics, GWS' (Hogben et al, 1990[13]).

Oceanographic data are also provided from instrumental measurements on sea (e.g. buoy, wave radar) or off sea (satellite). Buoys are operated by various organizations (public institutions such as National Oceanic and Atmospheric Administration, NOOA, universities, oil companies, etc.). Some of these data are available to the public, which

includes NOOA National Data Buoy Center, NDBC (www.ndbc.nooa.gov)[24]. The most massive instrumental observation is performed by using weather satellites. They can generate wave radar image of sea area or foot print, which could cover typical dimensions of several kilometers. Some of these data are available to the public by space agencies which operate those satellites. They include GEOSAT (1985-1989), Topex/Poseidon (1991~ 2005), ERS-1 (1991~ 2000), ERS-2 (1995~ 2011) and Jason 1 (2001 ~), and Jason-2 (2008 ~) (WMO, 1998[48]).

In recent years, hind-cast data are available as a substitute of measurement data. Hindcasting usually refers to a numerical model integration of a historical period where no observations are recorded. Since surface waves are generated by the wind, wave hindcasting is considered adequate for generating a reasonable representation of the wave climate. Many climatology data include the wave data generated by hindcasting.

2.2.1   The comparison of significant wave data

Before investigation in following sections, the significant wave, H_W, data of different data sources are compared. Two grid points are chosen in North Pacific Oceans. The locations and data period are presented in Table 2-1. H_W data are provided from the ERS-2 satellite, Japanese Weather Association (JWA)[1] hind-cast, Europe Centre for Medium-Range Weather Forecasts (ECMWF)[7]2 hind-cast and National Oceanic and Atmospheric Administration (NOOA) National data buoy center (NDBC)[24]3 buoys.

---

[1] JWA hind-cast data is used by permission from Research Initiative on Ocean Going Ship (RIOS) Osaka University.
[2] ECMWF hind-cast is owned by ECMWF, and it is accessed from http://data-portal.ecmwf.int/data/d/interim_full_daily/
[3] NDBC data is accessed from 'http://www.ndbc.noaa.gov/'.

Table 2-1 Chosen locations of H_W measurement (Mao et al, 2013[20b]).

Point	Latitude	Longitude	Period of Measurement
Pts-1	46ºN	131ºW	January 1, 2000 ~ December 31, 2010
Pts-2	41ºN	66ºW	January 1, 2000 ~ December 31, 2010

H_W's probability density function (p.d.f.) of different sources are compared in Figure 2-1. It is shown that H_W's p.d.f of all sources almost match each other for high wave region ($H_W > 4$m). The satellite data's p.d.f. is smaller than that of JWA and ECMWF hind-cast data in mid wave region (1m<H_W<4m) at Pts 2, while JWA hind-cast shows higher p.d.f. than that of ECMWF at Pts-1. Above results show that the difference between buoys, hind-casts (JWA and ECMWF) data are not significant.
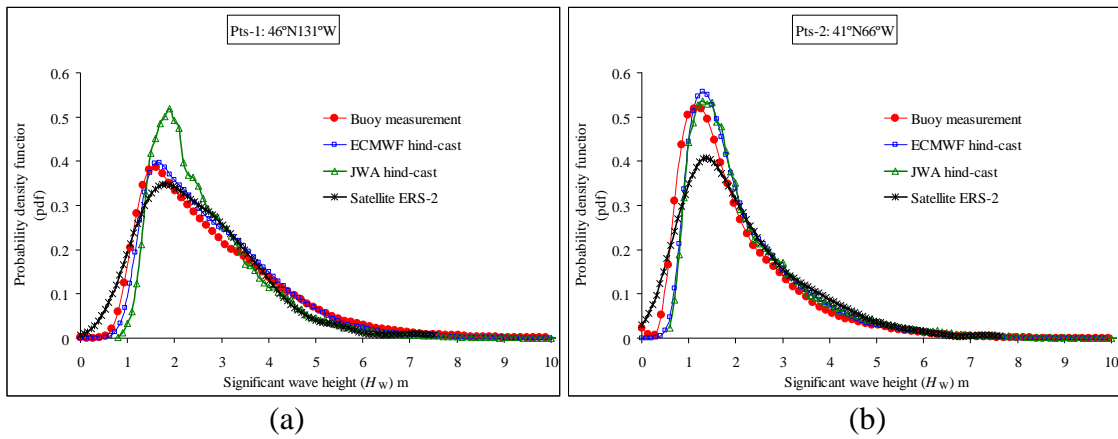
Figure 2-1 Probability density function of H_W measured from different sources at the locations described in Table 2-1 (Mao et al, 2013[20b]).

In the following analyses, JWA's hind-cast data is chosen as data source in this study because it has the longest record period in data examined in this study.

2.2   Wave Scatter Diagram
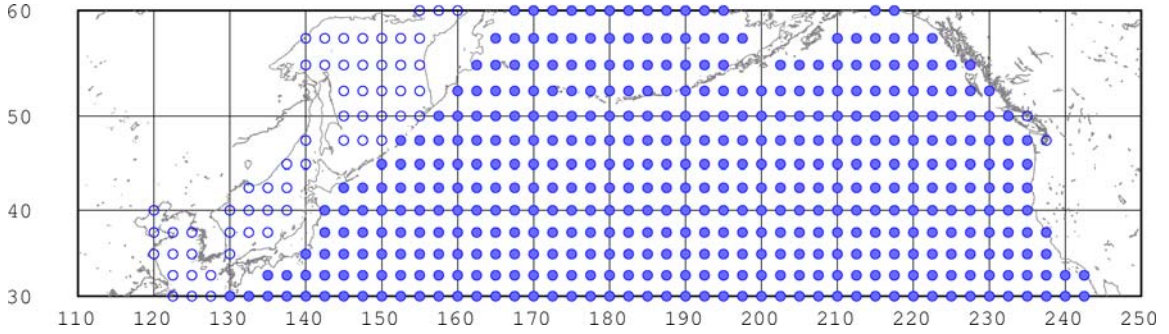
(a) North Pacific Ocean
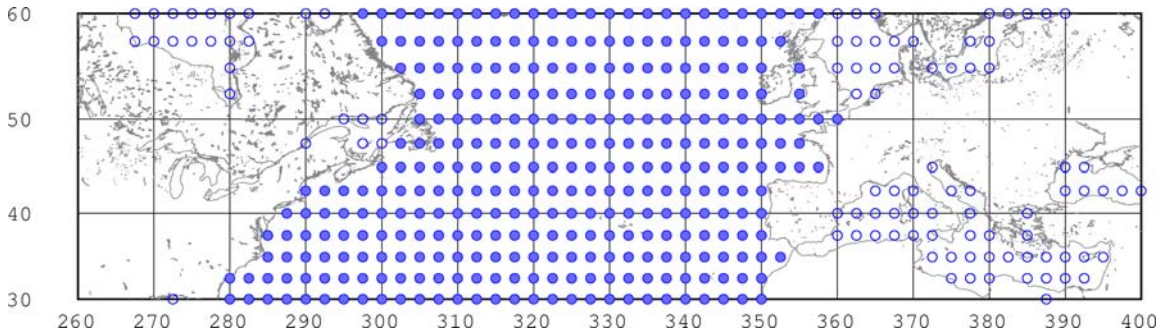
(b). North Atlantic Ocean

Figure 2-2 JWA hind-cast area on North Pacific (a) and North Atlantic (b) Oceans.

In the present work, JWA hind-cast data is chosen as the source data. The wave scatter diagram, the joint distribution of significant wave height and mean periods, is determined from this hind-cast data at each grid point. North Pacific area is between 30ºN ~ 60ºN and 110ºE ~ 110ºW (Figure 2-2(a)), and North Atlantic area 30ºN ~ 60ºN and 80ºW ~ 10ºE (Figure 2-2(b)). For each grid point, wave scatter diagrams are also assembled separately for each season.

Once a wave scatter diagram is assembled, the joint probability density of H_W and T_W, $p(H_W, T_W)$ can determined. $p(H_W, T_W)$ is determined by fitting the data with the conditional log-normal distribution proposed by Wan and Shinkai (1995)[45] given as:

$$p(H_W, T_W) = p(H_W) p(T_W \mid H_W)$$

$$p(T_W \mid H_W) = \exp\left\{-\frac{[\ln(T_W) - \mu]^2}{2\sigma^2}\right\} \alpha(T_W, H_W), \tag{2.1}$$

$$\alpha(T_W, H_W) = \frac{\sqrt{2\pi}}{2\pi T_W \sigma}, \quad \mu = \mathrm{E}\{\ln(T_W(H_W))\}, \quad \sigma^2 = \mathrm{Var}\{\ln(T_W(H_W))\}$$

in which, $p(H_W)$ is the marginal probability distribution of H_W, and $p(T_W|H_W)$ is the conditional distribution for T_W given H_W.

2.3   Modeling of Environmental Data

Hereafter, $F(H_W)$ and $P_{ex}(H_W)$ be H_W's cumulative probability distribution and its exceedance probability. It is well known that long-term probability distribution of H_W can be approximated by Weibull distribution. For a Weibull distribution, $F(H_W)$ is given by[8]

$$F(H_W) = 1 - \exp\left[-\left(\frac{H_W}{\lambda}\right)^k\right] \tag{2.2}$$

and, its p.d.f. is given as

$$\left(\frac{k.H_W^{k-1}}{\lambda^k}\right) \exp\left[-\left(\frac{H_W}{\lambda}\right)^k\right] \tag{2.3}$$

where, k and λ are the Weibull's shape and its scale parameters.

(a)   (b)

(c)
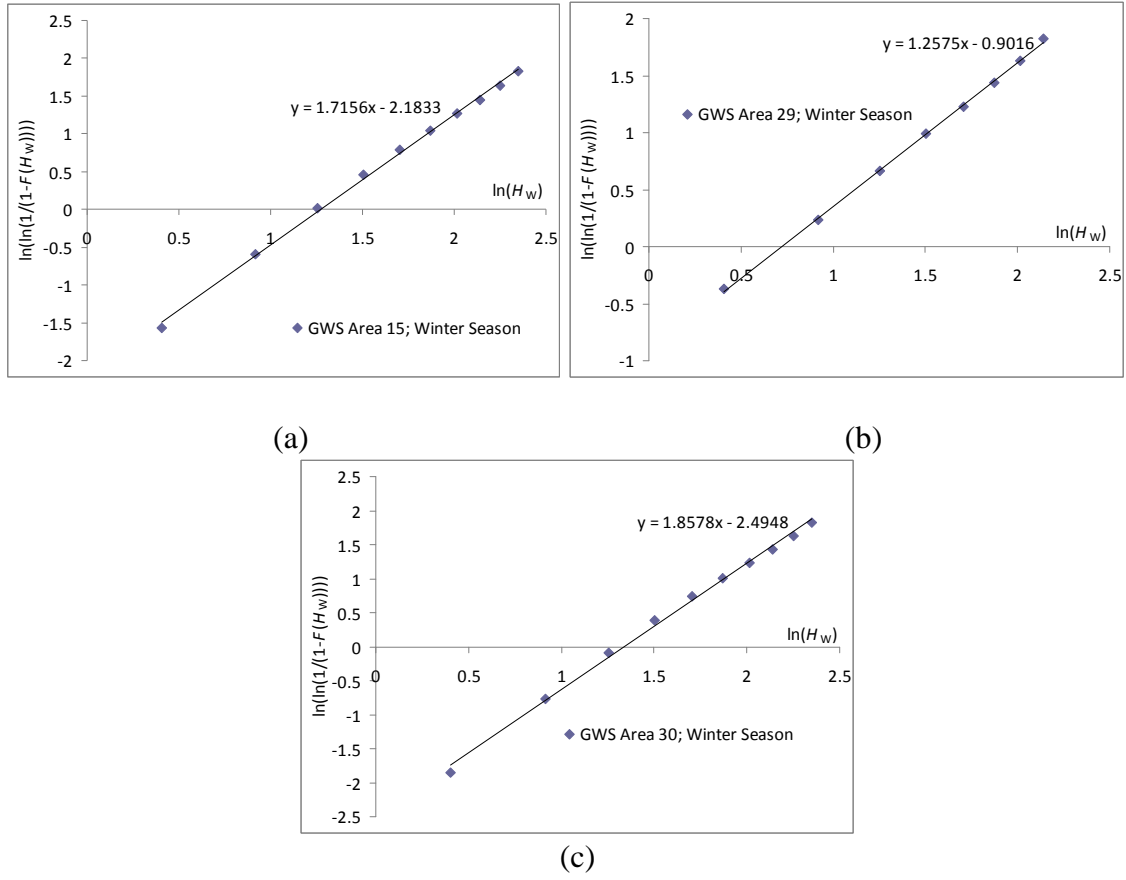
Figure 2-3 Weibull plot of severest season on GWS Area 15 (a), 29 (b) and 30 (c).

$F(H_W)$ of the GWS data at severest season in GWS area 15, area 29 and area 30 are examined. GWS area 29 is chosen as an example of the calm-sea area, area 15 of severe sea area in North Atlantic Ocean and area 30 of severe area in North Atlantic Ocean. Figure 2-3 shows the Weibull plot of $F(H_W)$ in chosen areas. The relation between $\ln(H_W)$ and $\ln(\ln(1/(1-F(H_W))))$ can be represented by a straight line, and Weibull's shape and scale parameters can be identified by using least square method. Figure 2-4 shows the comparison between $P_{ex}(H_W)$ of original data and that of the fitted Weibull distribution. This figure shows that $P_{ex}(H_W)$ of the fitted distribution matches with that of the original data.

(a)

(b)

(c)
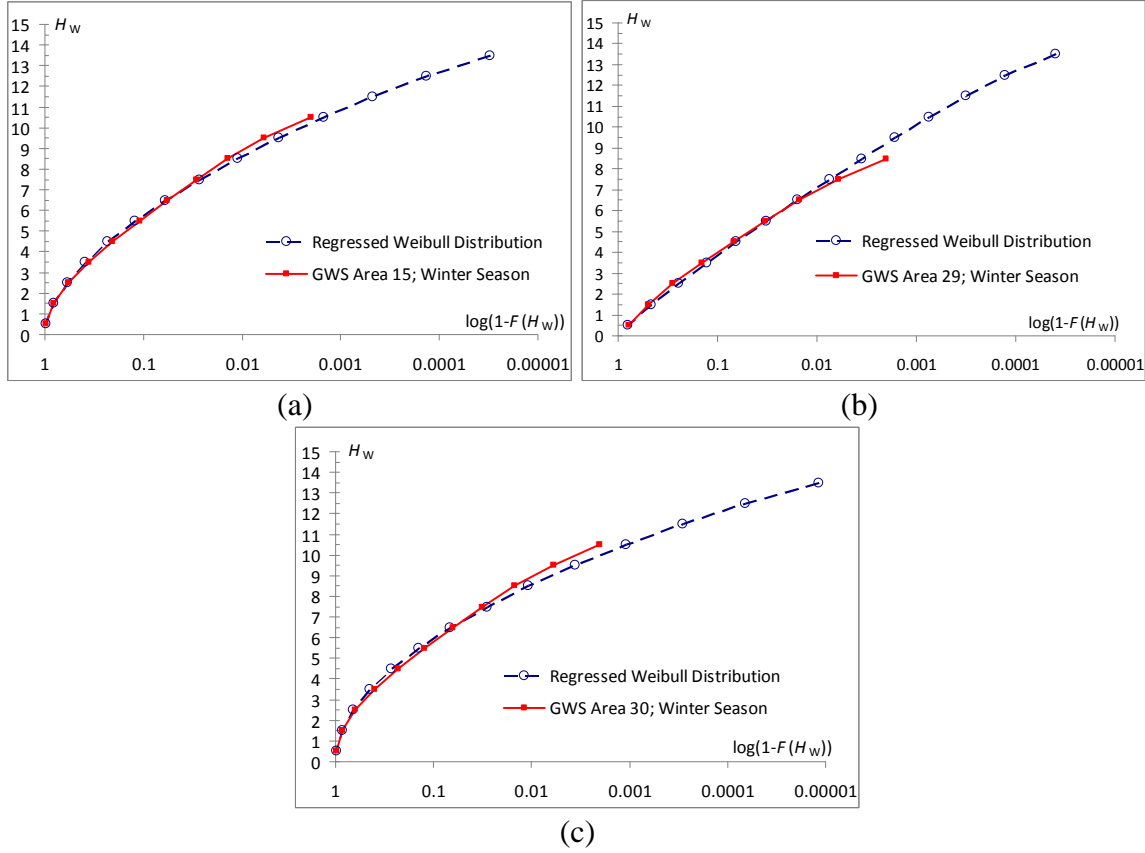
Figure 2-4 $P_{ex}(H_W)$ of severest season on GWS area 15 (a), 29 (b), and 30 (c). The regressed data based on Weibull distribution is compared with that of the original one.

$F(H_W)$ of JWA hind-cast data points, No. 1018 (35ºN145ºE), No. 1064 (40ºN160ºE), No. 1134 (52.5ºN175ºW), No. 2140 (52.5ºN40ºW) and No. 2193 (50ºN30ºW) are examined. Let $H_{W,mean}$ be the overall average of H_W. The Weibull plot of the severest season of points No. 1018, 1064 and 2140 are presented in Figure 2-5. In this figure shows the contrary with GWS that the correlation of $\ln(H_W)$ and $\ln(\ln(1/(1-F(H_W))))$ cannot be represented by a single straight line. However, they approximately show a linear relationship in the mid to high H_W region ($H_W < H_{W,mean}$). Because the number of short-seas with low H_W has relatively small effect on the crack propagation lives, $F(H_W)$ of JWA hind-cast diagram are determined by performing Weibull fitting for mid to high H_W ($H_W > H_{W,mean}$) data.

(a)

(b)

(c)
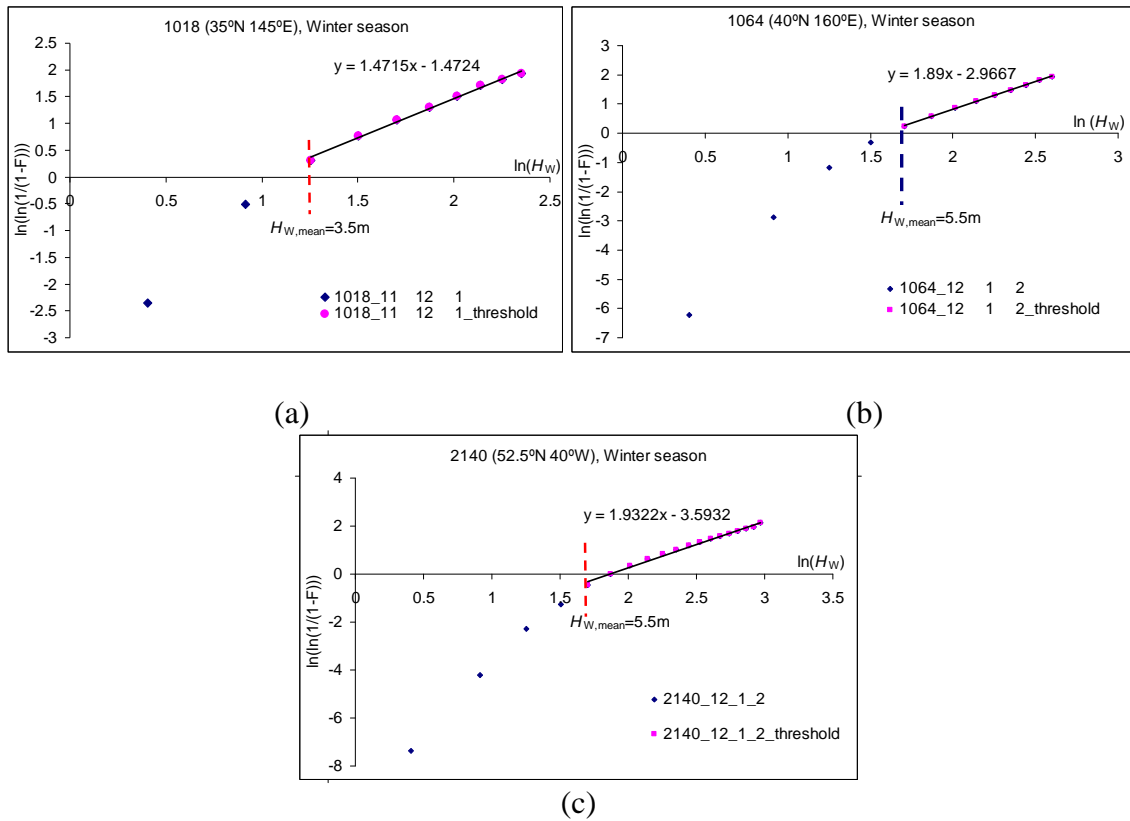
Figure 2-5 The Weibull plot of severest season on JWA hind-cast points No. 1018 (35ºN145ºE), No.1064 (40ºN160ºE) and No.2140 (52.5ºN40ºW).
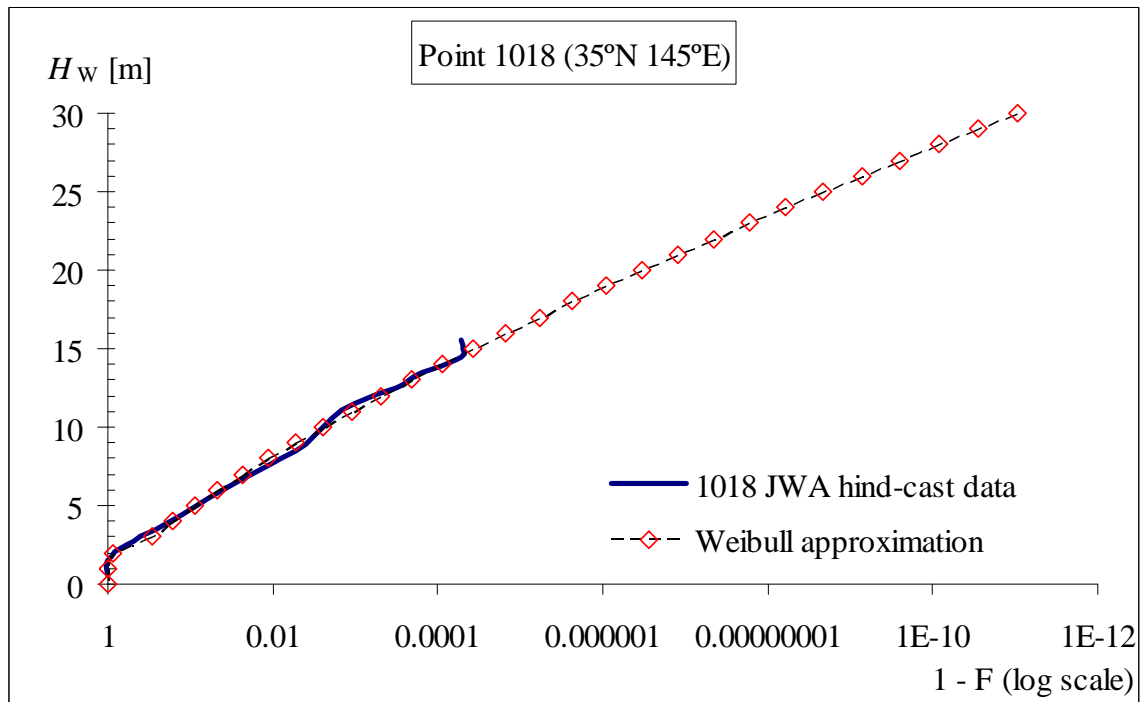
(a)
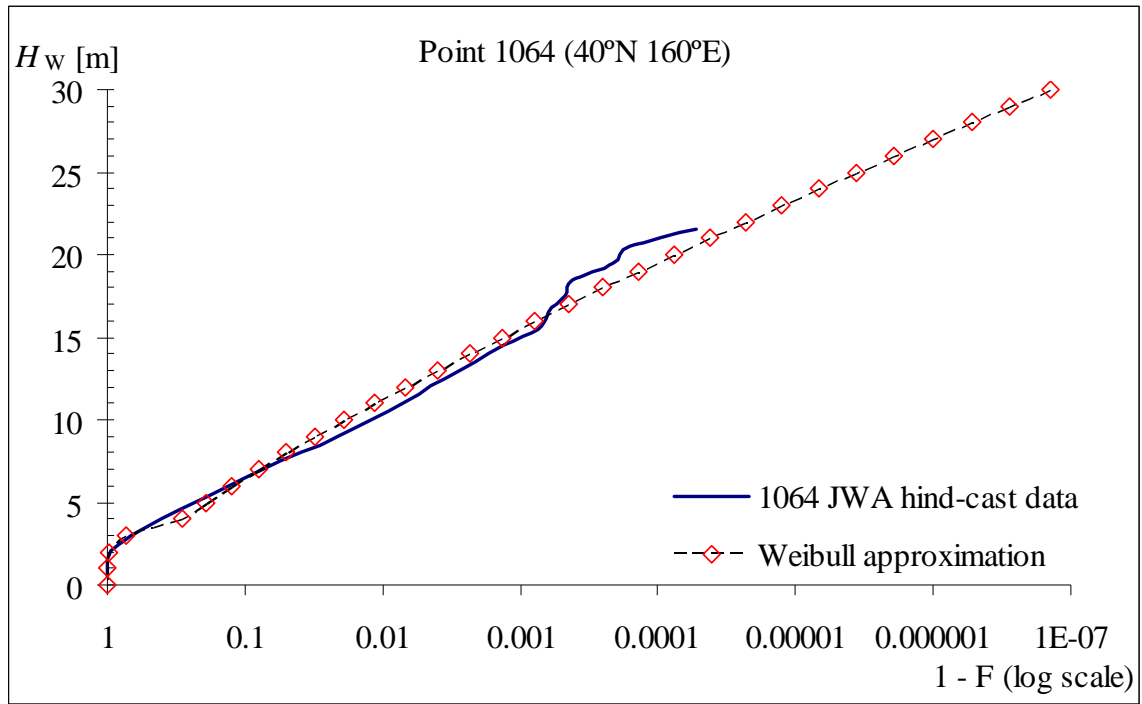
(b)
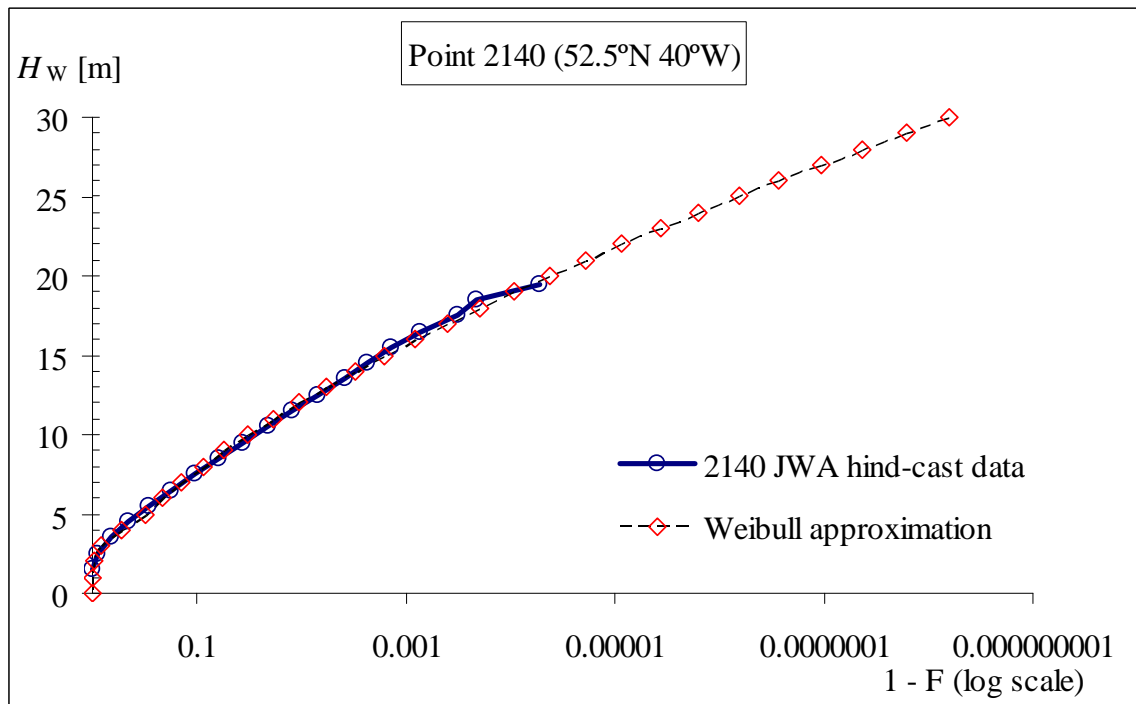
(c)

Figure 2-6 Comparison of H_W long-term exceedance probability between regressed Weibull distribution and that of JWA hind-cast in local location (a. 1018; b. 1064 and c. 2140)

Figure 2-6 shows H_W long-term exceedance probability for point 1018, 1064 and 2140. These figures show that the regressed Weibull approximations show fair agreement with that of original wave source, except point 1064. Point 1064 shows that the regressed Weibull approximation is slightly smaller than the original data for mid range of H_W (5m $< H_W <$ 7m), however, this difference can be neglected.

Finally, it can be concluded that the H_W's long term probability distribution can be approximated by Weibull distributions. For GWS data, Weibull can be fitted by using H_W in whole range. For JWA hind-cast, Weibull fitting can be performed using only mid to high H_W ($H_W > H_{W,mean}$) data.

3 STORM MODEL DEVELOPMENT WITH AUTOMATIC CONFIGURATION

The wave scatter diagram is assembled from the source oceanographic data chosen in the previous chapter. From this wave scatter diagram, the joint probability distribution of H_W and T_W, and H_W's long-term probability distribution are determined. In this chapter, the fully automated procedure to configure storm profiles is developed. These storm profiles consist of the waveform in a storm and the occurrence probability of storms with various maximum wave heights. In addition, H_W's frequency distribution in calm-sea is also determined.

3.1 Storm Models

In the first generation (1G) storm model proposed by Tomita et al. (1992, 1995)[37-39], it is assumed that ocean is divided into calm-sea and storm conditions. The storm duration is assumed to be 3.5 days (= 302,400 sec.) and it remains unchanged. In a storm consists of 48,000 individual wave height caused the mean wave period is 6.3 sec. Storms are modeled by crescendo de crescendo amplitude individual waveforms. Let h_W be the individual wave height. Discrete values of h_W in 1m steps are considered. Storm profiles are determined by considering that h_W's storm be a stationary short-term random process, so the frequency distribution of h_W in a storm follows Rayleigh distribution. In storm condition (h_W>5m), h_W increases with time until it reaches the maximum, then decreases gradually, as shown in Figure 3-1. The storms are classified in five storm classes based on maximum h_W in a storm (see Table 3-1). This model cannot be coupled

with sea keeping theory because it is impossible to determine T_W for given h_W. The relation between the stress response and the sea state (H_W and T_W) cannot be analyzed accuracy by using Tomita's model.
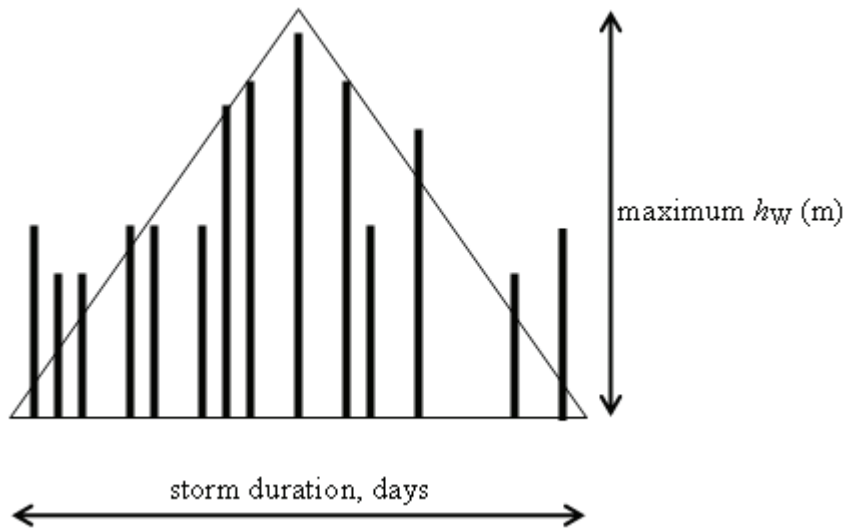
Figure 3-1 Tomita's storm model

Table 3-1 Maximum h_W of Calm-sea and storm conditions of Tomita's storm model

Sea condition	Maximum h_W (m)
Calm-sea Condition	5.0
Storm A	6.0
Storm B	7.0
Storm C	8.0
Storm D	9.0
Storm E	11.0
Storm F	15.0

Kawabe (2002, 2003)[17-18] proposed the second-generation (2G) model in which storms are modeled by short sea sequences with crescendo de crescendo amplitude H_W waveform. Let $H_{W,max|storm}$ be the maximum H_W in each storm waveform. This model can be coupled with sea keeping theory because T_W for given H_W can be determined by using a wave scatter diagram. Storm profiles of Kawabe's 2G model were determined by using

an averaged wave scatter diagrams. Discrete values of H_W in 1m steps are also considered and storm profiles are determined so that the frequency distribution of H_W in a storm is similar with the tail of H_W's long-term distribution. Wave statistics depends on sea area and season, however, the effect of these changes on the crack propagation behavior is neglected in Kawabe's model. In this model, storm profiles are needed to be adjusted in trial and error manner so that the overall H_W's frequency distribution of whole ship's life agrees with the long-term distribution and the number of storm increases with the decrease in $H_{W,max|storm}$. The adjustment process takes considerable man-hours and it is dependent on individual skill.

Osawa et al (2006)[28] proposed a modification of Kawabe's model so that the sea area/season wave statistics can be taken into account in crack propagation analysis. The storm profile is determined by using the local wave scatter diagram for each sea area and/or season. In Osawa's model, it was assumed that H_W increased or decreased linearly with time. This assumption makes storm profile easy to determine, therefore, the number of storms does not decrease monotonically with the increase in $H_{W,max|storm}$. This unnaturalness needs to adjust by using trial and error manner. The adjustment process dependent on individual skill and makes considerable additional man-hours while storm profiles configure for numerous sea areas. The emphasis to automate in the adjustment process is needed. Storm profiles of Kawabe's and Osawa's 2G models were determined by using GWS database with 2 hours observation period. It was also assumed that storm duration remained unchanged (=3.5 days).

Hereafter, Tomita's individual wave based storm model is called the 1G (1st generation) storm model. Kawabe's and Osawa's model based on significant wave height

data are called the 2G (2nd Generation) model. In this chapter, the automatic short sea number adjustment technique for 2G storm model is developed

3.2 Automatic Storm Profile Configuration for Constant storm duration (2G Storm profile)

3.2.1 Automatic waveform determination

3.2.1.1 Background method

Let $p(H_W)$ be the long-term probability density of H_W. Because we assume discrete values of H_W in 1m steps, $p(H_W)$ can be calculated as $p(H_W) = F(H_W) - F(H_W - 1)$. $p(H_W)$ follows a Weibull distribution with the scale parameter λ, and shape parameter k. Figure 3-2 shows the typical $P_{ex}(H_W)$ of Weibull distribution and its tail of $p(H_W)$. The relative frequency distribution of H_W, $p'(H_W)$ is also plotted and it is similar with tail of $p(H_W)$. This figure shows slightly difference between $p'(H_W)$ and $P_{ex}(H_W)$. This difference is the ratio between $p'(H_W)$ to $P_{ex}(H_W)$ as shown in Figure 3-3, that is $R_{tail}(H_W)$. $R_{tail}(H_W)$ can be approximated as the equation below:

$$R_{tail}\left(H_W\right) = a\left(H_W\right)^c ; a = \frac{1}{\lambda} ; c = k - \zeta \tag{3.1}$$

where, ζ varies with the sea area and season. For the source data chosen in this chapter, it is found that the exponent c of equation 3.1 is nearly independent of sea areas and seasons. Let $\bar{\zeta}$ be the mean value of ζ. $\bar{\zeta}$ is 0.65 regardless I_{OB} under the condition chosen.
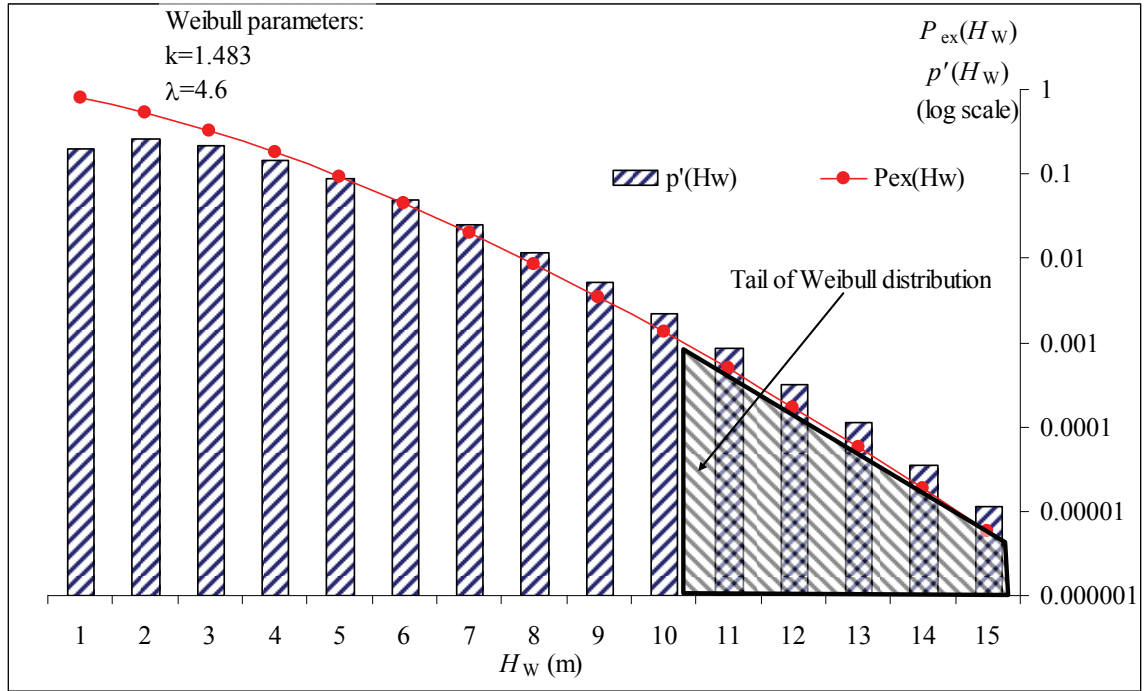
Figure 3-2 Typical tail of Weibull's long term exceedance probability and its tail distribution.
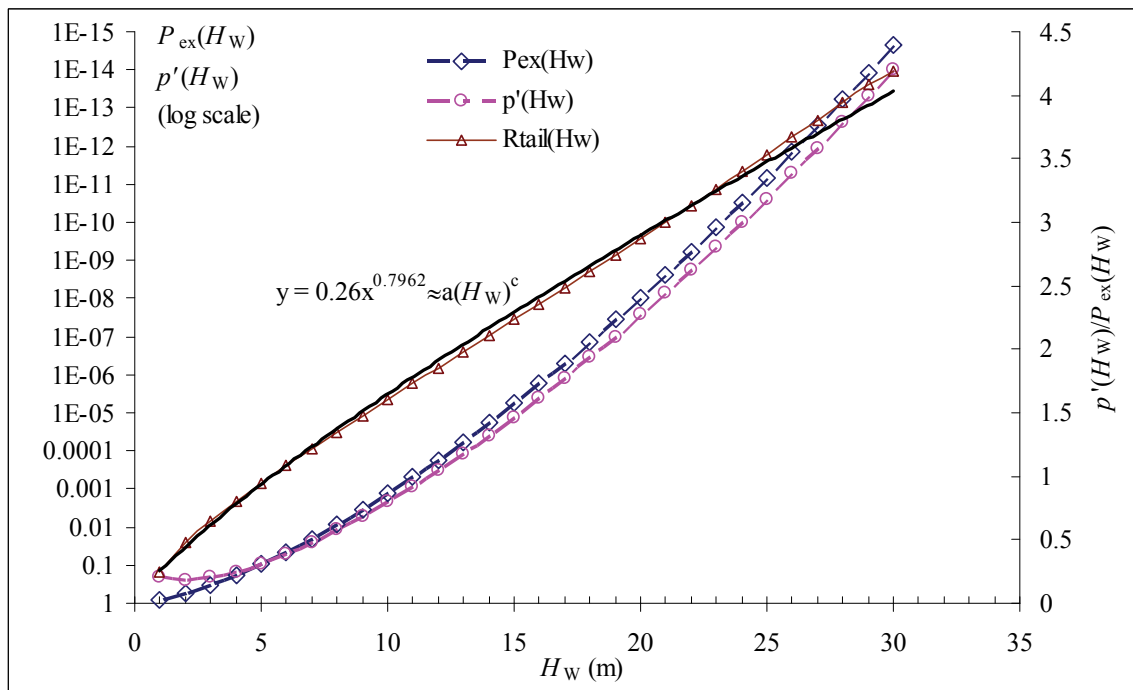
Figure 3-3 Correlation between $p'(H_W)$ and $P_{ex}(H_W)$.

3.2.1.2 Profile of Storms with constant storm duration (2G)

2G storm profiles with automatic adjustment process are configured by following procedure:

1. It is assumed that ship will be sailed for whole design life; L_D. L_D is dependent on design requirement, such as 20, 25 or 30 years. Discrete values of H_W in 1m steps are considered.

2. Let I_{OB} be the observation interval of sea state data (i.e. on-board measurement, hindcast or buoy data). It is assumed that storm duration, d remains unchanged to be 3.5 days as the same as 1G and 2G model's assumptions. Because 1G and 2G model were configured from oceanography data with 2 hours observation period, I_{OB} be 2 hours.

3. The total number of short-sea in whole ship's life, N_{total}, is given as

$$N_{total} = \text{int}\left[\frac{365 \times 24 \times L_D [\text{years}]}{I_{OB}[\text{Hr.}]}\right]$$
(3.2)

and the number of short-seas in each storm sea, N_{SS}, is given as

$$N_{SS} = \text{int}\left[\frac{d[days] \times 24}{I_{OB}[\text{Hr.}]}\right]$$
(3.3)

4. The $p(H_W)$, is given as the marginal probability distribution in which have correlation with H_W of $p(H_W, T_W)$ given by equation (2.1). $p(H_W)$ is approximated by obeying a Weibull distribution. Weibull parameters are identified from wave scatter diagram, while H_W is chosen source dependency as described in chapter 2.

5. In the same manner as Tomita (1995), it is assumed that $2H_{W,mean}$ is the maximum H_W in calm seas. Storms are classified according to $H_{W,max|storm}$. $H_{W,max|storm}$ ranges from $2H_{W,mean}+1$[m] to $H_{W,ext}$, where, $H_{W,ext}$ is that the extreme H_W occurs once in a

ship's life. The probability of exceedance of $H_{W,ext}$ is $1/N_{total}$. Hereafter, a storm class with $H_{W,max|storm}=H_{W,ext}-i+1$[m] is called 'the i-th storm class'. The number of short seas with H_W in ship's life, $N(H_W)$, is given as

$$N\left(H_{W,ext}\right)=1 \; ; 1-F\left(H_{W,ext}\right)=\frac{1}{N_{total}}=\frac{I_{OB}\left[\text{Hr.}\right]}{365\times24\times L_D\left[\text{years}\right]} \tag{3.4}$$

$$N\left(H_W\right)=\text{Int}\left[\frac{\left\{P_{ex}\left(H_W-1.0\right)-P_{ex}\left(H_W\right)\right\}\times L_D\left[\text{years}\right]\times365\times24}{I_{OB}\left[\text{Hr.}\right]}\right] \tag{3.5}$$

6. In the same manner as Kawabe (2002, 2003)[17-18], the crescendo de crescendo amplitude H_W waveform of the a i-th storm class is determined so that the frequent distribution of H_W in each storm is similar to the tail of $p(H_W)$. The maximum number of H_W levels in a storm, j_{end} is given by Eq.(3.6), where k and λ are the scale and shape parameters of the Weibull distribution.

$$j_{end}=\text{Int}\left[\exp\left\{\frac{\left(\ln\left(\ln\left(N_{ss}\right)\right)-\ln\left(\frac{1}{\lambda}\right)\right)}{k}\right\}\right] \tag{3.6}$$

7. A crescendo de crescendo waveform starts from $H_W=\min(1.0, H_{W,ext}-i-j_{end}+1)$. When $H_{W,max|storm}$ of i-th class storm is smaller than $2H_{W,mean}+j_{end}$, H_W in beginning of crescendo de-crescendo waveform, $H_W=H_{W,ext}-i-j_{end}+1$ is also smaller than $2H_{W,mean}$.

8. The frequent distribution of H_W in a clam sea, $p_{calm}(H_W)$, is determined from the numbers of short seas with $H_W<2H_{W,mean}$, which do not appear in storms.

9. Let $n^{(i)}$ be the number of occurrence of the i-th class storm in the ship's life. $H_{W,max|storm}$ of the 1st (severest) class storm is $H_{W,ext}$, and a ship encounters this storm only once in a lifetime. That is, $n^{(1)}$ is one. $H_{W,max|storm}$ of the 2nd severest short sea is $H_{W,ext}-1$ and the number of occurrence of the short sea with $H_W=H_{W,ext}-1$, $N_{ext}-1$, is

given as

$$N_{\text{ext}-1} = \text{Int}\left[N_{\text{total}}\left\{F\left(H_{\text{W,ext}}\right) - F\left(H_{\text{W,ext}}-1\right)\right\}\right]$$
$$= \text{Int}\left[N_{\text{total}}\left\{P_{\text{ex}}\left(H_{\text{W,ext}}-1\right)\right\} - n^{(1)}\right] \tag{3.6}$$

Let N_{SS} be the number of short seas in one storm, and $N^*_{\text{ext-1}}$ be the number of short-seas with $H_{\text{W}}=H_{\text{W,ext}}-1$ in the 1st storm class H_{W} distribution. In general, $N_{\text{ext-1}} > N^*_{\text{ext-1}}$. The number of 2nd severest short seas which not used in the 1st storm class, $N_{\text{ext-1}}-N^*_{\text{ext-1}}$, becomes the number of 2nd storm class, $n^{(2)}$. By repeating this procedure, numbers of storms in all classes, $n^{(i)}$ i=3,4,..., can be determined. The index i of the lowest $H_{\text{W,max|storm}}$ is $i_{\text{end}}=\text{Int}(H_{\text{W,ext}} - 2H_{\text{W,mean}})$. The total number of storms in ship's life, $n^{(\text{storm})}$, is the summation of $n^{(i)}$ from i equals 1 to i_{end}. The number of calm seas in ship's life, $n^{(\text{calm})}$ can be determined by subtracting $n^{(\text{storm})}$ from the total number of short seas as

$$n^{(\text{storm})} = \sum_{i=1}^{i_{\text{end}}} n^{(i)}, \quad i_{\text{end}} = \text{Int}\left[H_{\text{W,ext}} - H_{\text{W,mean}}\right]$$
$$n^{(\text{calm})} = \frac{N_{\text{total}}}{N_{\text{SS}}} - n^{(\text{storm})} \tag{3.7}$$

3.2.1.3 Waveform Determination

The waveform determination as described in procedure no.6 above is detailed below:

a) Let $H_{\text{W,max|storm}}$ be $H_{\text{W,ext}}-i+1$[m]. This is the i-th storm class. The number of short seas in this storm is N_{SS}. Let j be the sequential of H_{W} in descending order in this storm (j=1 for $H_{\text{W,ext}}-i+1$, j=2 for $H_{\text{W,ext}}-i$, …), and $N_{\text{j,i}}$ be the number of short sea with $H_{\text{W}}=H_{\text{W,max}}-j+1=H_{\text{W,ext}}-i-j+2$[m].

b) The first approximation of $N_{\text{j,i}}$ (j=1,2,3,…), $N_{\text{j,i}}^{(0)}$, are determined tentatively by following equations:

$$N_{1,i}{}^{(0)} = \mathrm{Int}\left[\frac{24 \times d\,[\mathrm{days}]}{I_{OB}\,[\mathrm{Hr.}]}\left\{P_{ex}\left(H_{W,\mathrm{ext}} - i + 1\right)\right\}\right] = 1$$

$$N_{2,i}{}^{(0)} = \mathrm{Int}\left[\frac{24 \times d\,[\mathrm{days}]}{I_{OB}\,[\mathrm{Hr.}]}\cdot\left\{P_{ex}\left(H_{W,\mathrm{ext}} - i\right)\right\} - N_{1,i}{}^{(0)}\right]$$

$$N_{3,i}{}^{(0)} = \mathrm{Int}\left[\frac{24 \times d\,[\mathrm{days}]}{I_{OB}\,[\mathrm{Hr.}]}\cdot\left\{P_{ex}\left(H_{W,\mathrm{ext}} - i - 1\right)\right\} - \left(N_{1,i}{}^{(0)} + N_{2,i}{}^{(0)}\right)\right]$$

$$\vdots$$

(3.8)

The summation of $N_{j,i}{}^{(0)}$ should be equal to N_{SS}, however, this requirement is not met

for some cases because the round-off errors.

c) $N_{j,i}{}^{(0)}$ of equation (3.8) can be adjusted so that the summation is equal to N_{SS} by the

equation given as

$$N_{j,i} = N_{j,i}{}^{(0)} + \mathrm{Int}\left[R_{tail}\left(H_{W,\max} - j + 1\right) \times \Delta_{SS} \times P_{ex}(H_{W,\max} - j + 1)\right];$$

$$R_{tail}\left(H_{W,\max} - j + 1\right) = \left(\frac{\left(H_{W,\max} - j + 1\right)^{k - \bar{\zeta}}}{\lambda}\right);$$

(3.9)

$$P_{ex}(H_{W,\max} - j + 1) = \exp\left\{-\frac{\left(H_{W,\max} - j + 1\right)^{k}}{\lambda}\right\}; \Delta_{SS} = N_{SS} - \sum_{j=jend}^{1} N_{j,i}^{(0)}$$

in which, k and λ are the shape and scale parameters of Weibull distribution. The

right hand side of Eq.(3.9) consists of two main part, the one is formula related to

$R_{tail}(H_W)$ and the other is that related with $P_{ex}(H_W)$. It is confirmed that $N_{j,i}$ is similar

with tail of $p(H_W)$. j_{end} in Eq. (3.9) is determined by Eq.(3.6) so that the difference

between N_{ss} and the summation of $N_{j,i}{}^{(0)}$ is minimized.

d) The sequence of H_W waveform in the i-th storm class is determined as shown in

Table 3-2. The sequence H_W in a calm sea is determined by random number

selection using $p_{\mathrm{calm}}(H_W)$.

Table 3-2 Significant wave height waveform in the i-th storm class.

J	H_W	Num. of repeat	
		*	**
j_{end}	$H_{W,ext}-i-j_{end}+1$	$0.5\,N_{jend,i}$	$\text{Int}(0.5\,N_{jend,i})$
$j_{end}-1$	$H_{W,ext}-i-j_{end}$	$0.5\,N_{jend-1,i}$	$\text{Int}(0.5\,N_{jend-1,i})$
$\vdots$	$\vdots$	$\vdots$	$\vdots$
2	$H_{W,ext}-i-1$	$0.5\,N_{2,i}$	$\text{Int}(0.5\,N_{2,i})$
1	$H_{W,ext}-i$	$N_{1,i}=1$	$N_{1,i}=1$
2	$H_{W,ext}-i-1$	$0.5\,N_{2,i}$	$N_{2,i}-\text{Int}(0.5\,N_{2,i})$
$\vdots$	$\vdots$	$\vdots$	$\vdots$
$j_{end}-1$	$H_{W,ext}-i-j_{end}$	$0.5\,N_{jend-1,i}$	$N_{jend-1,i}-\text{Int}(0.5\,N_{jend-1,i})$
j_{end}	$H_{W,ext}-i-j_{end}+1$	$0.5\,N_{jend,i}$	$N_{jend,i}-\text{Int}(0.5\,N_{jend,i})$

*. For $N_{j,i}$ is the even-number case. **. For $N_{j,i}$ is the odd-number case.

3.2.2 Validation of automatic configuration
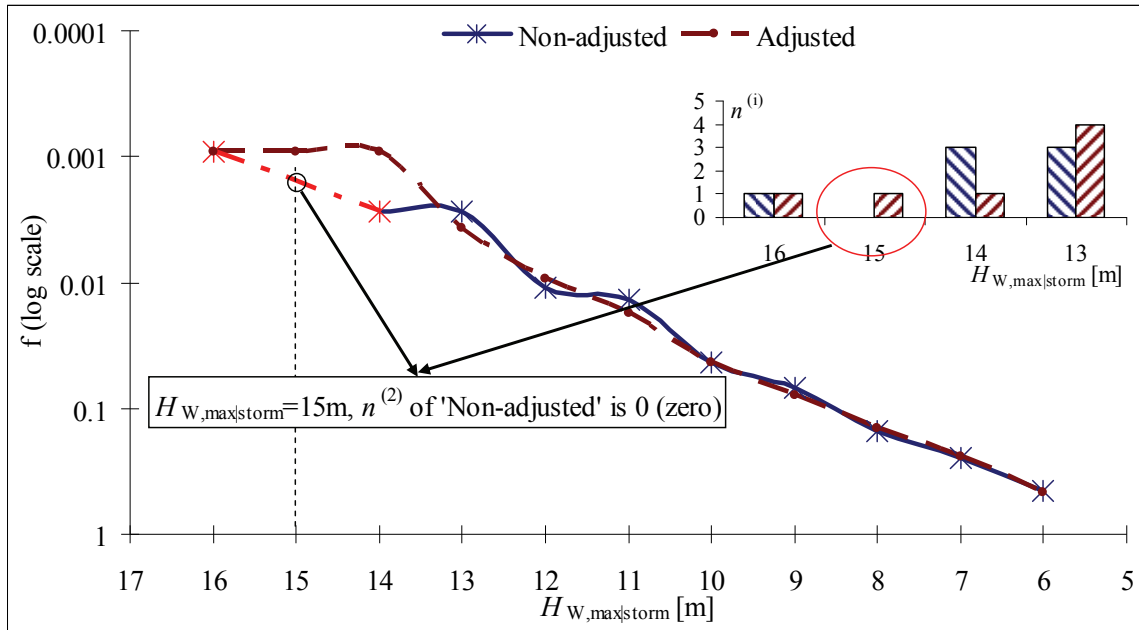
Figure 3-4 Comparison occurrence probabilities of storm classes in which derived from Eq.(3.8) and Eq.(3.9).

Figure 3-4 shows comparison of occurrence probabilities of storm classes (ratio of $n^{(i)}$ to $n^{(storm)}$ derived from Eq.(8) ('not adjusted') and Eq.(9) ('adjusted') profiles. $H_{W,max|storm}$ ranges from 16m to 6m. For 'adjusted' profile, $n^{(i)}$ increases smoothly with the

decrease in $H_{W,max|storm}$ and the changing nature is smooth. However, for non-adjusted profile, $n^{(i)}$ shows considerable fluctuation. This shows that the unnatural in 'non-adjusted' profile can be eliminated by the proposed adjustment technique.

3.2.3   Stress history generation

In the same manner as Osawa's model, a stress history is generated by taking into account the change in loading condition, sea area/ grid point and season. In a chosen sea area/ grid point and season, randomize short sea sequence is generated by using a local storm profiles as described in section 3.2.2 and following the procedure below:

a) Storm or calm sea is decided by random number selection. The occurrence probability of a storm and calm seas, P_{storm} and P_{calm}, are given as:

$$P_{storm} = \frac{n^{(storm)}}{n^{(storm)} + n^{(calm)}}, \quad P_{calm} = \frac{n^{(calm)}}{n^{(storm)} + n^{(calm)}} \tag{3.10}$$

b) For a calm sea case, generate a random sequence of H_W which obeys $p_{calm}(H_W)$.

c) For a storm sea case, the storm class is decided by random number selection. The occurrence probability of the *i*-th storm class is determined as the ratio of $n^{(i)}$ to $n^{(storm)}$.

d) For the *i*-th storm class, generate a crescendo de-crescendo sequence of H_W as presented in Table 3-2.

e) Once we determine H_W, the mean period T_W is determined by random number selection using the conditional probability of T_W given H_W as in equation 2.1.

A sequence of storm and calm sea is generated by sampling with replacement. Once sea state sequence (H_W and T_W) is determined, stress range in each individual wave height, S_a, is calculated in which the calculation conditions are:

a) The heading angle of the ship is determined by using all-heading model.

b)   The stress response amplitude operator (RAO) of the wave-induced stress in which acting on the structural member can be derived by performing ship's sea keeping and structural analyses.

c)   In each short-sea (H_W and T_W), the individual wave height is generated by assuming the individual wave height obeys Rayleigh distribution whose energy spectrum is given by International Ship structure Congress (Warnsink, 1964[46]). The wave energy spectrum is given as

$$\frac{S(\omega)}{H_w^2} = 0.11 \times \left(\frac{\omega T_w}{2\pi}\right)^{-4} \times \exp\left\{-0.44\left(\frac{\omega T_w}{2\pi}\right)^{-4}\right\}$$
(3.11)

where, ω and $S(\omega)$ are the wave's angular frequency in rad/s and that specified wave spectrum ($m^2 s$). The cumulative probability distribution function of S_a is assumed to obey Rayleigh distribution[8] and given by the equation below:

$$F(S_a) = 1 - \exp\left(-\frac{S_a^2}{2R^2}\right)$$
(3.12)

where, R is the standard deviation of the stress response.

3.3   Short-sea sequence generation

The short-sea sequences are generated by using the 2G storm profile configured by using the proposed procedure. The storm profile is configured using the wave scatter diagram assembled from JWA hind-cast data as described in chapter 2. A hundred random short sea sequences are simulated in a point of North Pacific Ocean, that is point No. 1228 (45ºN 167.5ºW).

3.3.1   Exceedance probability of H_W

15 years short-sea sequences are generated at the chosen point. $P_{ex}(H_W)$ of the simulated short-sea sequences is plotted in Figure 3-5. In this figure, $P_{ex}(H_W)$ of the regressed Weibull distribution and the source hind-cast data are also presented. This figure shows that $P_{ex}(H_W)$ of the simulated sequence agrees well with JWA hind-cast data and the regressed Weibull distribution. This result shows that the statistical characteristics of the short sea sequence generated from the 2G storm profile almost agrees with those derived from the joint probability distribution of H_W and T_W.
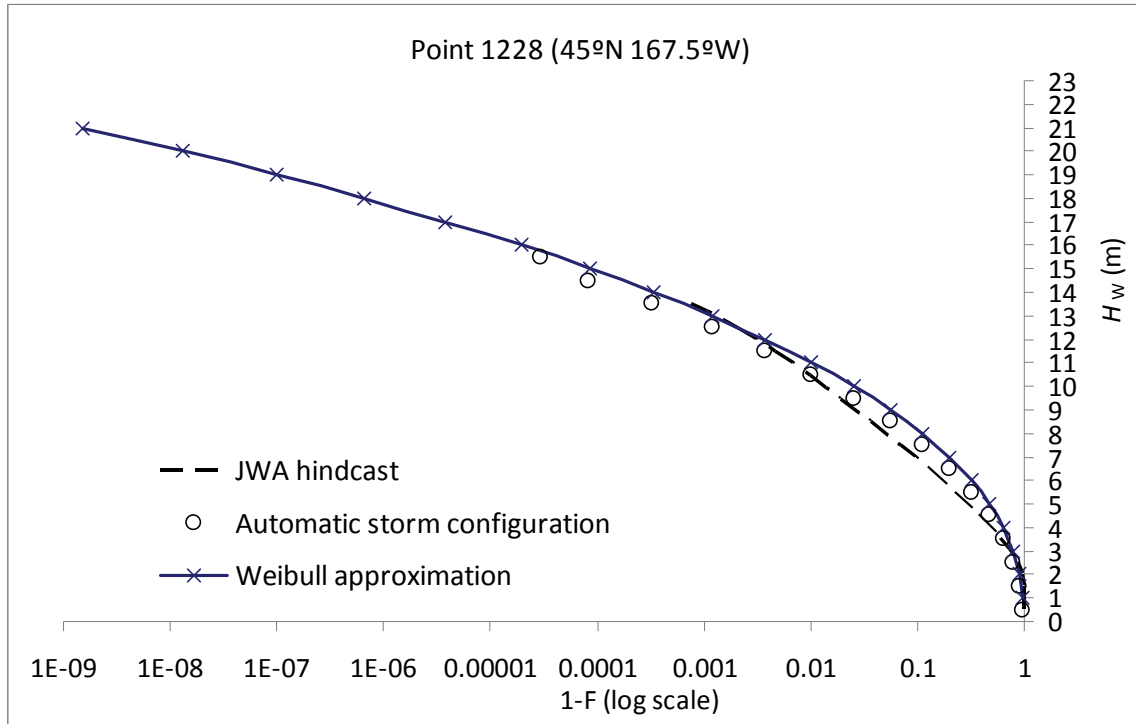
Figure 3-5 Long-term exceedance probability of H_W at point 1228 (45ºN 167.5ºW).

3.3.2   Occurrences frequency of storm classes

The comparison of the occurrences frequency of storm class of the simulation result and that of the source of hind-cast data is compared in Figure 3-6. The frequencies of hind-cast data are calculated by analyzing Equivalent Triangle Storm (ETS) explained

in Chapter 4. This figure shows that the frequency of simulation result is about the same as that of source hind-cast data. This demonstrates that the 2G storm profile configured by the proposed method can emulate the relation between the storm's maximum wave height and storm's occurrence probability of the source data.
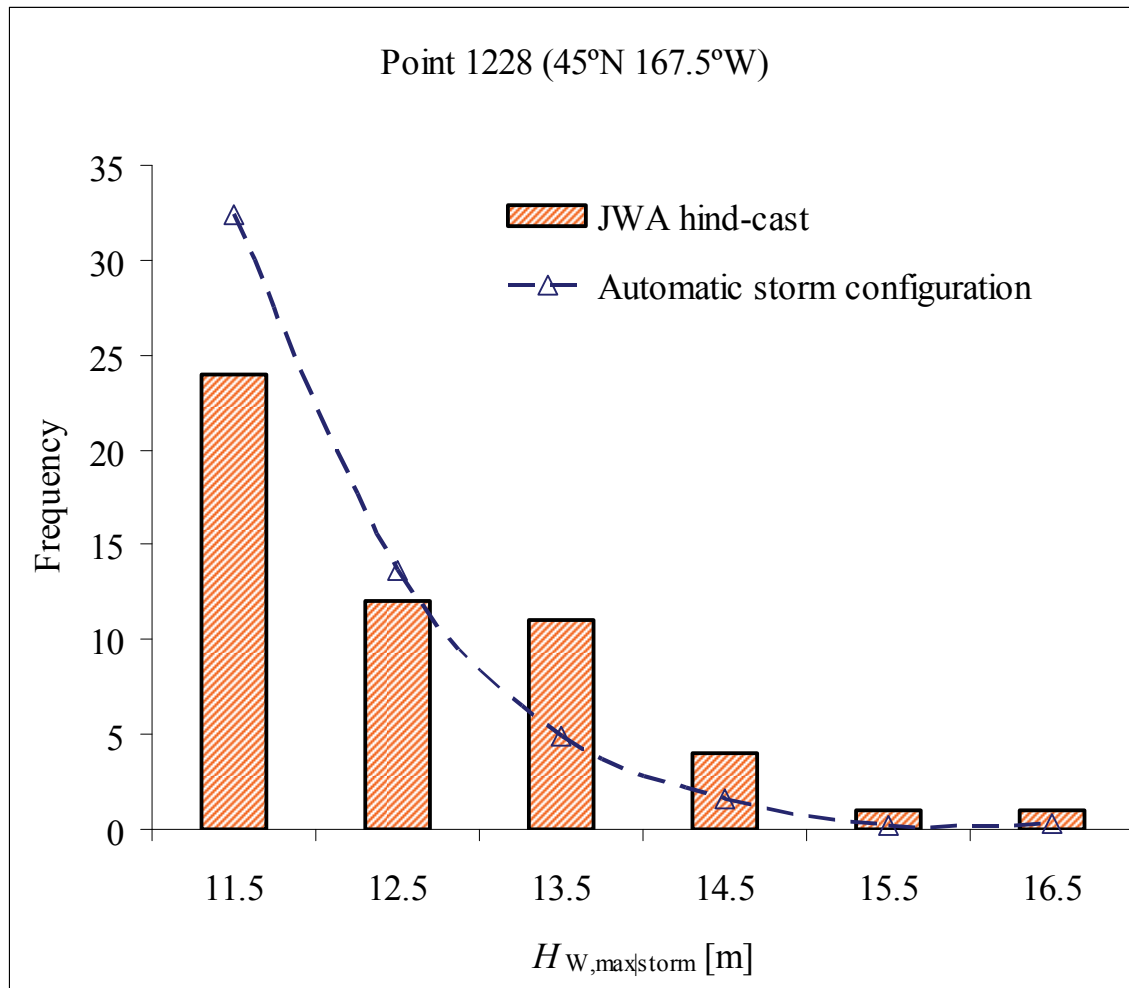
Figure 3-6 Occurrence frequency of storm classes at point 1228 (45ºN 167.5ºW). Storms occurrence derived from source hind-cast and storm model generation are compared.

4 STORM MODEL DEVELOPMENT WITH VARIATION OF STORM DURATION

In the previous chapter, a fully automatic storm profile configuration technique is developed. In 1G (Tomita model) and 2G (Kawabe and Osawa models) storm models, it is assumed that storm duration remains unchanged, 3.5 days. This assumption is in contradiction with the real ocean condition, where storms duration varies substantially. This may deteriorate the accuracy of fatigue life estimation based on storm model. In this chapter, the statistical nature of storm duration is investigated in North Pacific and North Atlantic Ocean. The statistical characteristics of storm duration are modeled and new (the 3rd generation, 3G) storm model, which can simulate variable storm duration, is developed. The effectiveness of the developed 3G storm model is examined by comparing the stochastic characteristic of short sea sequences derived from the developed model and the source hind-cast data.

4.1 Storm Duration Investigation

The stochastic characteristics of storm/rough sea duration, d, can be examined by using the oceanographic data in which wave sequence is recorded. In Chapter 1, it is shown that the difference in H_W sequences recorded in various sources is small. In this work, JWA hind-cast data in North Pacific and North Atlantic Oceans is chosen as the source data. Boccoti (2000)[1] proposed a simplified model of the short-sea sequence in rough seas, "Equivalent Triangular Storm (ETS)". In ETS, it is assumed that H_W exceeds $1.5H_{W,mean}$ and it does not fall below this threshold in a certain period. Here, d can be

defined as this period. The H_W's threshold is sea area dependency. In study on 1G storm model, Tomita presented that the threshold can be set at $2H_{W,mean}$ by analyzing the onboard wave data in which ships sailed on North pacific (1976~1989), and Indian - Japan Ocean (1976~1989). In the present work, $2H_{W,mean}$ is chosen as the threshold. H_W history is prepared based on JWA hind-cast data and according to the following procedure:

i)   The design life, ship speed, sailing routes, ratio of the total navigation time of each route to the whole life are determined.

ii) The route and the departure date and time of the maiden voyage are chosen in random manner.

iii) During the voyage, the ship location is determined in the observation intervals (I_{OB}) of chosen oceanography data by calculating travel distance from the departure port, and H_W at the ship location of the source data is appended to the H_W history.

iv) The following route is determined by random number selection when the maiden voyage is done, and the process iii) is repeated in the second voyage.

v)   The process iii) and iv) are repeated up to the end of the ship's life, and the H_W's history of the first trial is established.

vi) The different route and departure of the maiden voyage from those of process ii) are chosen randomly, and the processes iii) ~v) are repeated in order to prepare H_W histories of successive trials.
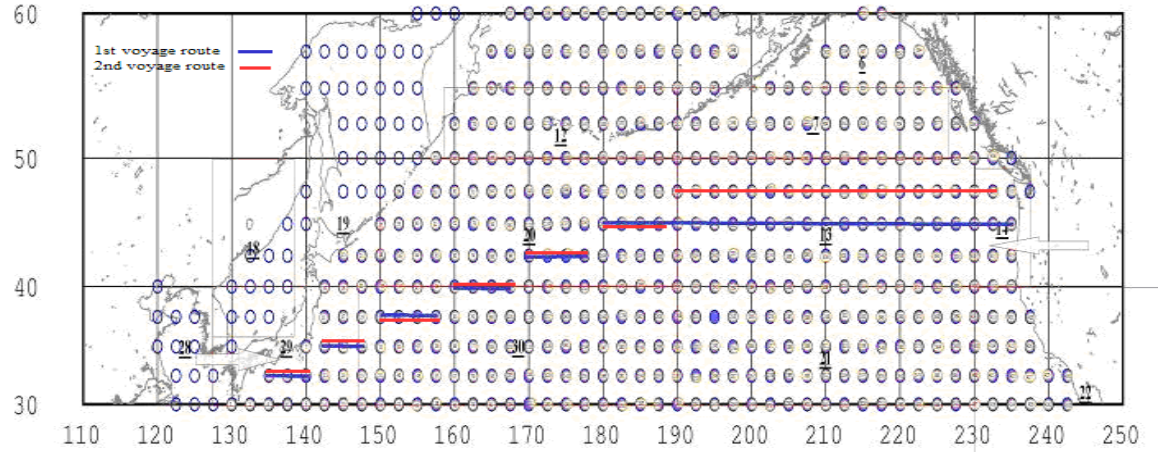
(a) Fictitious route is between Kobe to Portland.
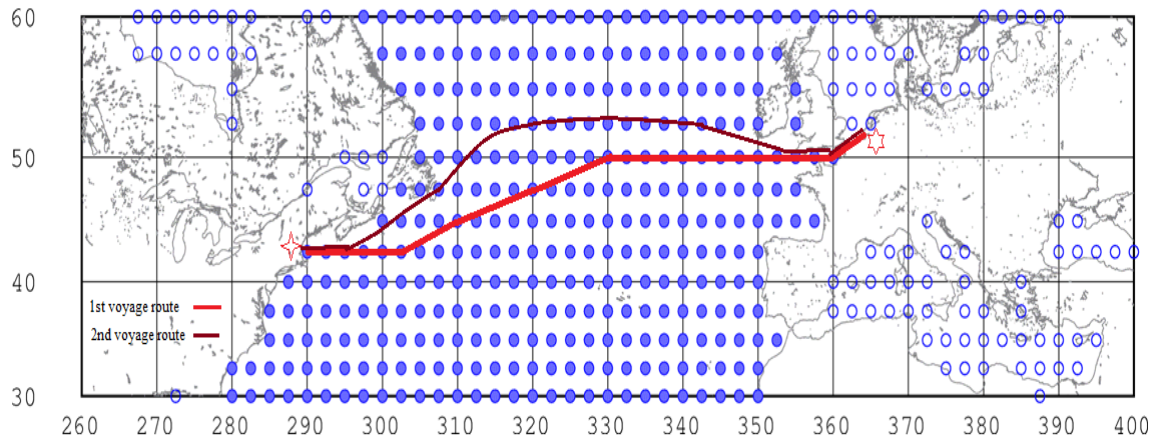
(b) Fictitious route is between Boston to Rotterdam.

Figure 4-1 Fictitious routes in North Pacific and North Atlantic Oceans.

In the present investigation, H_W histories are prepared for ship routes as shown in Figure 4-1(a) (North Pacific, Kobe - Portland route) and (b) (North Atlantic, Boston - Rotterdam route). The ship's sailing time set up to 15 years because JWA hind-cast data from 1994 to 2009 are chosen as the source data. Then, H_W's histories are smoothed by using moving average method. The period of ETS, *d*, is determined by analyzing those of H_W histories as in the following procedure:

a) Find the ETSs (certain periods in which $H_{W,max(j)}>2H_{W,mean}$) and number in consecutive order (j=1,2,3,…).

b) Determine the local maximum of H_W in the j-th ETS, $H_{W,max(j)}$ as the crest of a storm.

c) Find the time of the local minimum of H_W which appears just before the j-th ETS occurs, $t_{B,j}$ and that the local minimum just after the j-th ETS occurs, $t_{E,j}$.

d) The duration of j-th ETS, $d_{(j)}$ is determined as $t_{E,j} - t_{B,j}$. The procedures a) to c) are described in Figure 4-2.
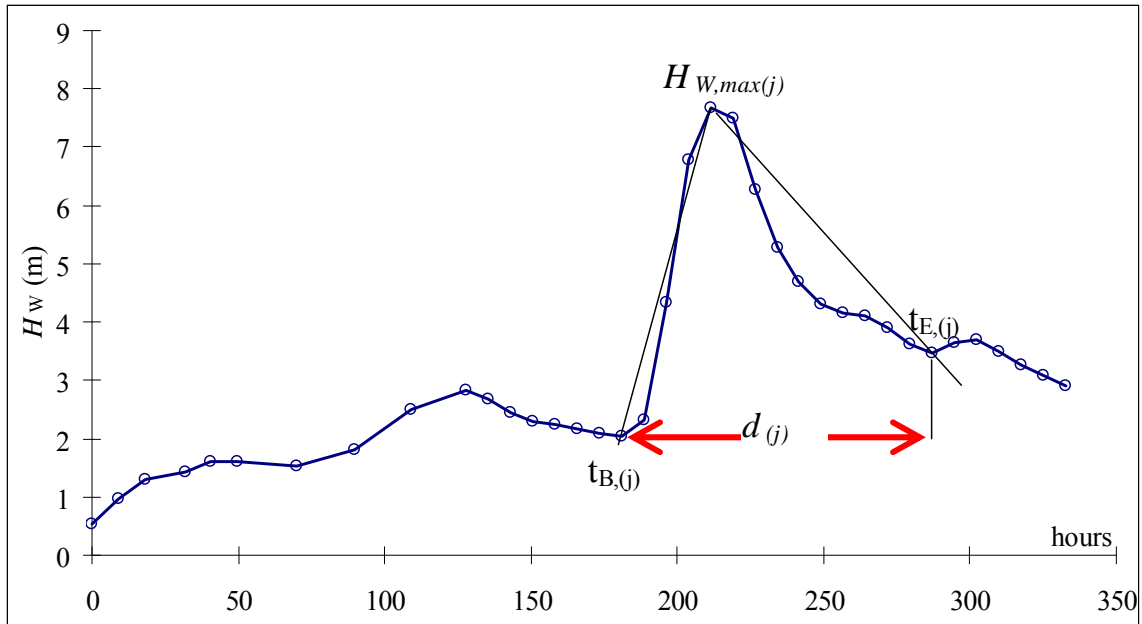
Figure 4-2 Definition of equivalent triangular storm (ETS) and its duration.

Figure 4-3(a) shows the correlations $d_{(j)}$ and $H_{W,max}^{(j)}$ in which derived from H_W's histories in North Pacific (Kobe to Portland) route. Figure 4-3(b) and (c) shows the scatter plot $d_{(j)}$ of H_W's histories in North Pacific (Kobe to Portland) and North Atlantic (Boston to Rotterdam) routes. Figure 4-3(a) shows there is not much correlation between $d_{(j)}$ and $H_{W,max(j)}$. Consequently, it is needed a tool so that $d^{(j)}$ can be modeled for practical engineering and can fluctuate in time domain. We assumed that the variation of d can be approximated by using a normal distribution regardless of $H_{W,max(j)}$. The mean

value μ and the variance σ^2 are μ=3.398 days and σ^2=1.446 for the North Pacific route, and μ=3.988 days and σ^2=1.822 for the North Atlantic route. In 1G and 2G storm models, it is assumed that *d* remains unchanged to be 3.5 days for North Pacific Ocean. This fixed duration approximately agrees with the mean value of North Pacific route analyzed in this section, while the mean storm duration of North Atlantic is longer than that of assumed duration.

Figure 4-4(a) and (b) show the frequency distribution of $d_{(j)}$ for North Pacific and North Atlantic routes. The probability density function of the regressed normal distribution and the relative frequencies are compared in those figures. These figures show that the fitness of *d* with the regressed normal distribution is reasonable. These results show that according to variation of storm duration the load sequence simulation can expand its application not only in North Pacific as studied in 1G model, but, it also be applicable for severe Ocean such as North Atlantic Ocean. In this study, we assume that *d* is 3.5 days regardless Ocean for numerical simplicity.
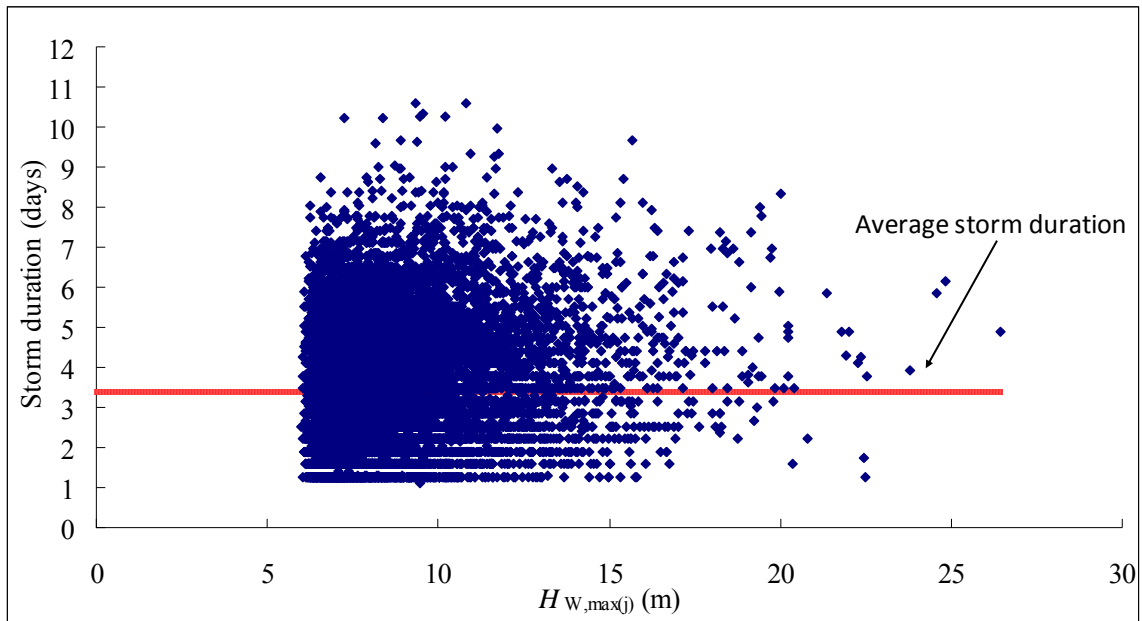
(a) Relation between $d_{(j)}$ to $H_{W,max(j)}$ for North Pacific Ocean.
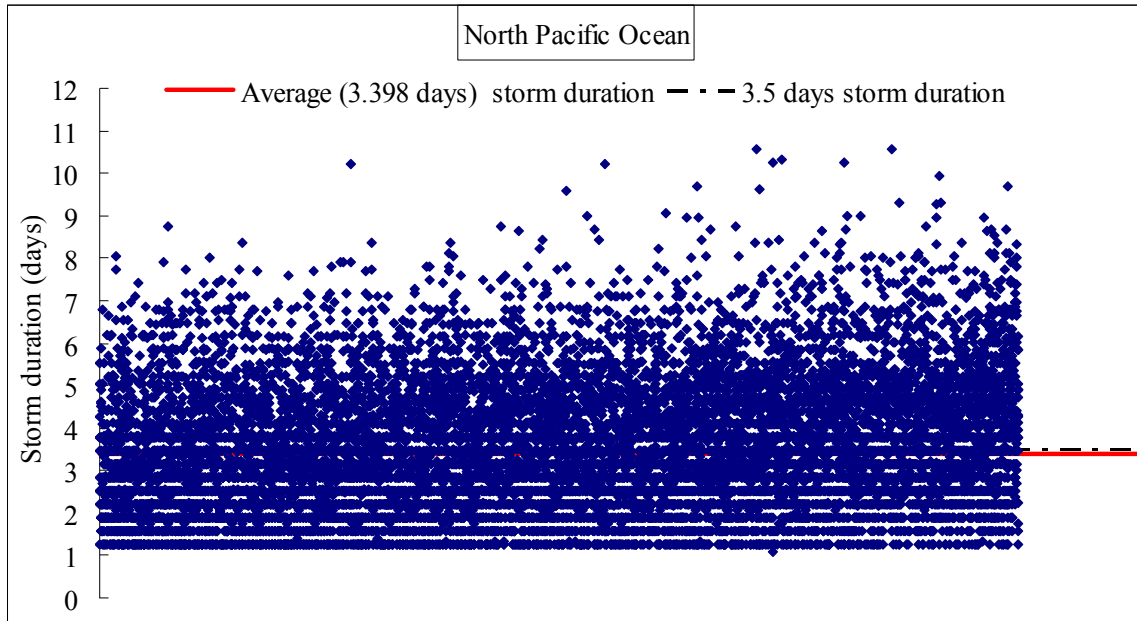
(b) $d_{(j)}$ of H_W's histories in North Pacific route.
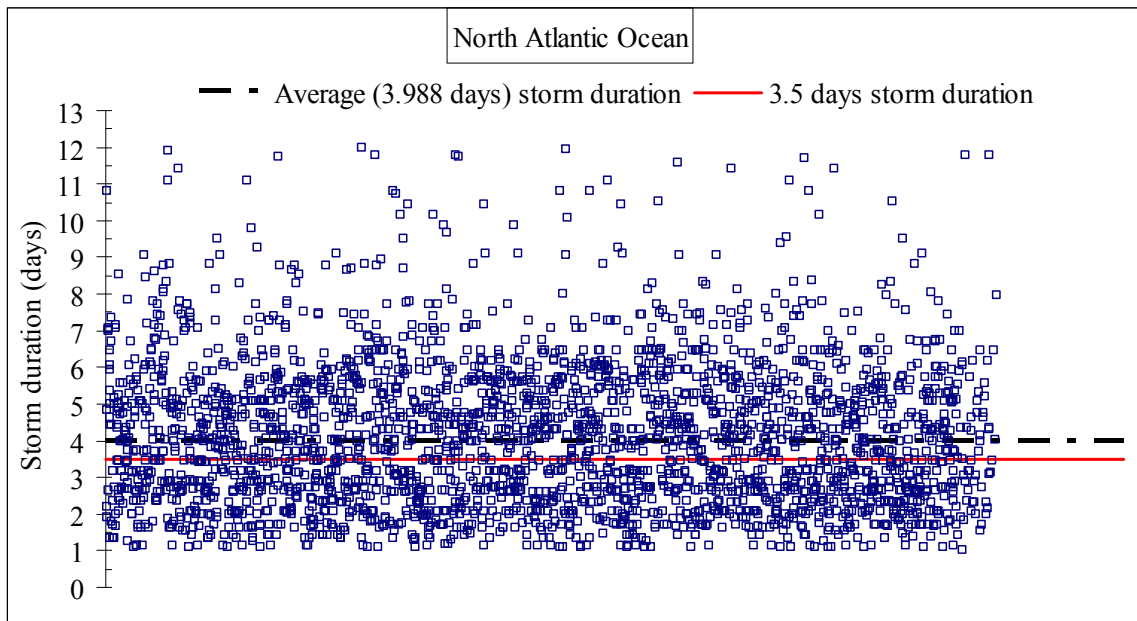
(c) $d_{(j)}$ of H_W's histories in North Atlantic route.

Figure 4-3 $d_{(j)}$ of H_W's histories in North Pacific and North Atlantic Oceans derived by using modified Equivalent Triangular Storm (ETS).
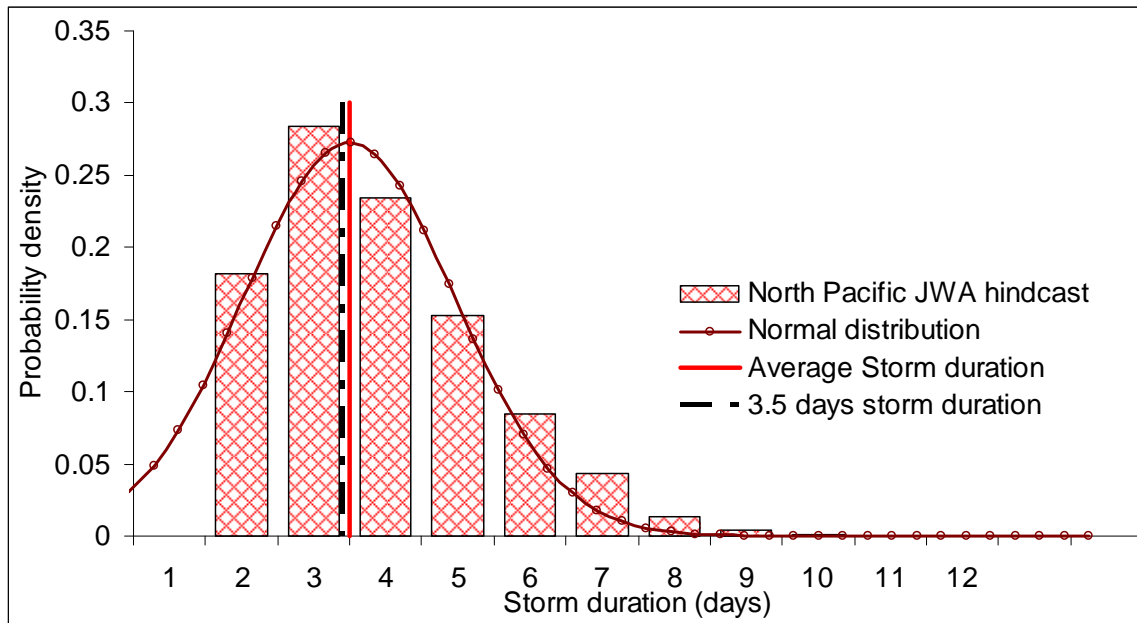
(a) North Pacific route.
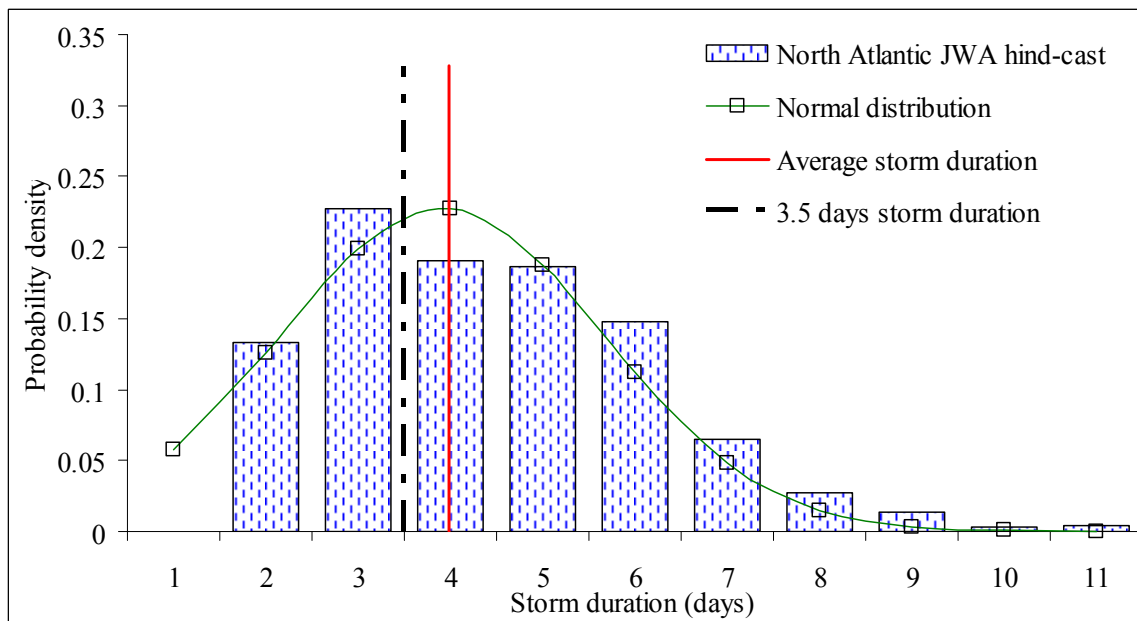
(b) North Atlantic route.

Figure 4-4 Frequency distribution of $d_{(j)}$ for North Pacific (a) and North Atlantic (b) routes. The probability density function of regressed a Normal distribution and relative duration are comparable.

4.2   Storm Profiles with Variation Storm Duration (3G Storm Profile)

4.2.1   2G Storm profile configuration for arbitrary observation period

Recently, various oceanography data with different observation period are available. For example, the observation period I_{OB} is 1 or 6 hours for JWA hind-cast data, 6 hours for ECMWF hind-cast, 0.5 or 1 hour for satellite data, and 2 hours for GWS. Beside I_{OB}, the short-sea duration, that is period in which H_W remains unchanged, I_{SM}, is considered. In this study, storm profiles are configured for JWA hind-cast data with I_{OB}=1, 2 and 6 hours.
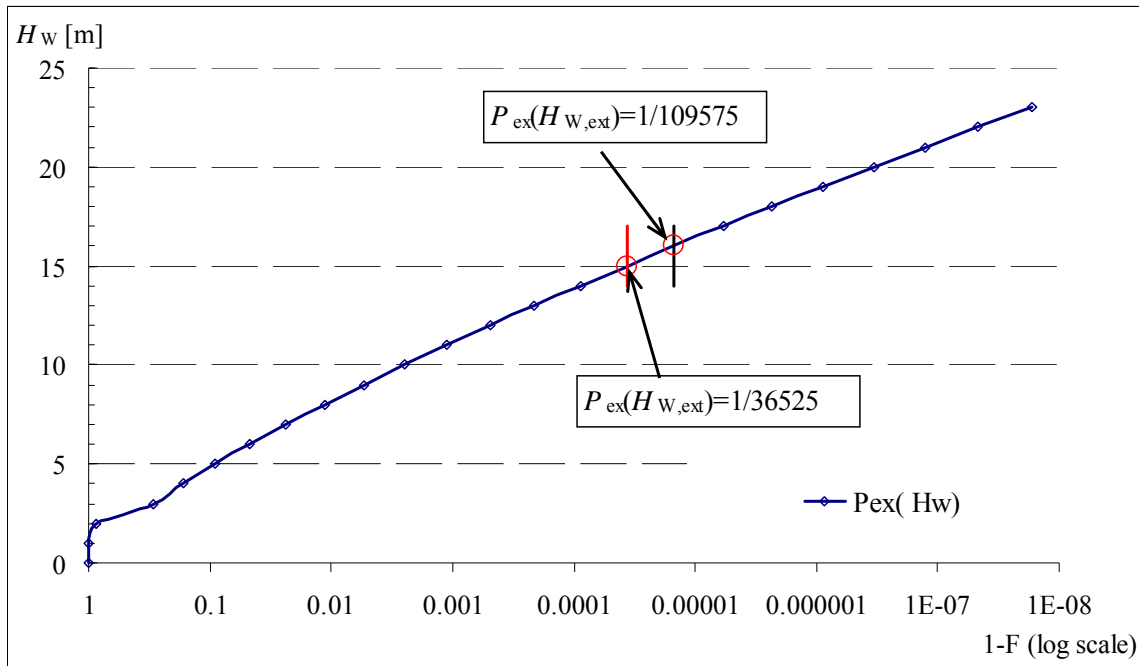
Figure 4-5 The comparison $P_{ex}(H_{W,ext})$ of I_{OB}=6 and that of I_{OB}=2 hours plotted in $P_{ex}(H_W)$ of I_{OB}=1 hours.

Figure 4-5 shows an example of the relation between H_W and $P_{ex}(H_W)=1-F(H_W)$ for the case with I_{OB}=1 hour. The occurrence probabilities of the once-in-life extreme

short sea, $P_{ex}(H_{W,ext})$ for I_{OB}=2 and 6 hours are also plotted in this figure. N_{total} for I_{OB}=6 hours is 36525 and that for I_{OB}=2 hours is 109575. This figure shows that larger I_{OB} gives lower $H_{W,ext}$.

For the cases with arbitrary I_{OB}, Eq. (3.2), (3.3), (3.4), (3.5), (3.8) are modified and given as:

$$N_{Total} = \mathrm{int}\left[\frac{365 \times 24 \times L_D\left[years\right]}{I_{OB}\left[Hr.\right]}\right]; N_{SS} = \mathrm{int}\left[\frac{d[days] \times 24}{I_{SM}\left[Hr.\right]}\right] \tag{4.1}$$

$$N\left(H_W, ext\right) = 1; 1 - F(H_{W,ext}) = \frac{I_{OB}\left[Hr.\right]}{365 \times 24 \times L_D\left[years\right]}$$

$$N\left(H_W\right) = \mathrm{Int}\left[\frac{\left\{P_{ex}\left(H_W - 1.0\right) - P_{ex}\left(H_W\right)\right\} \times L_D\left[years\right] \times 365 \times 24}{I_{OB}\left[Hr.\right]} \times \frac{I_{OB}\left[Hr.\right]}{I_{SM}\left[Hr.\right]}\right] \tag{4.2}$$

$$N_{1,i}^{(0)} = \mathrm{Int}\left[\frac{24 \times d\left[days\right]}{I_{OB}\left[Hr.\right]}\left\{P_{ex}\left(H_{W,ext} - i + 1\right)\right\}\frac{I_{OB}\left[Hr.\right]}{I_{SM}\left[Hr.\right]}\right] = 1$$

$$N_{2,i}^{(0)} = \mathrm{Int}\left[\frac{24 \times d\left[days\right]}{I_{OB}\left[Hr.\right]} \cdot \left\{P_{ex}\left(H_{W,ext} - i\right)\right\}\frac{I_{OB}\left[Hr.\right]}{I_{SM}\left[Hr.\right]} - N_{1,i}^{(0)}\right] \tag{4.3}$$

$$N_{3,i}^{(0)} = \mathrm{Int}\left[\frac{24 \times d\left[days\right]}{I_{OB}\left[Hr.\right]} \cdot \left\{P_{ex}\left(H_{W,ext} - i - 1\right)\right\}\frac{I_{OB}\left[Hr.\right]}{I_{SM}\left[Hr.\right]} - \left(N_{1,i}^{(0)} + N_{2,i}^{(0)}\right)\right]$$

$$\vdots$$

Hereafter, 2G storm profiles are configured by applying the procedure as described in section 3.2 and the modified equations in section 4.2.1.

4.2.2 Storm profile configuration with variation storm duration (3G storm profile)

In chapter 3 and section 4.2.1, the storm profile is configured assuming that the duration of rough sea/storm remains unchanged (3.5 days). This assumption is in contradiction with the real ocean condition, and it is needed to configure storm profiles taking into account the variation of storm duration. Hereafter, storm model, which can

simulate the variation of storm duration, is called the 3rd generation, 3G, storm model.

3G storm profile is configured according to the following procedure:

1) Decide the tentative storm profiles, which is identical with 2G storm profiles with the given $p(H_W)$. 2G storm profile is configured by assumed that d equals to 3.5 days for North Pacific nor North Atlantic Oceans and according the procedure as described in section 3.2. The 2G storm profile is $n^{(i)}$, $n^{(storm)}$, $n^{(calm)}$, $p_{calm}(H_W)$, $N_{j,i}$. Let $N_{j,i}^{2G}$ be this tentative.

2) Let d_{var} be the variable storm duration. In a load sequence simulation, d_{var} of each storm is determined by random number selection so that d_{var} follows the normal distribution determined in section 4.1. The parameter of normal distribution is ocean dependency. The load sequence is generated by following procedure as described in section 3.2.3.

3) $N_{j,i}$ of a class storm with d_{var}, $N_{j,i}^{3G}$, is recalculated by expanding or contracting the time axis. The process is described by the following equation:

$$N_{j,i}^{3G} = \begin{cases} N_{j,i}^{2G} & (j=1) \\ \text{Int}\left[\dfrac{d_{var}}{d} N_{j,i}^{2G}\right] & (j>1) \end{cases} \tag{4.4}$$

4) H_W's sequence in the i-th class sorm with dvar is determined from $N_{j,i}^{3G}$ and Table 3.2 (which $N_{j,i}^{3G} \neq N_{j,i}^{2G}$).

An example of H_W's waveform for the case with $H_{W,max|storm}=8m$ and variable storm duration is presented in Figure 4-6. In this case, storm duration ranges from 3.0 to 4.0.
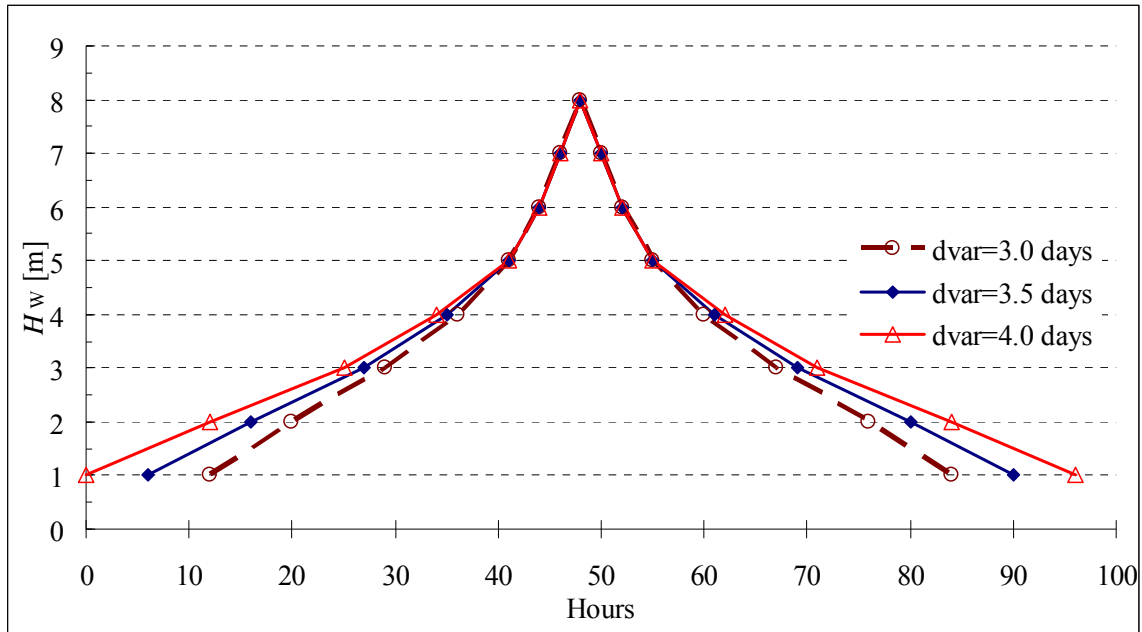
Figure 4-6 An example of H_W's waveform with difference storm duration.

4.3   Application Storm Model and Variation of Storm Duration

The appropriateness of proposed storm models (2G and 3G) is examined by simulating the loading sequences in North Pacific and North Atlantic Ocean routes. The load sequences on chosen routes are simulated by using 2G and 3G storm profiles described in section 4.2. Simulations are carried out by using storm profiles with I_{OB}=2 hours and 6 hours. Let 2G-storm be short-sea sequence simulated by using 2G storm profiles and 3G-storm that simulated by using the 3G storm profile. In this simulation, the storm profile is configured by using the wave scatter diagram assembled from JWA hind-cast data from 1994 to 2009 with I_{OB}= 6 hours. The hind-cast's area is between 30ºN ~ 60ºN and 110ºE ~ 110ºW for North Pacific Ocean. North Atlantic Ocean is between 30ºN ~ 60ºN and 80ºW ~ 10ºE. The data point grid interval is 2.5 degree in longitude and latitude direction.

4.3.1   Short-sea history generation

Short-sea sequences are simulated in several locations in North Pacific and North Atlantic Oceans. For North Pacific Ocean, point 1064 (40ºN 160ºE) is chosen as an example of moderate sea, point 1018 (35ºN 145ºE) of calm-sea and point 1134 (52.5ºN 175ºE) of severe sea. For North Atlantic Ocean, point 2140 (52.5ºN 40ºW) and 2193 (50ºN 30ºW) are chosen as example of severe sea. Short-sea sequences experienced by a ship, which sails two fictitious routes Kobe to/from Portland (Figure 4-1(a)) and Boston to/from Rotterdam (Figure 4-1(b)), are also simulated. In these simulations, 62 sequences are generated randomly in each point and route by following those routes. Hereafter, 2G-storm be short-sea sequence are simulated by using 2G storm profiles and 3G-storm is that of 3G storm profiles. The example of generated H_W sequences is shown in Figure 4-7. Figure 4-7 (a) and (b) shows the simulated short-sea sequences at point 1134 in which generated from 2G and 3G storm profiles when ships sails after about 1.6 years voyage. These figure shows that crescendo de-crescendo of H_W's sequence of $I_{OB}=2$ hour (thin lines with marks) and 6 hours (thick lines with marks) are symmetrically according to Table 3.2.
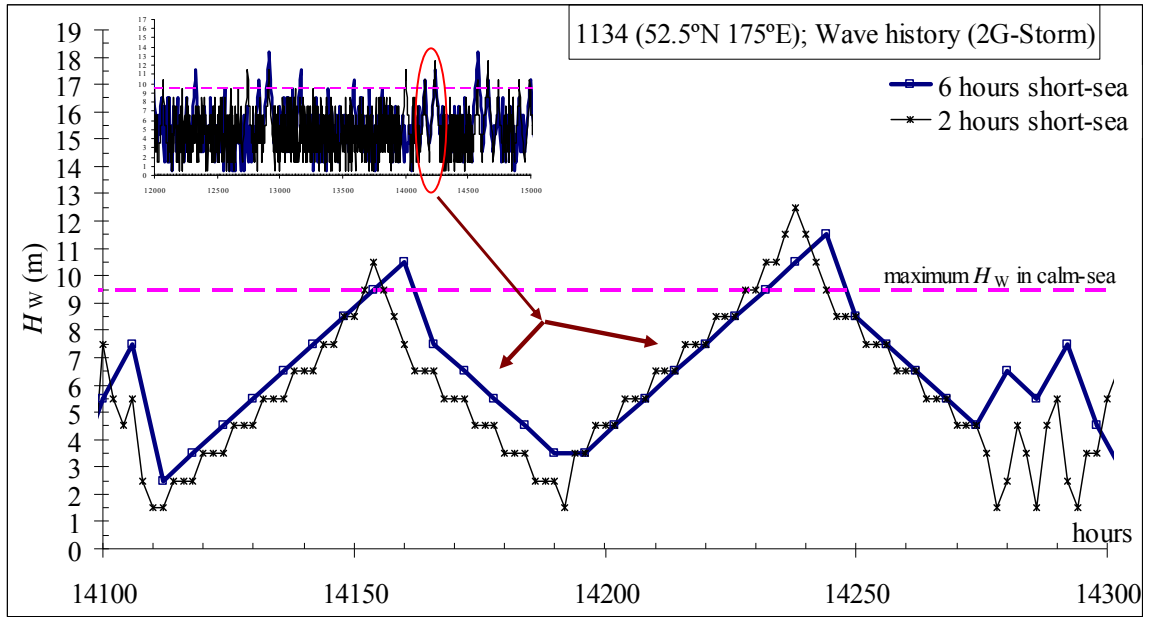
(a) H_W's sequences generated by using 2G storm profile at point 1134 (52.5ºN 175ºE).
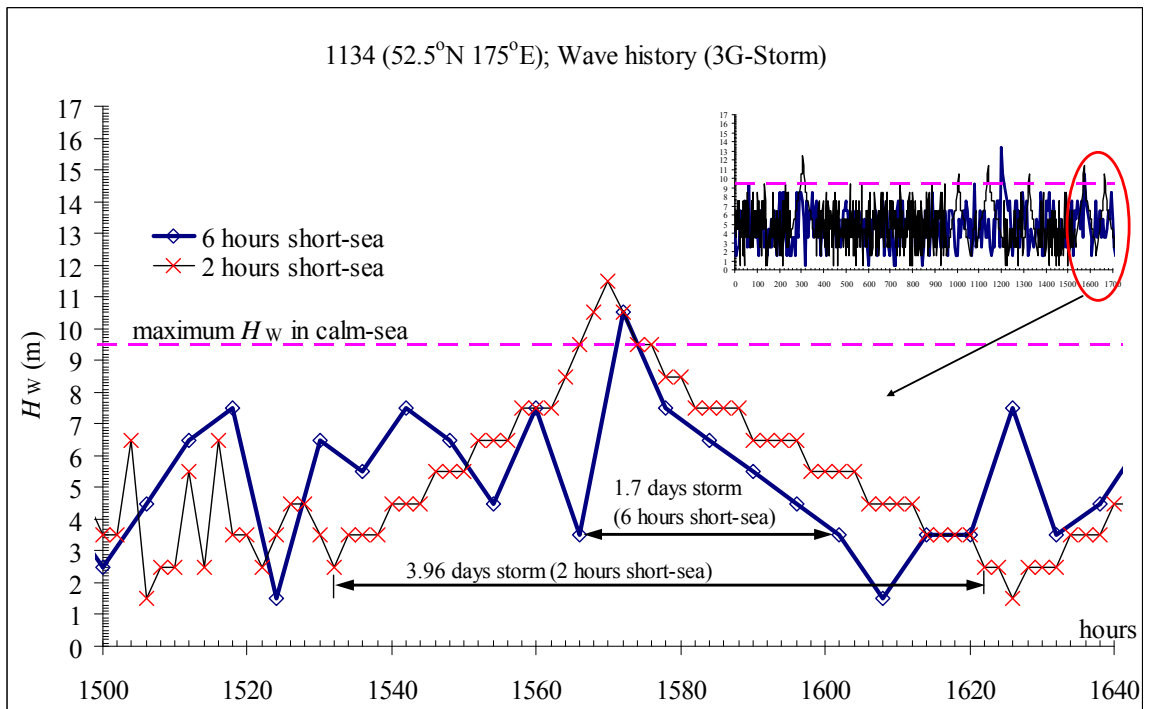
(b) H_W's sequences generated by using 3G storm profile at point 1134 (52.5ºN 175ºE).

Figure 4-7 the example of generated H_W's sequences based on 2G and 3G storm profiles in a certain period at Point 1134 (52.5ºN 175ºE).

4.3.1.1 H_W histories with different I_{OB}

Figure 4-8(a) and (b) show the comparisons of H_W waveforms of storms derived for different I_{OB}. They are the sequences of the 2nd and 3rd class 2G-storms determined for I_{OB}=2 and 6 hours. For cases with I_{OB}=6 hours, $\bar{\zeta}$ of Eq. (3.1) is set at 0.65, which is the same as that for I_{OB}=2 hours. Figure 4-8(a) and (b) show that $H_{W,\max|storm}$ for I_{OB}=2 hours (=15.5m) is higher than that for I_{OB}=6 hours (=14.5). Eq. (4.2) shows that $P(H_{W,ext})$ becomes larger with the increase in I_{OB}. This makes the $H_{W,ext}=H_{W,\max|storm}$ of the 1st class storm for I_{OB}=6 hours be lower than that for I_{OB}=2 hours. The 1st approximation of the number of short seas with $H_{W,\max}$-j in the i-th class, $N_{ji}^{(0)}$ is given by Eq. (4.3). In this equation, larger I_{OB} leads to smaller $N_{ji}^{(0)}$. The smallest time unit in which H_W is constant is proportional to I_{OB}. This makes the duration of the period with the same H_W for I_{OB}=6 hours be not so different from that for I_{OB}=2 hours. Accordingly, the waveforms of the same class storm for different I_{OB} becomes about the same shape. This is the explanation of the difference in $H_{W,\max|storm}$ and similarity of the waveforms in mid-to-low H_W region in Figure 4-8 (a) and (b). Figure 4-8(c) and (d) show the comparison of 3G-storm waveforms. In the storm profile determination, $\bar{\zeta}$ is set at 0.65 again. In the same manner for 2G-storm cases, $H_{W,\max|storm}$ for I_{OB}=6 hours is lower than that for I_{OB}=2 hours, and similarity of the waveforms in mid-to-low H_W region is calculated. In summary, it is shown that the proposed storm profile determination technique can generate equivalent sea state histories from data with different observation period by using the same $\bar{\zeta}$ (=0.65).
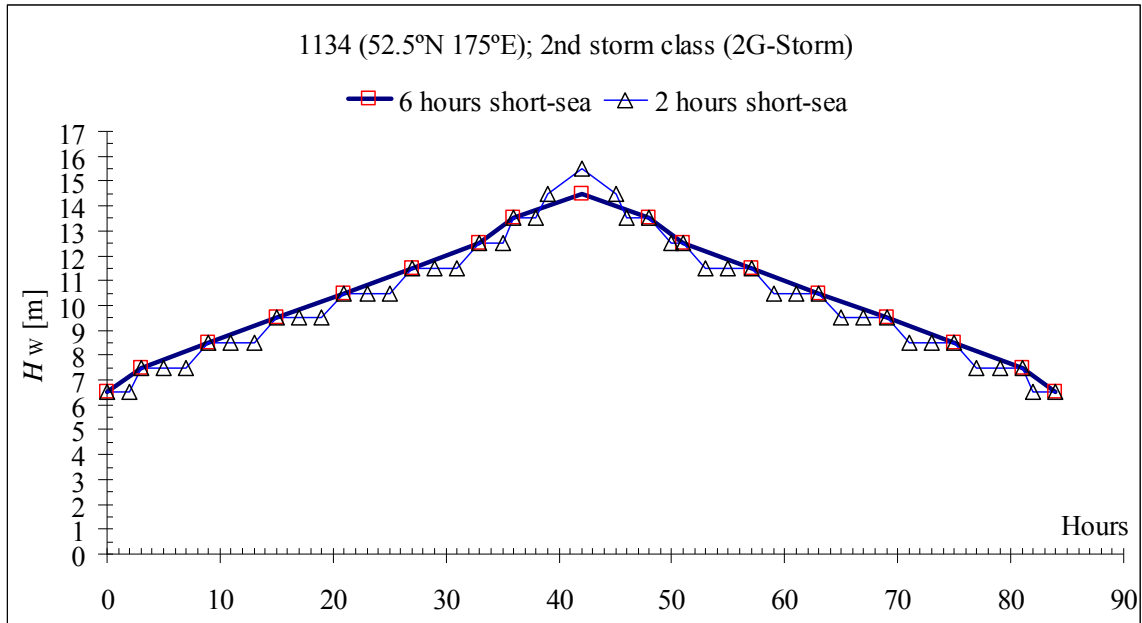
(a) 2nd storm class generated by using 2G storm profile.
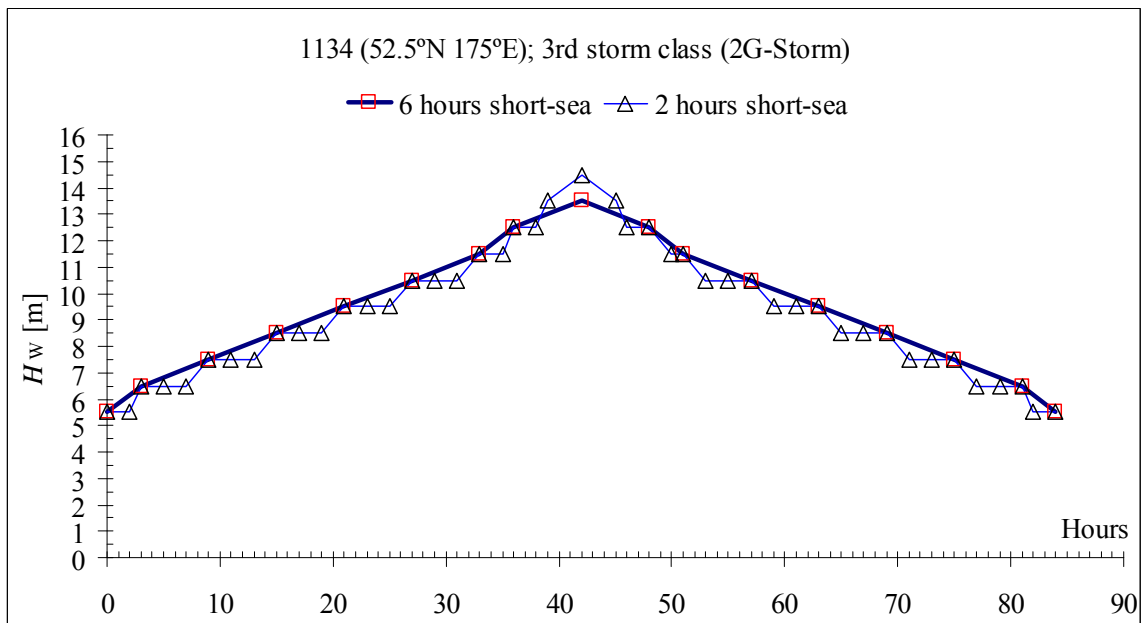
(b) 3rd storm class generated by using 2G storm profile.
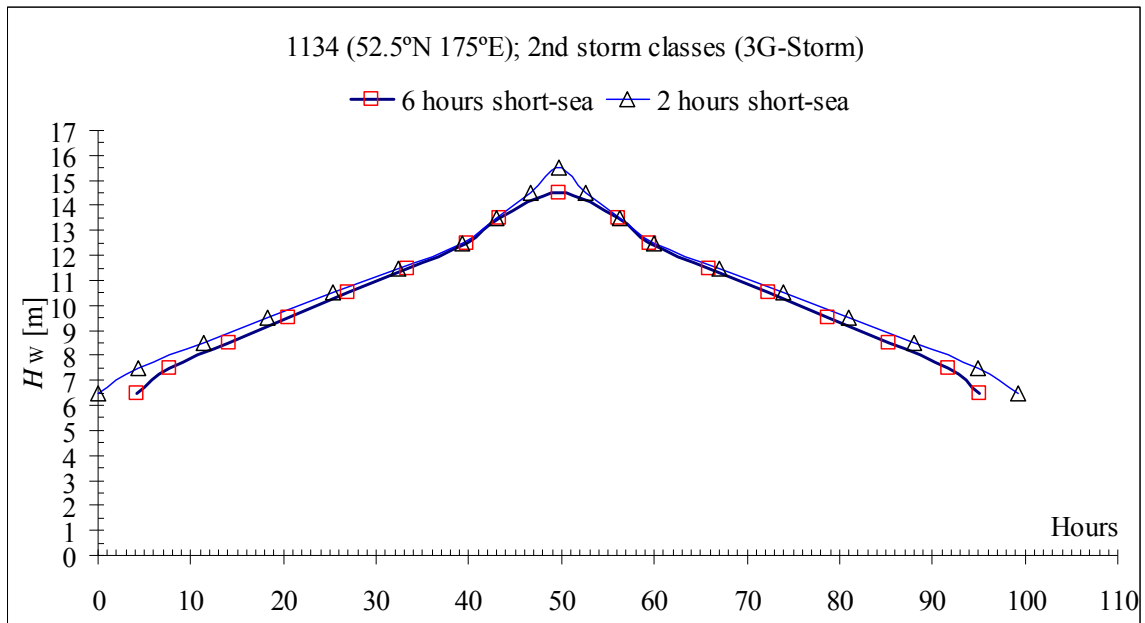
(c) 2nd storm class generated by using 3G storm profile.
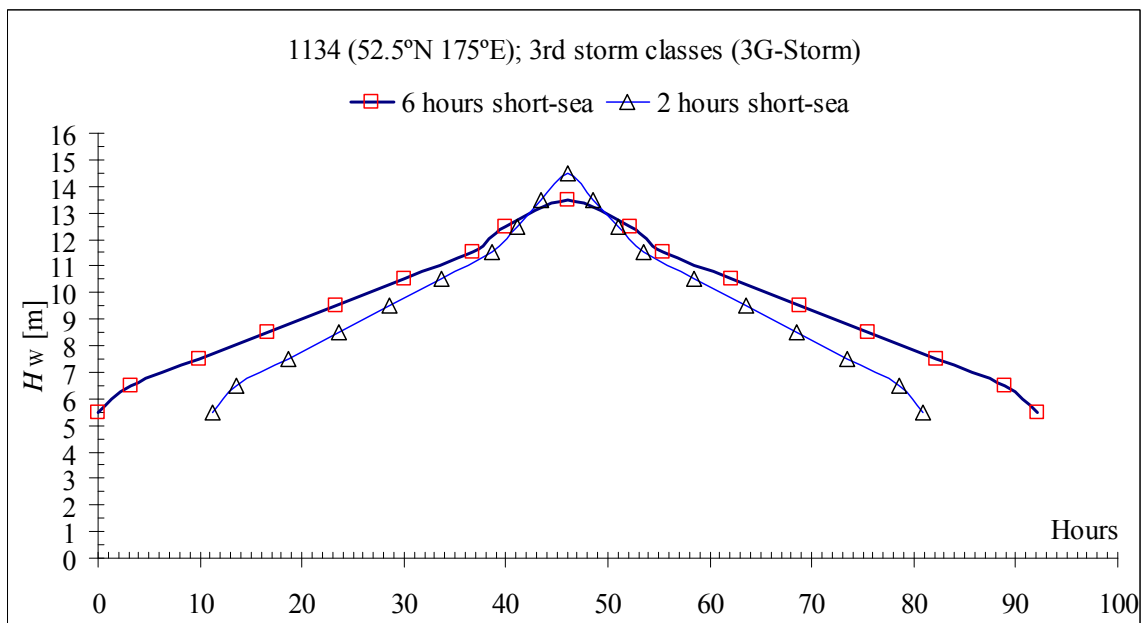
(d) 3rd storm class generated by using 3G storm profile.

Figure 4-8 H_W sequence of a chosen storm class simulated by using 2G and 3G storm profiles at point 1134 (52.5ºN 175ºE).

4.3.1.2 The exceedance probability of H_W

15 years short-sea sequences experienced by ship which sails on the chosen routes are generated. $P_{ex}(H_W)$ of simulated short-sea sequences based on 2G and 3G storm profiles with I_{OB}=2 hours and =6 hours are plotted in Figure 4-9. Figure 4-9 (a), (b), and (c) show $P_{ex}(H_W)$ for point 1018 (35ºN 145ºE), 1064 (40ºN 160ºE) and 1134 (52.5ºN 175ºE). Figure 4-9 (d) and (e) are for point 2140 (52.5ºN 40ºW) and 2193 (50ºN 30ºW). The relative frequency of local JWA hind-cast data and the regressed Weibull distribution are also plotted. Those figures show that $P_{ex}(H_W)$ shows reasonable agreement with JWA hind-cast data and those Weibull approximation regardless storm model generation and I_{OB}. This result means that 2G and 3G storm profiles satisfy long-term joint probability distribution of H_W and T_W.
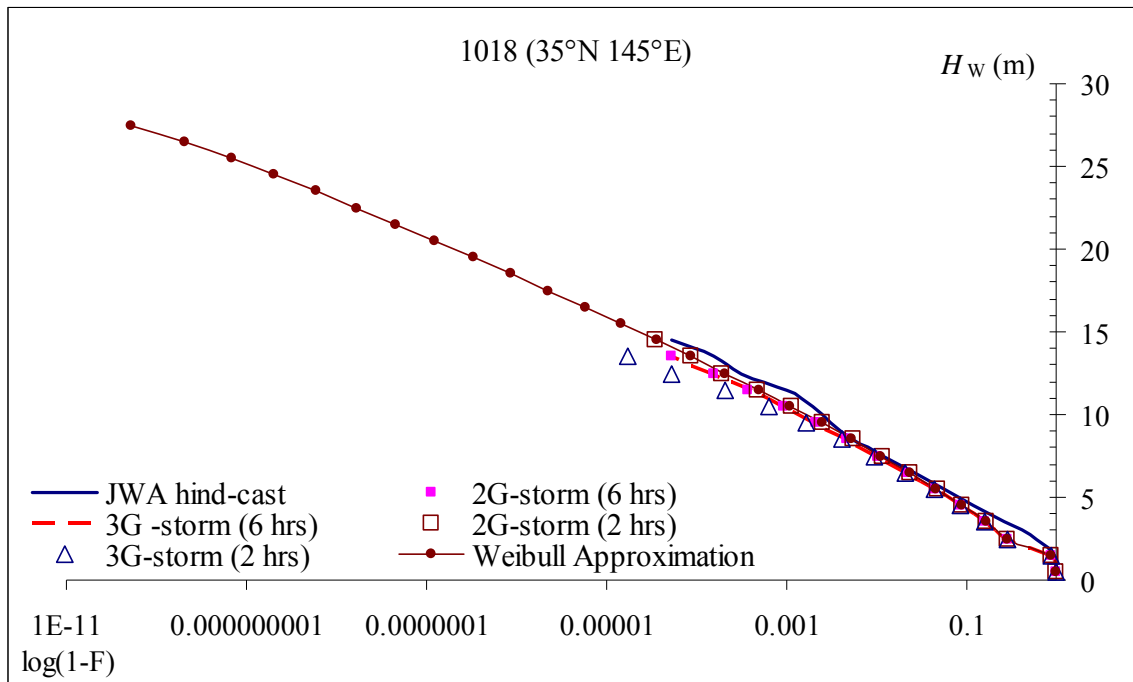
(a) Point 1018 (35ºN 145ºE)
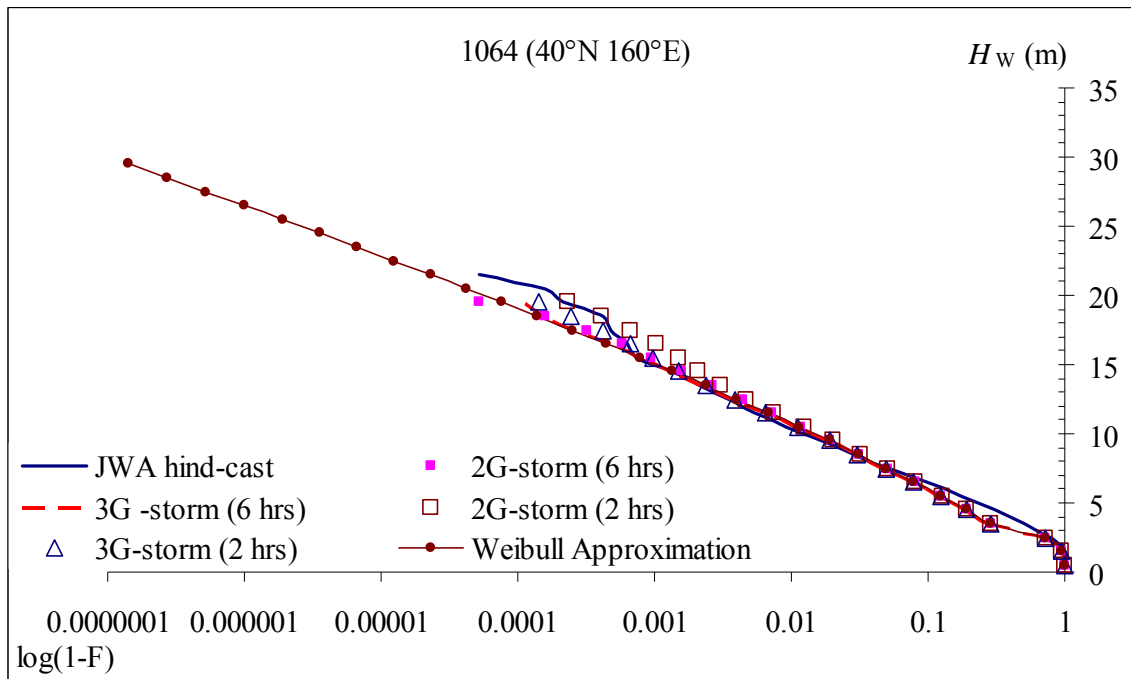
(b) Point 1064 (40ºN 160ºE)
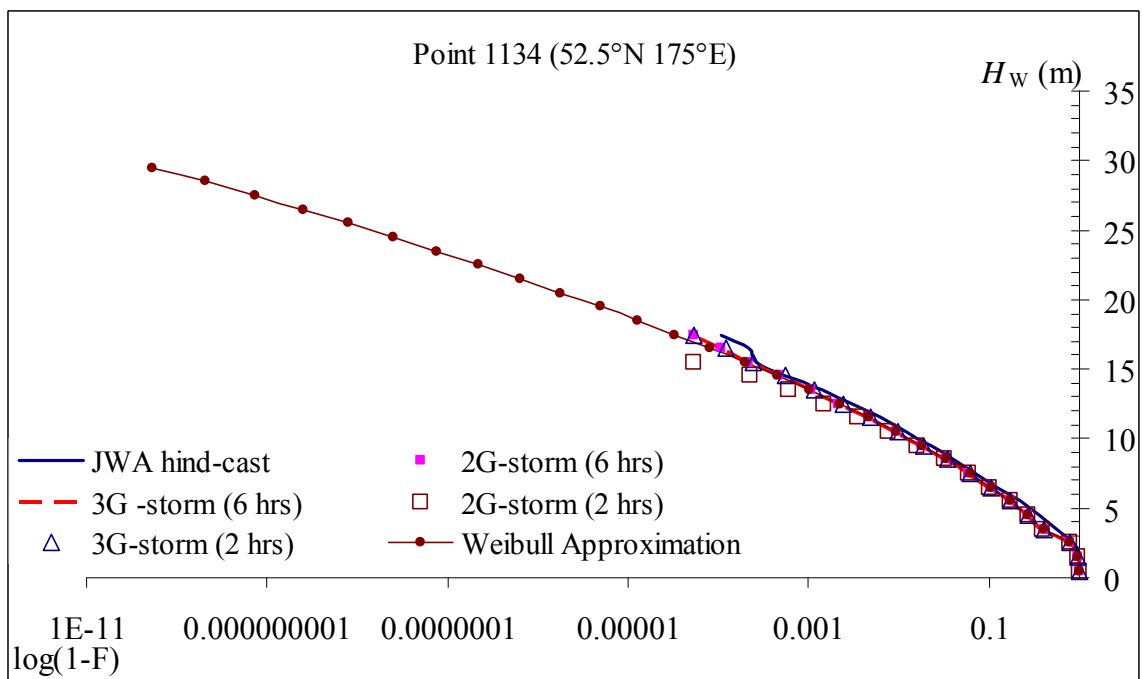
(c) Point 1134 (52.5ºN 175ºE)
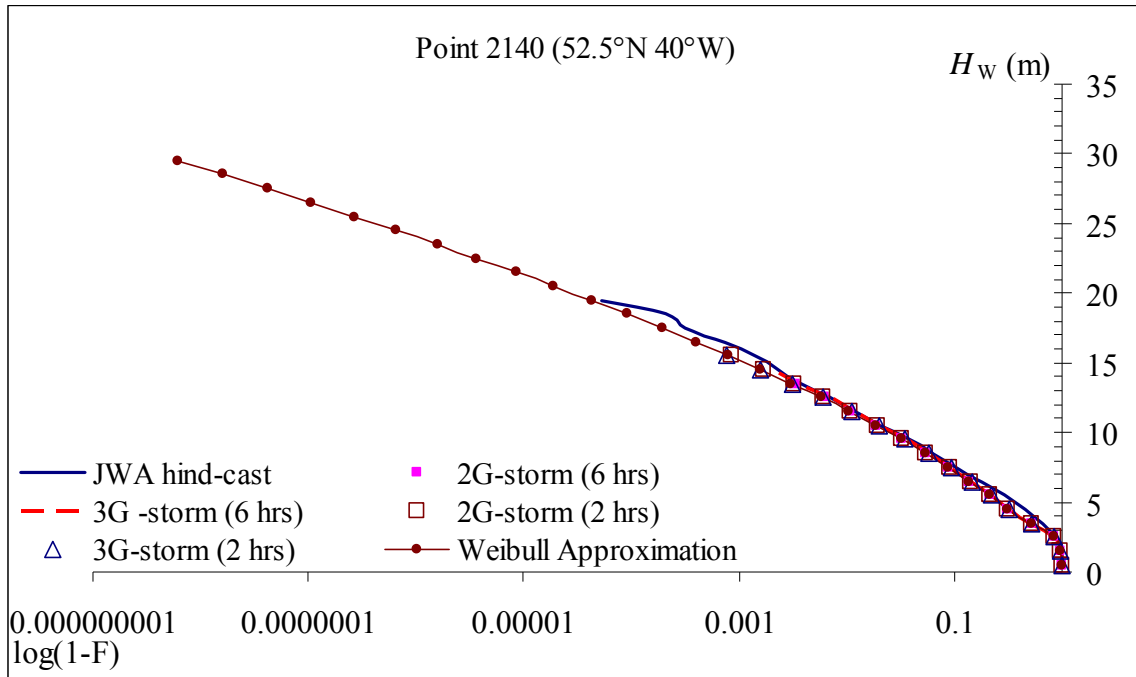
(d) Point 2140 (52.5ºN 40ºW)
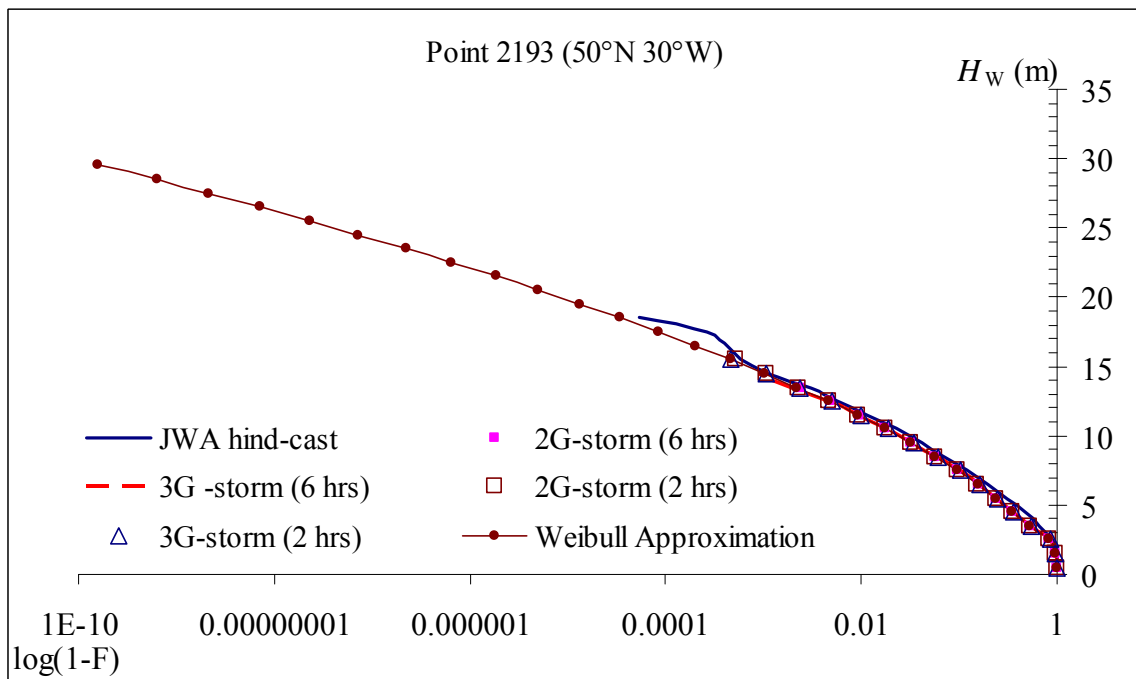
(e) Point 2193 (50ºN 30ºW)

Figure 4-9 H_W's exceedance probability at the chosen points in North Pacific and North Atlantic Oceans.

4.3.1.3 Occurrences frequency of storm classes

The comparison of occurrences frequency of storm classes of simulations and the local source data are shown in Figure 4-10 and Figure 4-11. Figure 4-10 (a), (b), (c), (d) and (e) show data at point 1018 (35ºN 145ºE), 1064 (40ºN 160ºE), 1134 (52.5ºN 175ºE), 2140 (52.5ºN 40ºW) and 2193 (50ºN 30ºW). Figure 4-11(a), (b) and (c) show occurrence frequency of storm classes for Kobe to/from Portland (see Figure 4-1(a)) and Boston to/from Rotterdam (Figure 4-1(b)) routes. Simulation results for both 2G-storm and 3G-storm in which I_{OB}=2 hours and 6 hours are used to configure storm profiles, are plotted in these figures. The frequencies of the hind-cast data are calculated by classifying ETS as described in section 4.1. These figures show that the frequency occurrences of 2G-storm and 3G-storm are about the same with those of hind-cast data. It is also shown that the difference in simulation results with different storm model generation and I_{OB} are negligible. This means that 2G and 3G profiles satisfy occurrence frequency of storm classes.
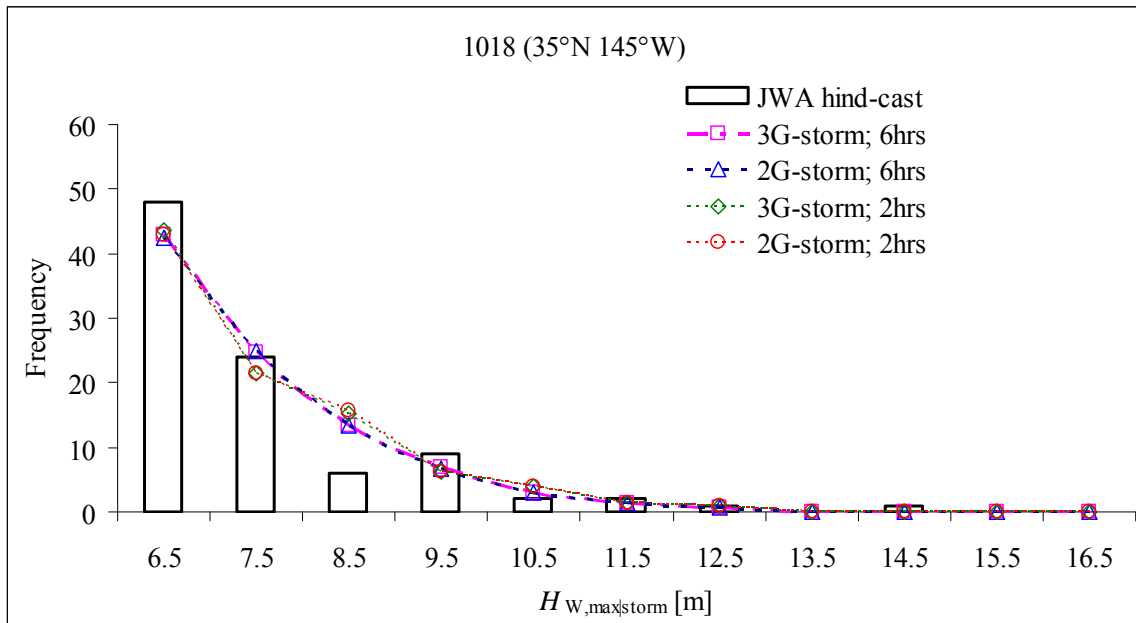
(a) Point 1018 (35ºN 145ºE).
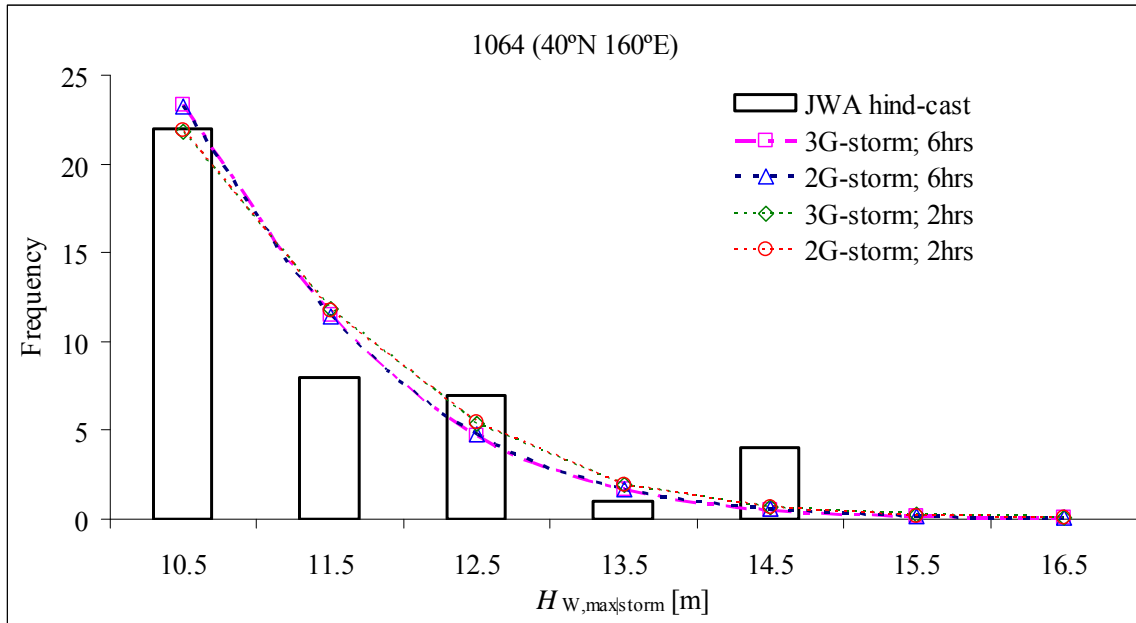
(b) Point 1064 (40ºN 160ºE).
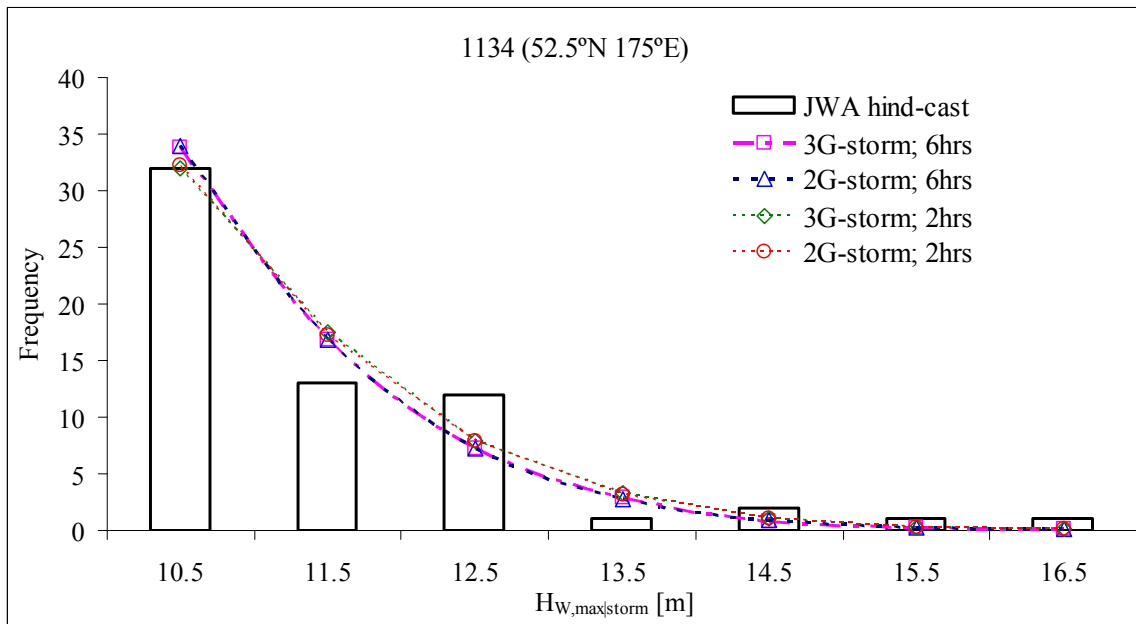
(c) Point 1134 (52.5ºN 175ºE).
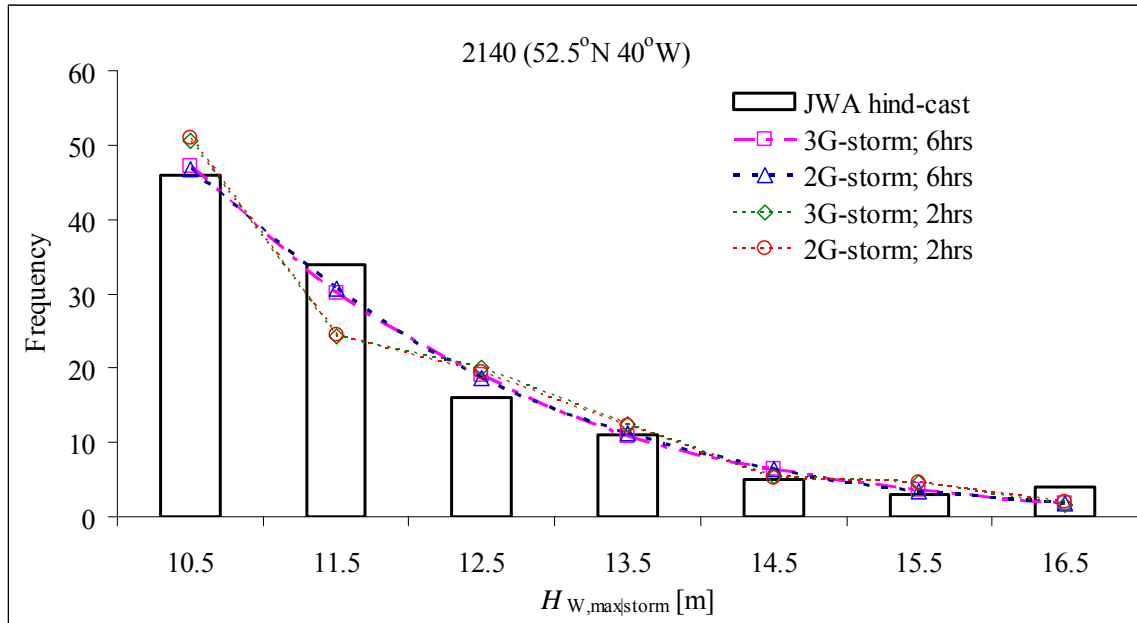
(d) Point 2140 (52.5ºN 40ºW).
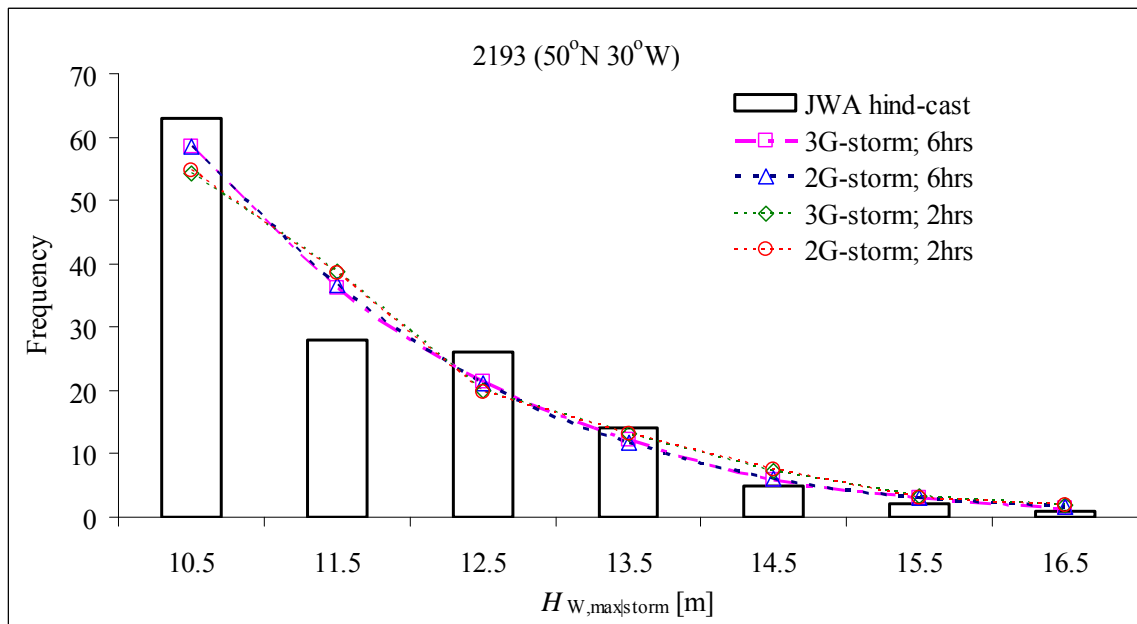
(e) Point 2193 (50ºN 30ºW).

Figure 4-10 Occurrence frequency of storm classes at chosen points in North Pacific and North Atlantic Oceans.
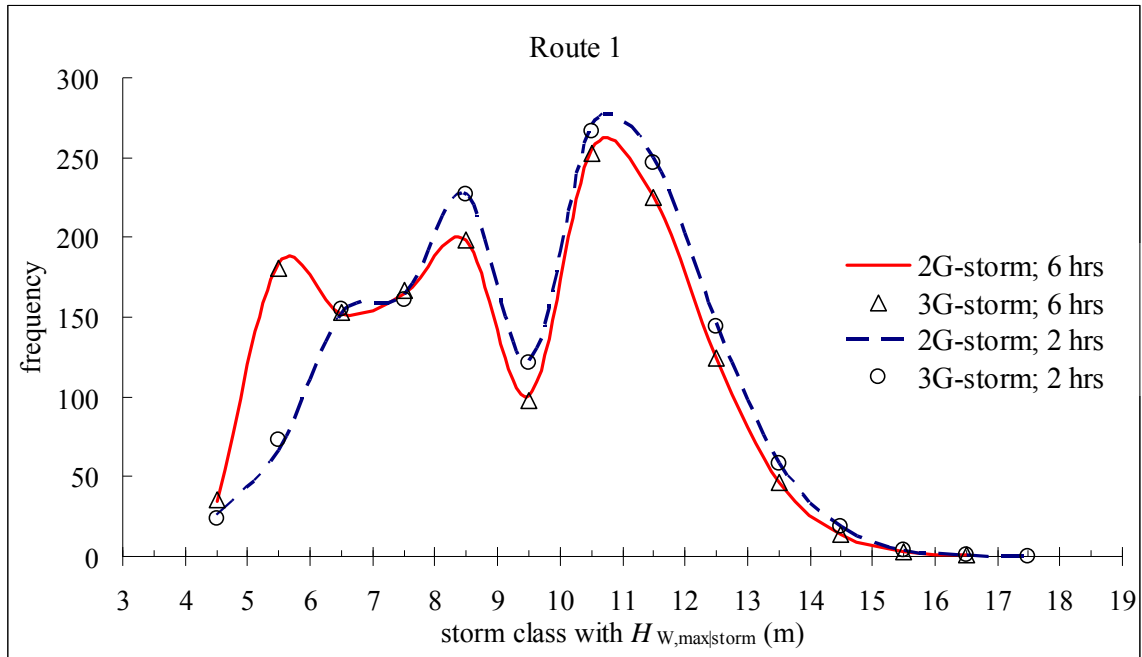
(a) Kobe to/from Portland route 1.
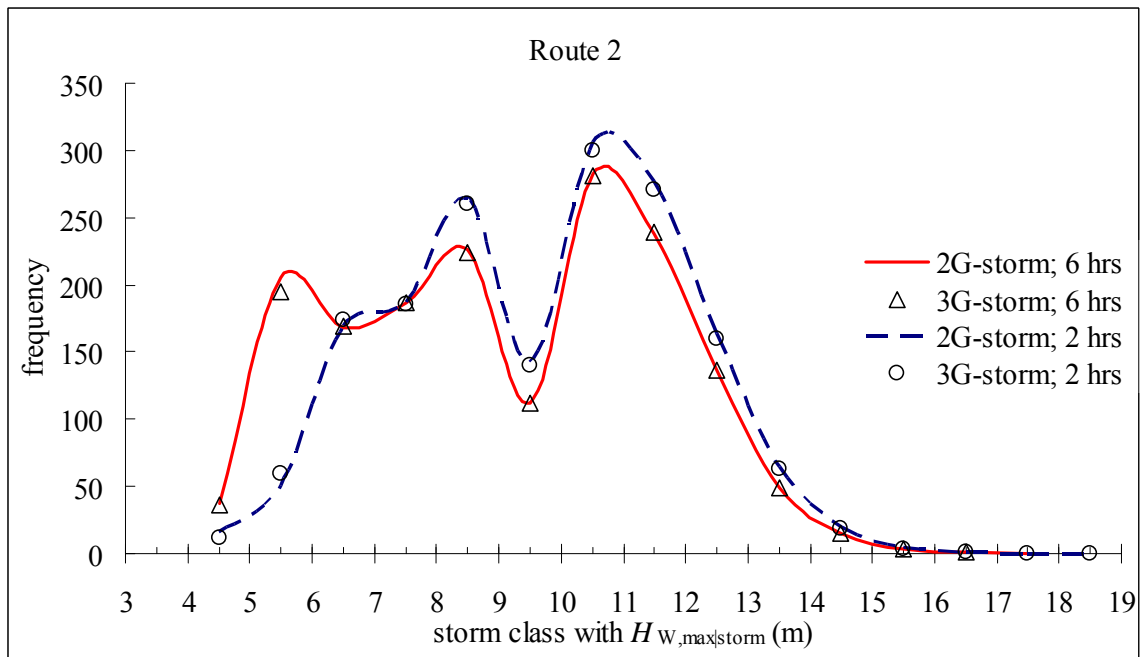
(b) Kobe to/from Portland route 2.
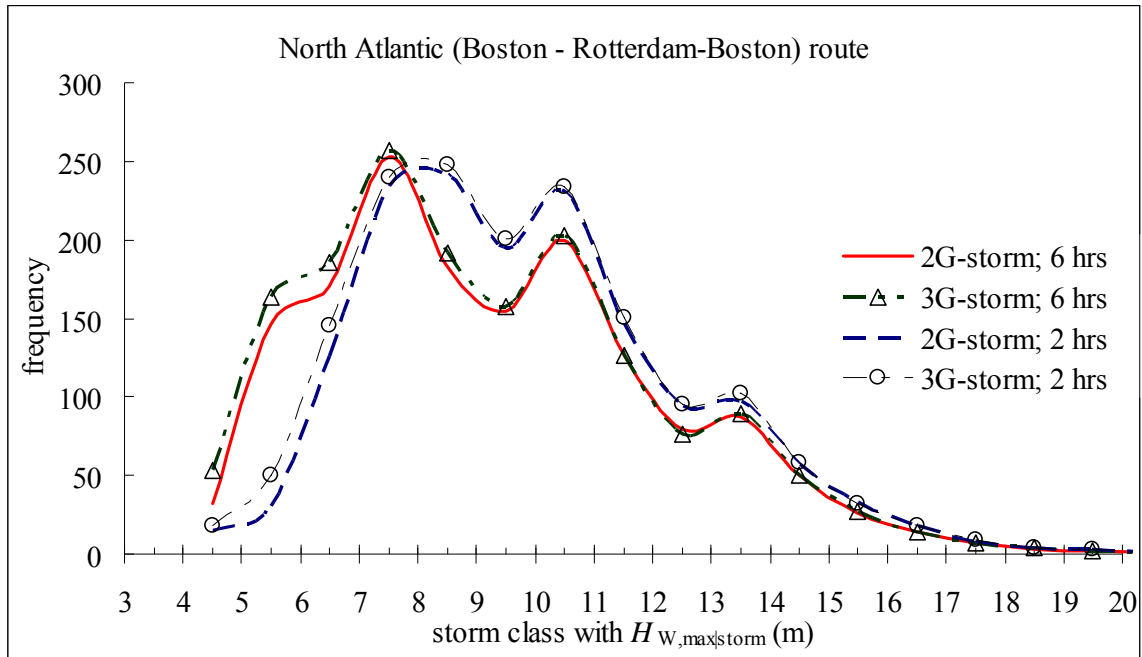
(c) Boston to/from Rotterdam route.

Figure 4-11 Occurrence frequency of storm classes for North Pacific (Kobe to/from Portland) and North Atlantic (Boston to/from Rotterdam) routes.

4.3.1.4 Variation in storm duration

Short-sea sequences are analyzed by collecting storm duration simulated in those histories of the fictitious ship routes. Figure 4-12 shows the normalized frequency distribution of the simulated storm duration for the cases all ship routes. Figure 4-12(a) and (b) present the simulation results of Kobe to/from Portland routes and Figure 4-12(c) is that of Boston to/from Rotterdam route. Both of regressed normal distribution determined (dash lines) and the data of JWA hind-cast (solid lines) in the fictitious routes are plotted. These figures show that the simulation results are acceptable agreement with that of regressed normal distribution and JWA hind-cast data.

The mean storm duration of simulation results for the cases of Kobe to/from Portland routes are 3.47 days. They are approximately equal to the mean duration of North Pacific Ocean's JWA hind-cast (3.398 days). The mean storm duration for Boston to/from Rotterdam also show acceptable agreement with that of North Atlantic Ocean' JWA hind-cast (3.988 days). These results show that the statistical nature of the simulated short-sea sequences is about the same as that of original JWA hind-cast data. The 2G and 3G storm profiles have capability to reproduce statistical nature of storm duration in real Ocean: mean value of storm duration for 2G-storm and probability distribution of storm duration for 3G-storm.
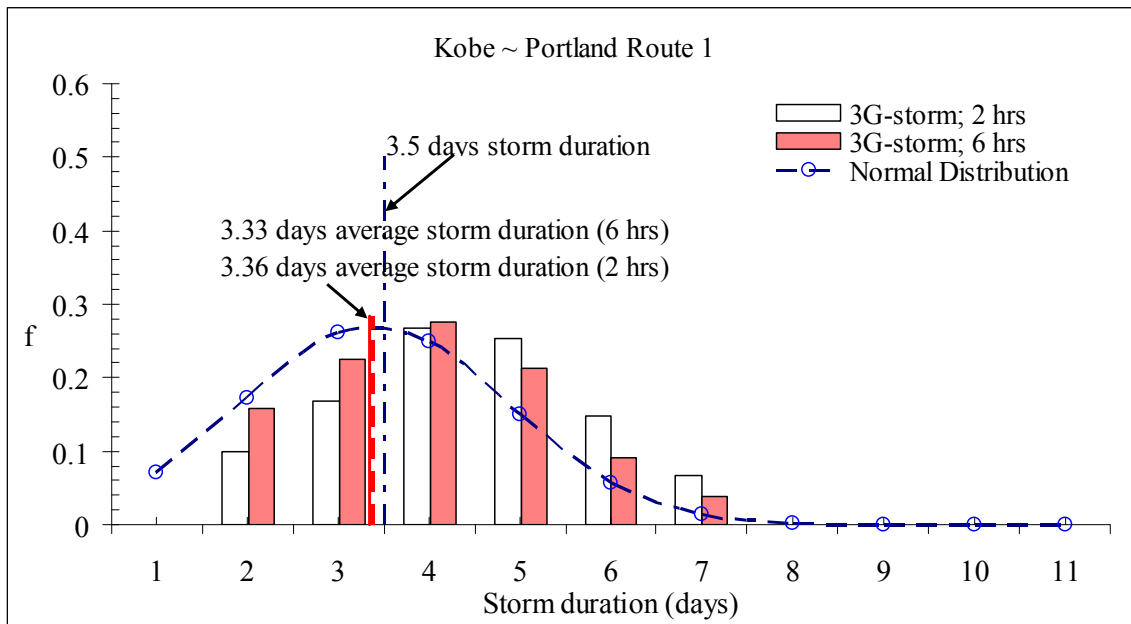
(a) Kobe to/from Portland route1.
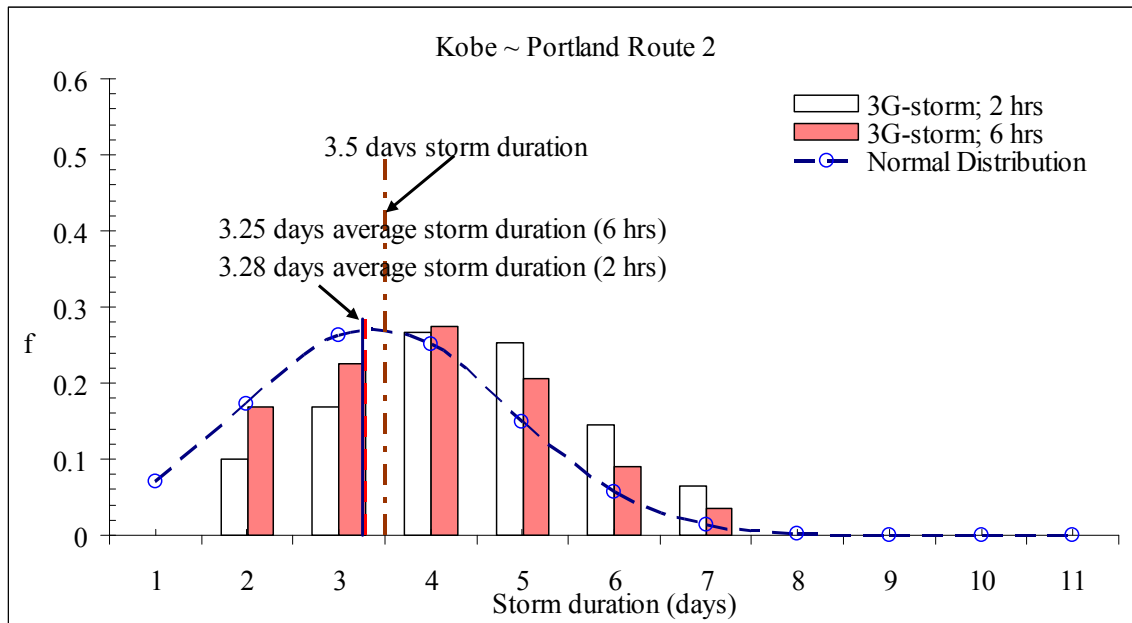
(b) Kobe to/from Portland route 2.
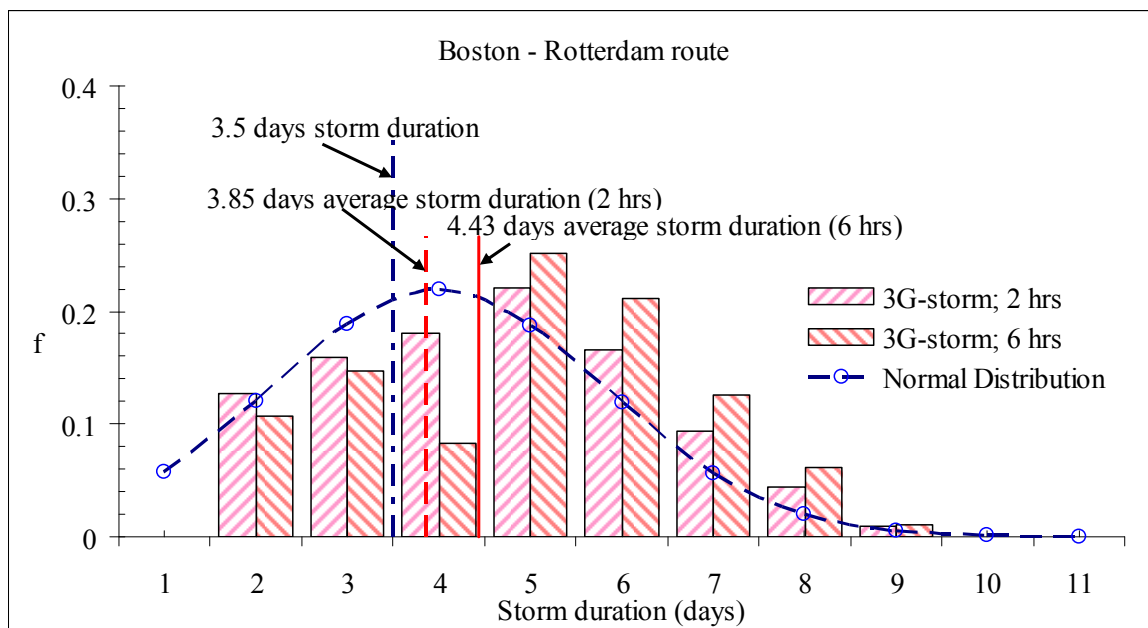
(c) Boston to/from Rotterdam route.

Figure 4-12 Probability distribution of storm duration for all fictitious ship routes.

4.3.2   Stress history generation

Let S_a and $P_{ex}(S_a)$ be the stress range on each individual waveform and its long-term exceedance probability. S_a sequences are simulated so that the stress energy spectrum are calculated by using the stress RAO of a bulk carrier's web-stiffened cruciform weld joint which is supplied by shipbuilding company. It is assumed that the wave-induced load is applied on plate and the stress concentration factor on structure detail, K_S, becomes one (1).
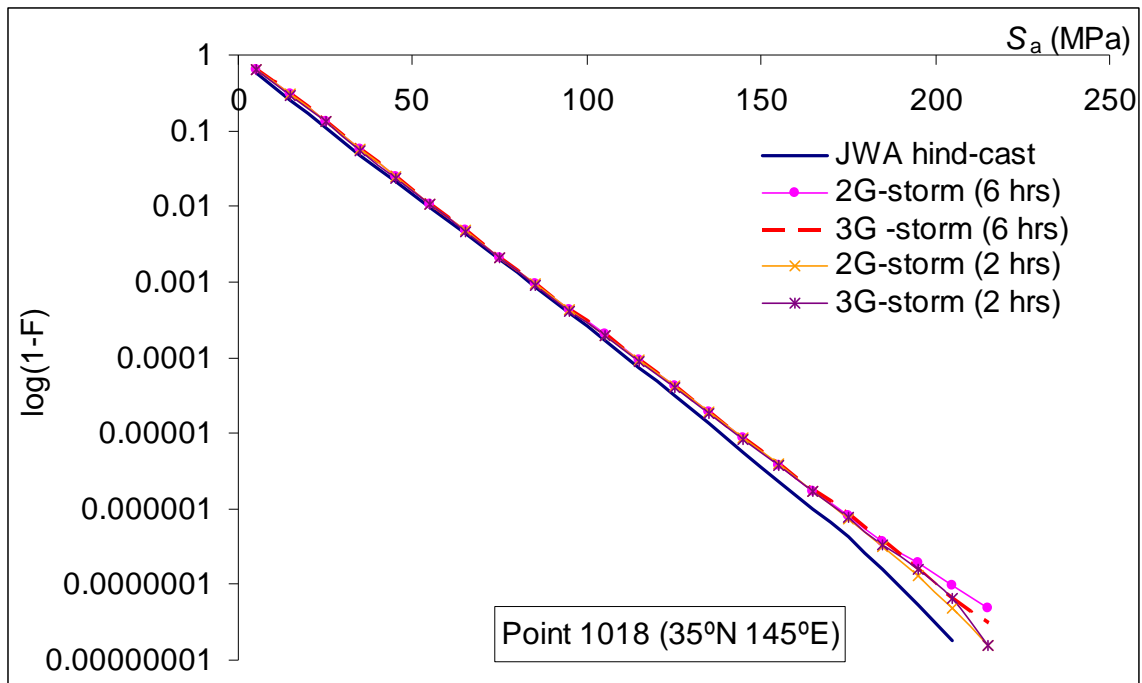
(a) Point 1018 (35ºN 145ºE).
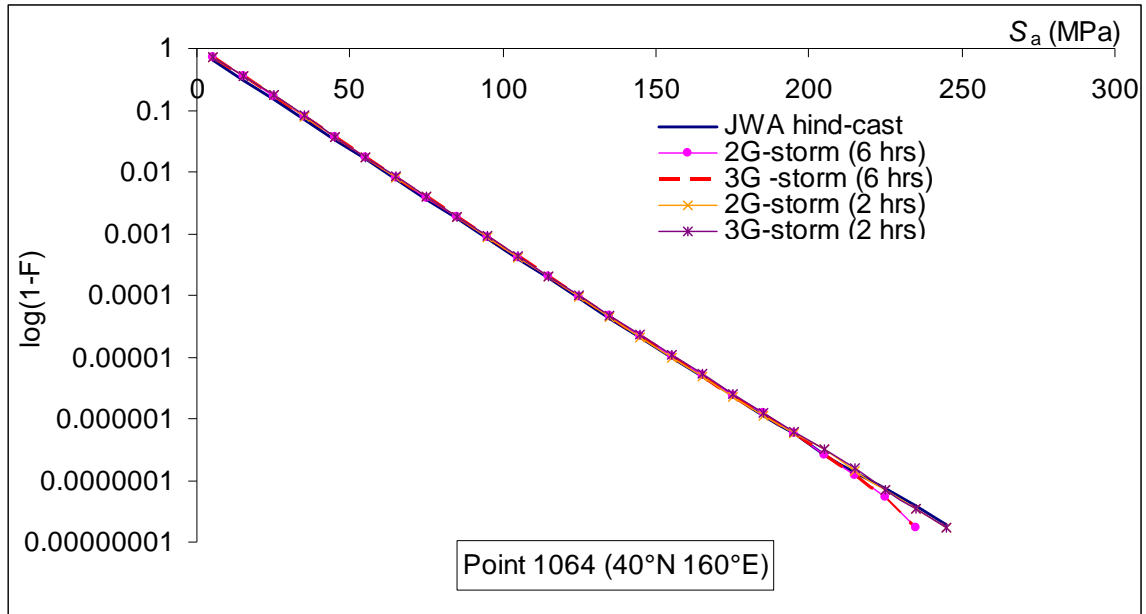
(b) Point 1064 (40ºN 160ºE).
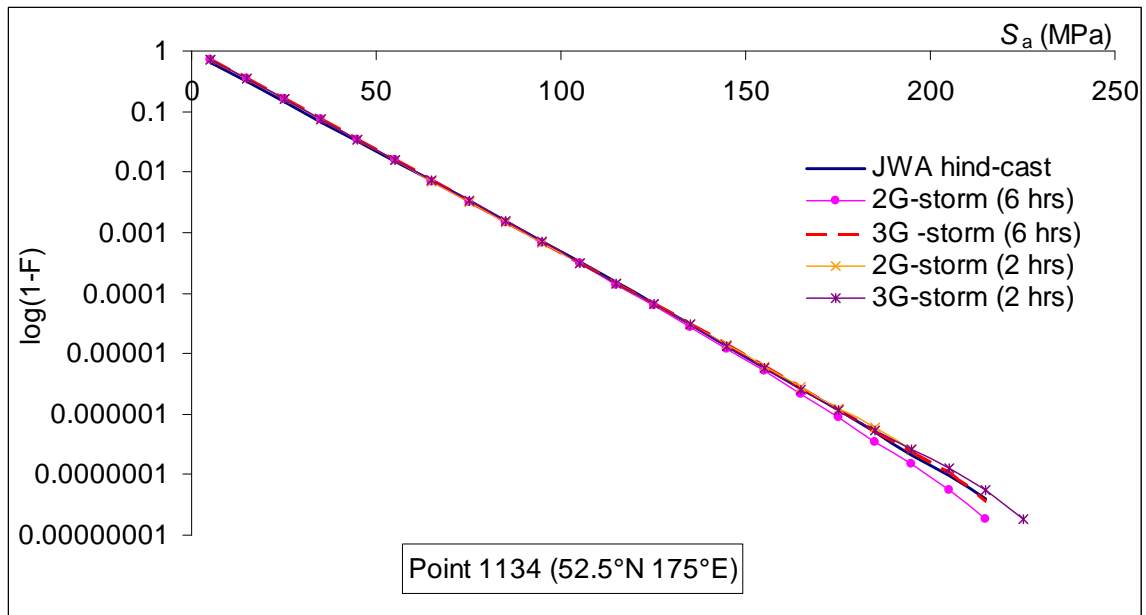
(c) Point 1134 (52.5ºN 175ºE).
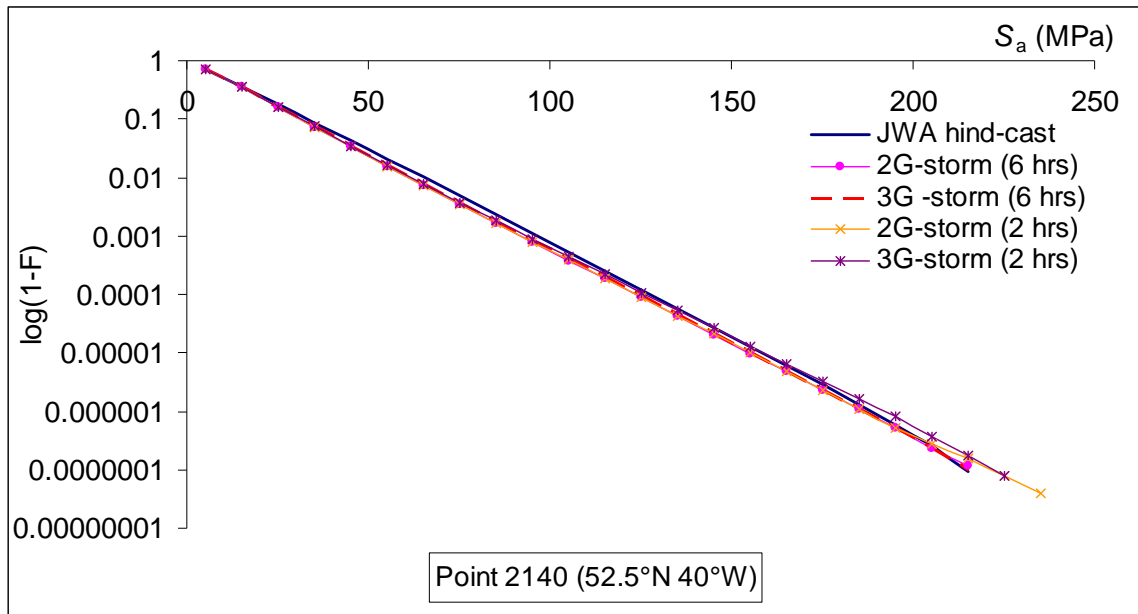
(d) Point 2140 (52.5ºN 40ºW).
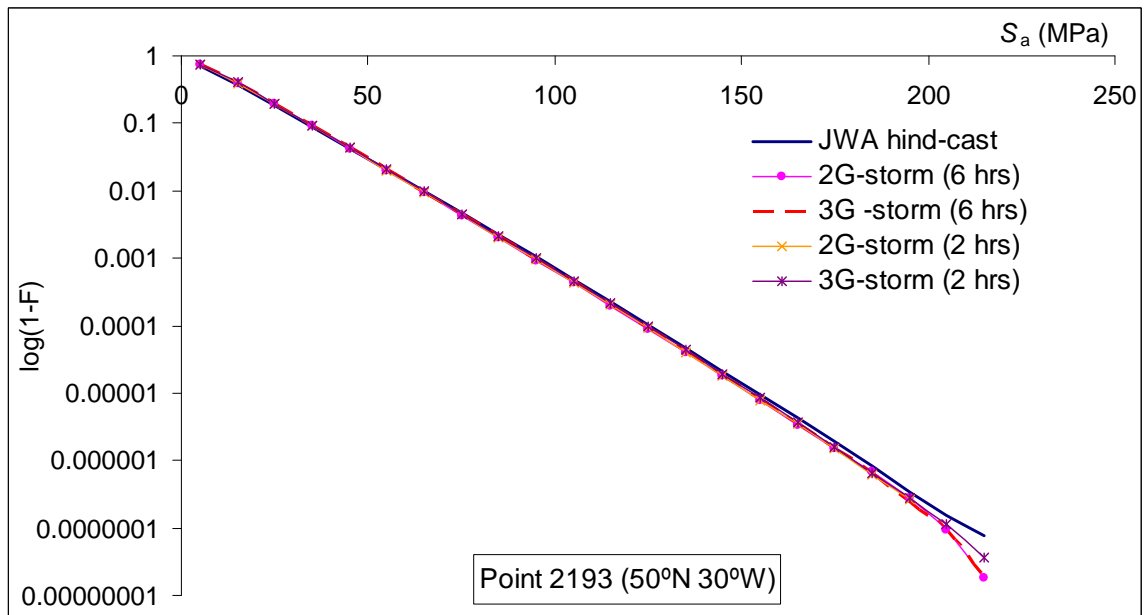
(e) Point 2193 (50°N 30°W).

Figure 4-13 Long-term exceedance probability of stress-range of the locations in North Pacific and North Atlantic Oceans.

Figure 4-13 shows $P_{ex}(S_a)$ for chosen points simulated according to the procedure described in section 3.2. Figure 4-13(a), (b), (c), (d) and (e) are show $P_{EX}(S_a)$ of point 1018 (35ºN 145ºE), 1064 (40ºN 160ºE), 1134 (52.5ºN 175ºE), 2140 (52.5ºN 40ºW) and 2193 (50ºN 30ºW). Simulation results by using 2G and 3G storm models with I_{OB}=2 hours and =6 hours are presented in these figures. $P_{ex}(S_a)$ calculated from the source hind-cast wave histories and the random number selection ship's heading angle also presented for reference. These figures show that $P_{ex}(S_a)$ derived by using 2G and 3G storm profiles are good agreement with that from the source hind-cast data regardless of I_{OB}.

From all results, it can be conclude that the 2G and 3G storm models developed in these report posses following capabilities:

i)   They can be coupled with the sea keeping theory;

ii) Long-term joint probability of H_W and T_W of the source data can be reproduced;

iii) Statistics characteristics of distribution of storm/rough sea duration (mean value of storm duration for 2G model only and the mean storm duration and its probability distribution for 3G model);

iv) Relation between, $H_{W,max|storm}$ and the storm's occurrence probability (frequent distribution of storm class) recorded in the source data can be emulated.

v)   Long-term probability of wave-induced stress, which is generated by a ship on given route, can be reproduced.

vi) Equivalent short-sea sequence can be generated from the data with arbitrary observation period.

5 STORM MODEL IN VARIOUS APPLICATIONS

The capability of storm model is advanced by taking into account the variation of storm duration in which the storm profiles are configured with different I_{OB} and the detailed procedures are confirmed in chapter 4. The advanced (new generation) storm model is improved by examined the observed wave data provided by Japan Weather Association (JWA). Two types' storm profiles are configured, (a) with constant storm duration (2G storm profile, 2G-storm) and (b) with variation storm duration (3G storm profile, 3G-storm). An example of fatigue assessment is demonstrated on a surface crack in a weld of a bulk carrier, which sails in North Atlantic Ocean. Two different approaches in fatigue assessment are utilized; 1) fatigue crack propagation analysis, and 2) Cumulative fatigue damage S-N approach. Crack growth in fatigue crack propagation analysis use two laws: a) modified Paris-Elber rule and FASTRAN II program.

5.1 Fatigue assessment of a ship structure member

As discussed in chapter 4, the new generation (3G) storm model is developed. 3G storm model is validated against the source hind-cast data and its predecessor in the emulated capability to reproduce loading sequence as in real Ocean. The effect of those loading sequence in fatigue assessment based on fatigue crack propagation analyses can be described based on that used in simulations.

The fatigue assessment based on fatigue crack propagation analyses of a surface crack in a bulk carrier's web-stiffened cruciform weld joint at bottom of a lower stool (see Figure 5-1) is conducted by using the stress sequence experienced by a ship which

sails on the Boston to/from Rotterdam route (see Figure 4-1(b)). Following two types of stress sequences are used in the simulations: a) S_a sequence derived from the source hind-cast wave sequence (H_W and T_W), JWA hind-cast; b) S_a sequence derived by using 2G storm (2G) and 3G storm (3G) profiles. Simulations are carried out by using storm profiles with I_{OB}=2 hours and 6 hours. In this analyses, the stress's energy spectrums are calculated by using the stress RAO of the weld joint, which was determined in Japanese Ship research Panel 219 research project (SR219, 1996)[29] (see Figure A1.1). The crack propagation analyses are proceed until the crack depth exceeds the main plate thickness, t=20mm.
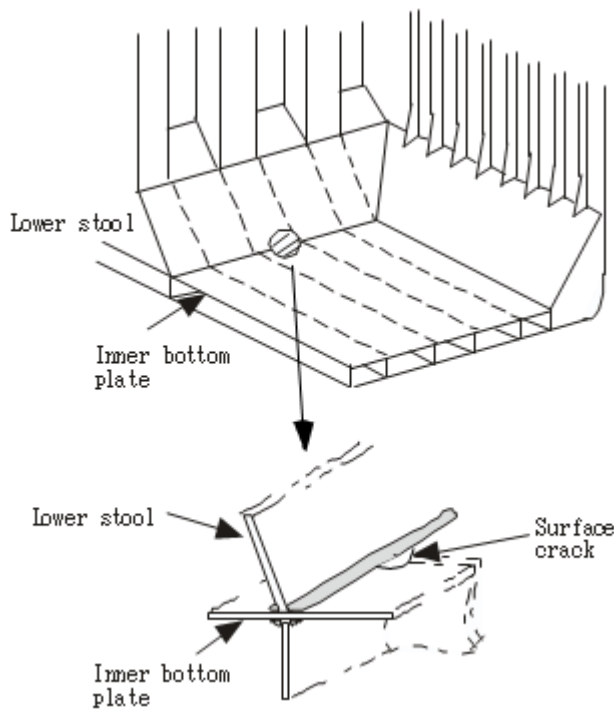
Figure 5-1 Target ship structure for fatigue assessment.

Figure 5-2 shows the comparison of $P_{ex}(S_a)$ for the chosen route and chosen periods (5.5 years) derived from 2G and 3G storm profiles with I_{OB}=2 hours and 6 hours. $P_{ex}(S_a)$ derived from source hind-cast data is also presented in this figure. This figure

shows that $P_{ex}(S_a)$ of source hind-cast data has good agreement with that of storm profiles regardless I_{OB}. Let $\bar{h}_W$ and $\bar{s}_a$ be normalized individual wave height and normalized stress amplitude. These values are normalized by the once-in-(128) trials values of h_W and S_a. Figure 5-3 shows the relative frequency of $\bar{h}_W$ and $\bar{s}_a$ of each trial calculated by using 3G-storm with I_{OB}=6 hours. It is shown that the difference in $\bar{s}_a$'s frequency of individual trial is much smaller than that of $\bar{h}_W$. It is supposed that this difference arises from large variance in stress RAO shown in figure A1.1.
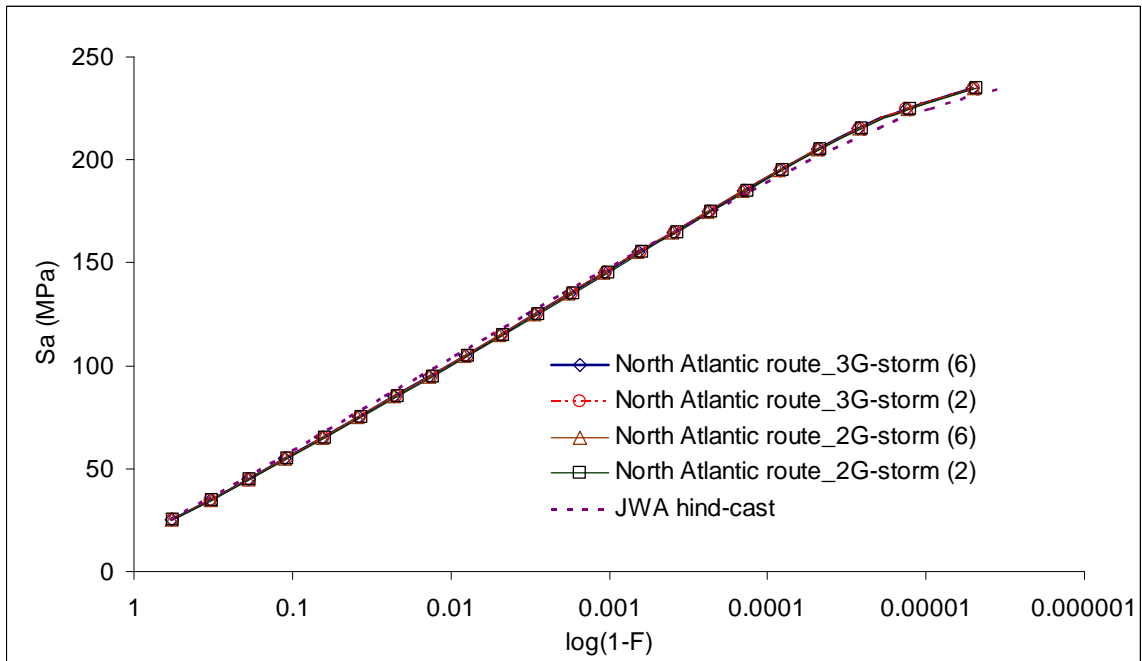
Figure 5-2 5.5 years S_a's exceedance probability experienced by a ship which sails in Boston to/from Rotterdam route.
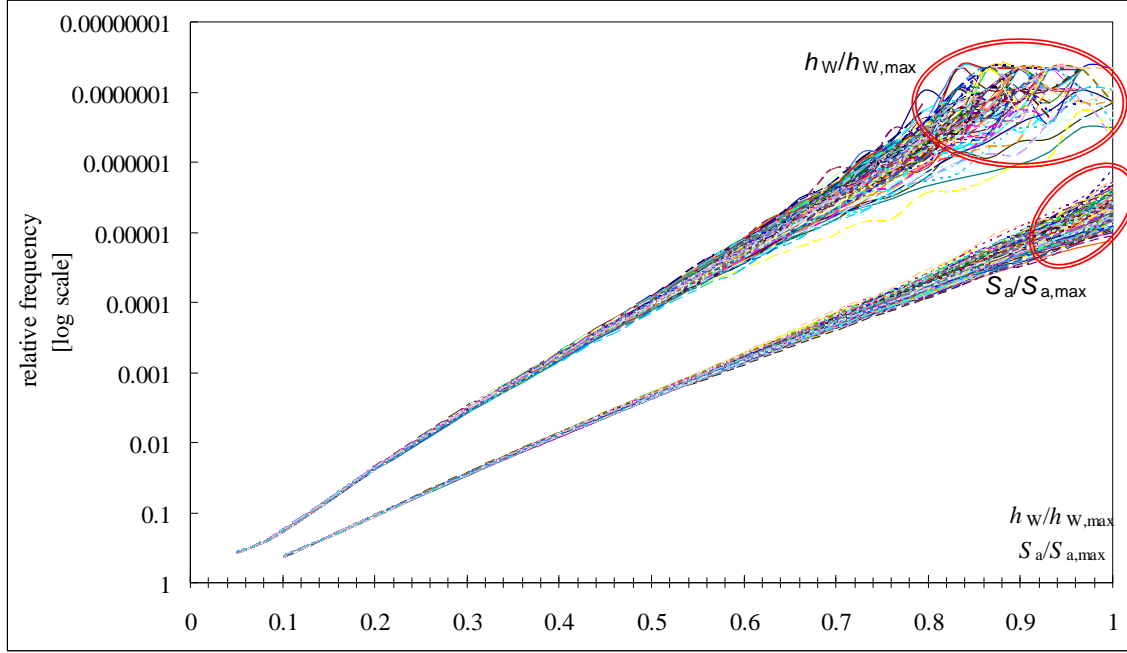
Figure 5-3 The relative frequency of normalized h_W and S_a of each trial (128 trials) calculated by using 3G-storm with I_{OB}=6 hours.

Fatigue crack propagation is simulated by applying two different crack growth laws: the modified Paris-Elber rule and FASTRAN II program, which is based on modified Dugdale model (Newman, 1981, 1992[25-26]). Hereafter, the modified Paris-Elber rule is called 'conventional law' given as:

$$\frac{da}{dN} = C\left\{\left(K_{max} - K_{op}\right)^m - \left(\Delta K_{eff}\right)_{th}^m\right\} \tag{5.1}$$

$$K_{op} = \begin{cases} -30.6 & K_{max} \leq -31.5 \text{ MPa.m}^{1/2} \\ 0.75 * K_{max} - 7 & -31.5 \text{ MPa.m}^{1/2} < K_{max} < 38.5 \text{ MPa.m}^{1/2} \\ 21.9 & K_{max} \geq 38.5 \text{ MPa.m}^{1/2} \end{cases} \tag{5.2}$$

$$SIF = K_s.M_k.\left(S_m.F_m\left(c,a,t\right) + S_b.F_b\left(c,a,t\right)\right)\sqrt{\pi a} \tag{5.3}$$

where, C and *m* are the material parameters. K_{max} and K_{op} are maximum stress intensity factor and crack opening stress intensity factor. K_{op} are obtained by using engineering formula proposed in Japanese Ship Research panel 245 Project (SR245, 2001[30]).

$(\Delta K_{\text{eff}})_{\text{th}}$ is the effective stress intensity factor. K_s is the stress concentration factor of structural detail, and it can be calculated by finite element direct calculation or by using the engineering formula provided by classification society rules. M_k, F_b and F_m are correction factor for weld base and finite plate size, and they are presented in SR219 report (1996)[29]. S and S_a are applied stress and its stress range. In FASTRAN II program, crack growth is formulated as:

$$\frac{da}{dN} = C\left(\Delta K_{eff}\right)^m \frac{\left[1 - \left(\frac{\Delta K_0}{\Delta K_{eff}}\right)^2\right]}{\left[1 - \left(\frac{K_{max}}{C5}\right)^2\right]} \tag{5.4}$$

$$\Delta K_0 = \left(\Delta K_{eff}\right)_{th}\left(1 - C4 \times \frac{S_{min}}{S_{max}}\right) \tag{5.5}$$

$$\Delta K_{eff} = \left(K_{max} - K\left(S_X\right)\right) \tag{5.6}$$

$$S_X = \begin{cases} S_0^{'} & S_0^{'} > S_{min} \\ S_{min} & S_0^{'} \le S_{min} \end{cases} \tag{5.7}$$

where,

$C4$ is the threshold constant of the effective SIF, it is equal to zero;

C5 is cyclic fracture toughness or limiting value of maximum SIF;

K_{max} and $K(S_x)$ are SIF at S_{max} and SIF at applied load S_x;

S_{max} and S_{min} are the maximum and minimum applied load;

$S_0^{'}$ is the crack opening stress.

A semi elliptical surface crack with 0.2mm depth, a, and 0.4mm length, c is setup as the initial condition. In the same manner of conventional laws, SIF of surface crack for FASTRAN II program is calculated by using modified Newman-Raju formula (see

Appendix 2). Material properties are shown in Table 5-1 and they are used in both propagation laws. These properties were determined by measuring the propagation rate of fatigue cracks in the weld residual stress field (SR219, 1996)[29]. K_s is set at 2.0 in accordance with DnV CN 30.7 (2010)[5]. K_S=1.9 for cruciform joint (grounded) is modified due to the stress concentration caused by the web stiffener on the back-face. The loading condition is full ballast condition, and the mean stress is set at 25MPa in order to avoid FASTRAN II calculation error.

Table 5-1 Material parameters.

C	1.45e-11m/cycle
M	2.75
$\left(\Delta K_{eff}\right)_{th}$	2.45MPa.m$^{1/2}$

Let L_p be the crack propagation life, and D the fatigue damage accumulated before L_p. Table 5-2 and Table 5-3 show the statistical data of crack propagation life calculated by the conventional law and FASTRAN II. Table 5-4 shows the statistical data of D. In damage calculation, S-N data of DnV CN.30.7 (2010)[5] is used (see Appendix 3). Figure 5-4 shows the mean calculated crack propagation lives and its standard deviation (which presented with error bars) for various calculation conditions (different of crack growth laws, type of stress sequences generation, I_{OB}). Figure 5-5 and Figure 5-6 show frequency distributions of crack propagation lives for various conditions. Figure 5-7, Figure 5-8 and Figure 5-9 show comparison of crack propagation lives for various crack growth laws with different type of stress sequence.

Table 5-2 Crack propagation lives of North Atlantic route perform by using Modified Paris-Elber rules.

Crack Propagation Lives	Modified Paris-Elber rules				
	Hind-cast	2G Storm	3G Storm	2G Storm	3G Storm
		I_{OB}=6 hours		I_{OB} =2 hours	
Longest life	1.4739 years	1.5007 years	1.4835 years	1.4913 years	1.4888 years
Shortest life	1.3647 years	1.3640 years	1.3530 years	1.4119 years	1.4137 years
Average life	1.4191 years	1.4294 years	1.4273 years	1.4486 years	1.4525 years
Coefficient of variance (C.V)	1.48%	1.75%	1.73%	1.18%	1.23%
Ratio of 2G to 3G	--	1.001		0.997	

Table 5-3 Crack propagation lives of North Atlantic route perform by using FASTRAN II (Based on modified Dugdale model).

Crack propagation Lives	FASTRAN II				
	Hind-cast	2G Storm	3G Storm	2G Storm	3G Storm
		I_{OB} =6 hours		I_{OB} =2 hours	
Longest life	3.7788 years	4.4124 years	4.2829 years	3.5975 years	3.5705 years
Shortest life	3.3220 years	3.4767 years	3.5416 years	3.0782 years	3.1517 years
Average life	3.5224 years	3.8785 years	3.8521 years	3.3932 years	3.4049 years
Coefficient of variance (C.V)	2.77%	6.08%	5.02%	3.38%	2.52%
Ratio of 2G to 3G	--	1.006		0.997	

Table 5-4 Cumulative Fatigue damage and fatigue life perform based on DnV CN.30.7.

	Hind-cast	2G Storm	3G Storm	2G Storm	3G Storm
		I_{OB} =6 hours		I_{OB} =2 hours	
Cumulative fatigue Damage, D=$\sum \dfrac{n_i}{N_i}$	1.979	1.782	1.766	1.707	1.710
Fatigue life, FL=$\dfrac{L_D[years]}{D}$	12.62 years	14.03 years	14.15 years	14.02 years	14.62 years
Ratio of 2G to 3G	--	1.009		0.998	
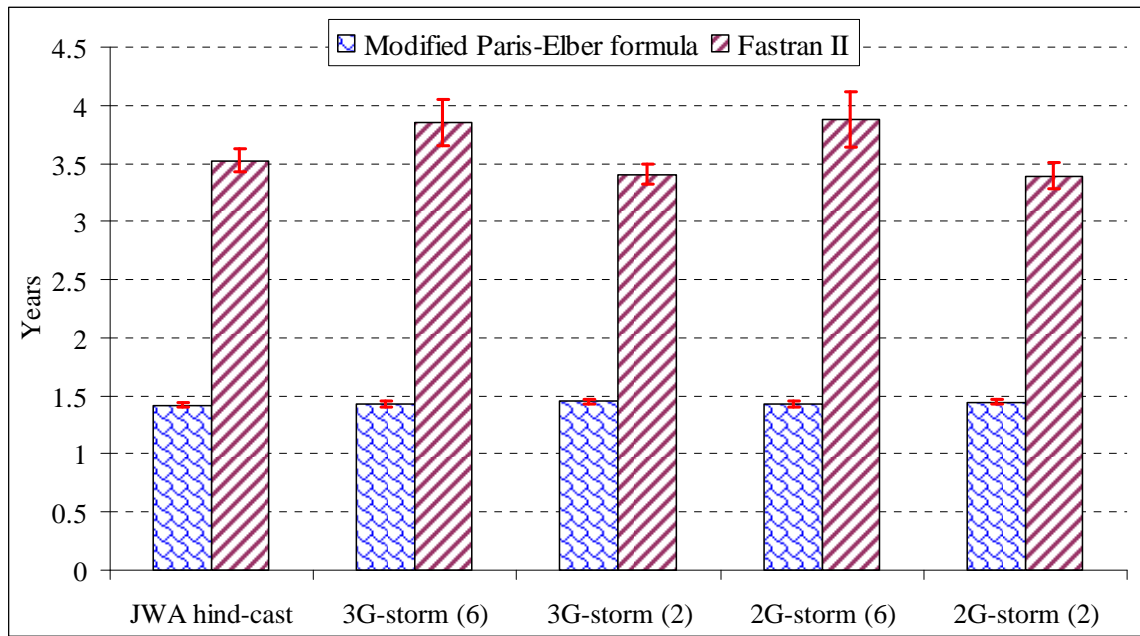
Figure 5-4 Comparison the mean calculated propagation lives that derived by modified Paris-Elber rule and FASTRAN II program.
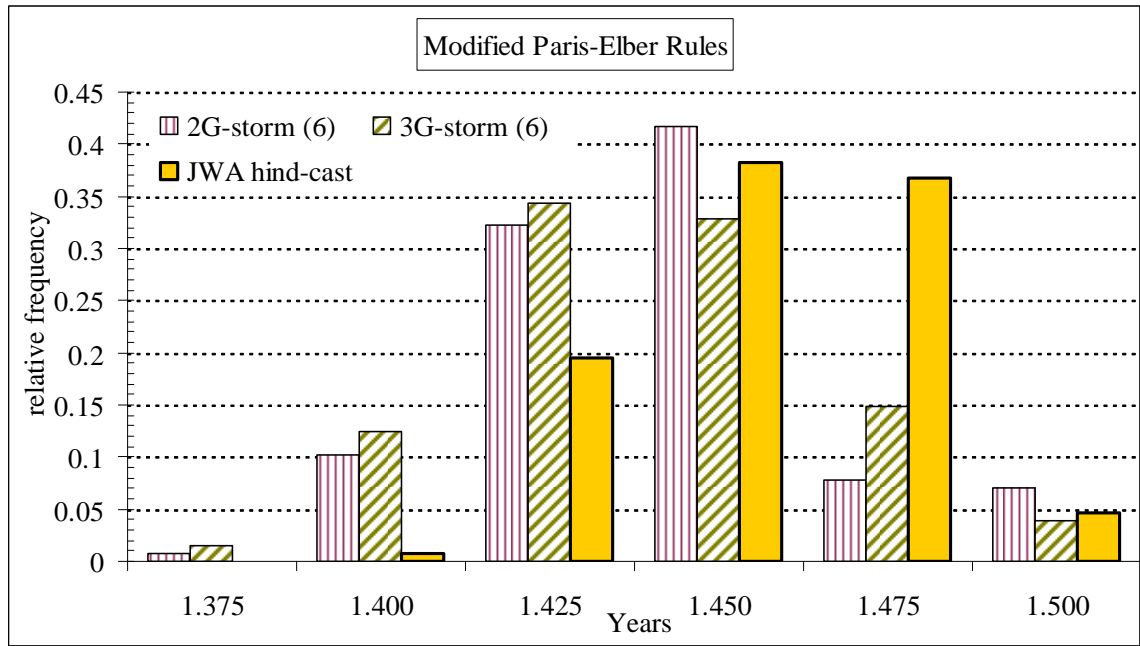
(a) I_{OB} equals to 6 hours (0.025 years/range).
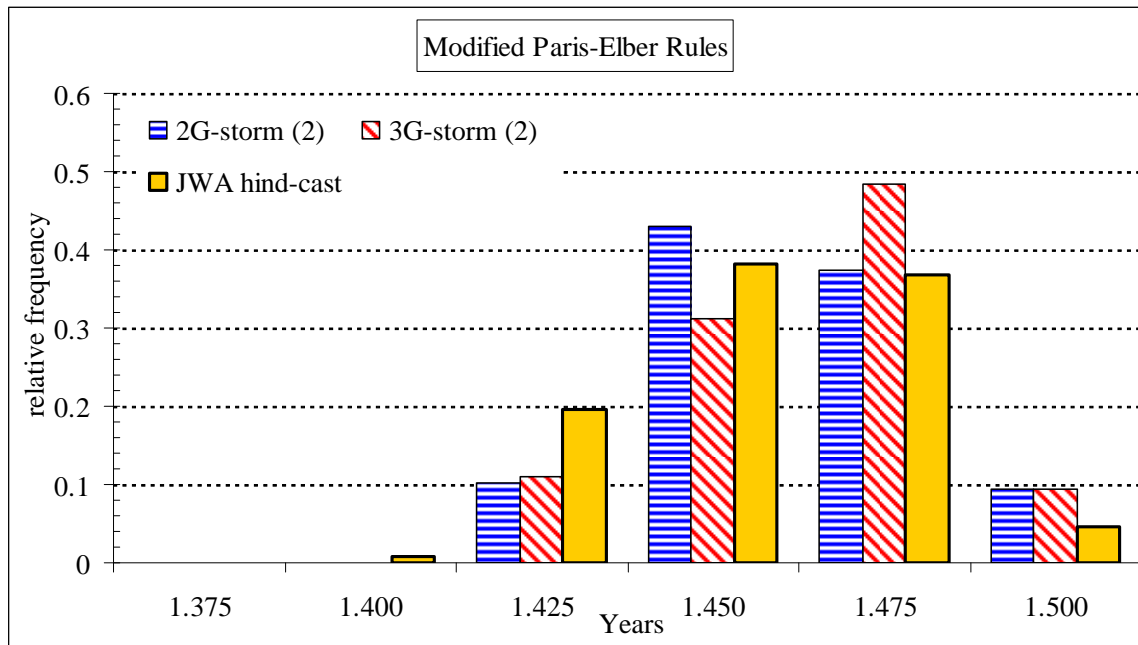
(b) I_{OB} equals to 2 hours (0.025 years/range).

Figure 5-5 Histogram of calculated crack propagation lives performed by modified Paris-Elber rule with stress sequence generated based on 2G and 3G storm profiles with I_{OB}=2 and 6 hours.
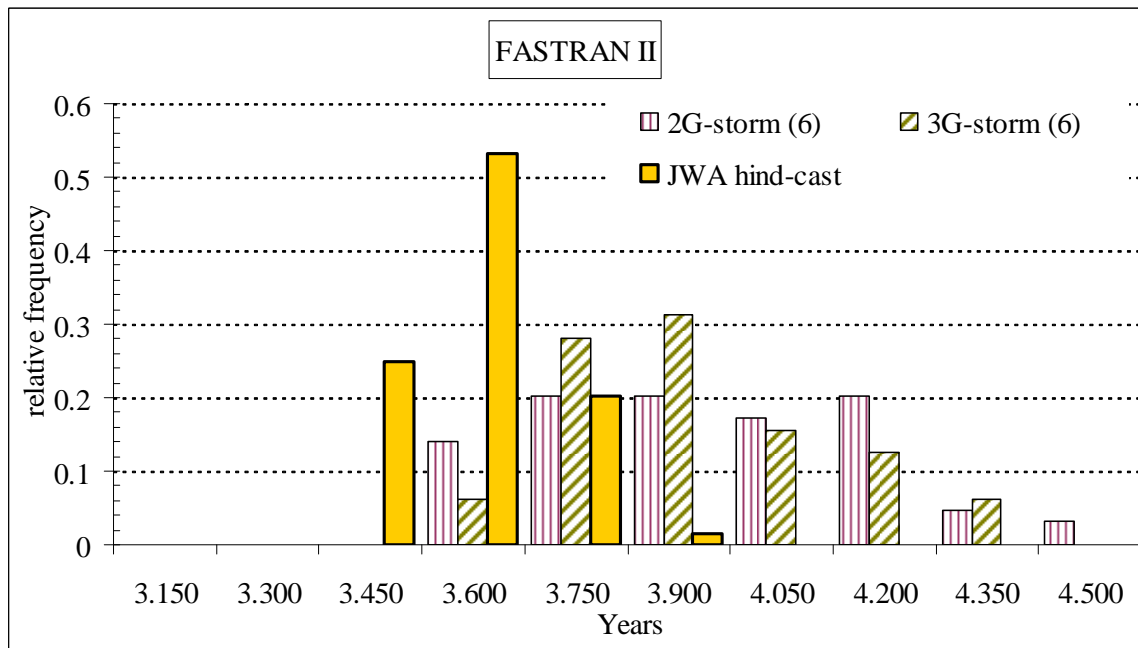
(a) I_{OB} equals to 6 hours (0.15 years/range).
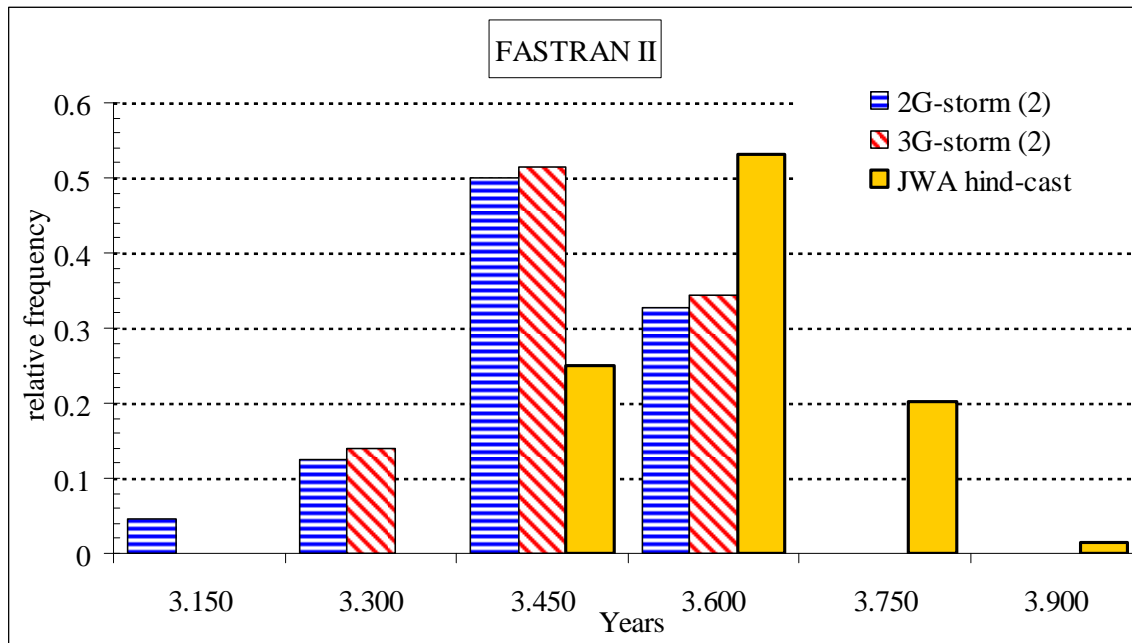
(b) I_{OB} equals to 2 hours (0.15 years/range).

Figure 5-6 Histogram of calculated crack propagation lives performed by FASTRAN II with stress sequence generated based on 2G and 3G storm profiles with I_{OB}=2 and 6 hours.
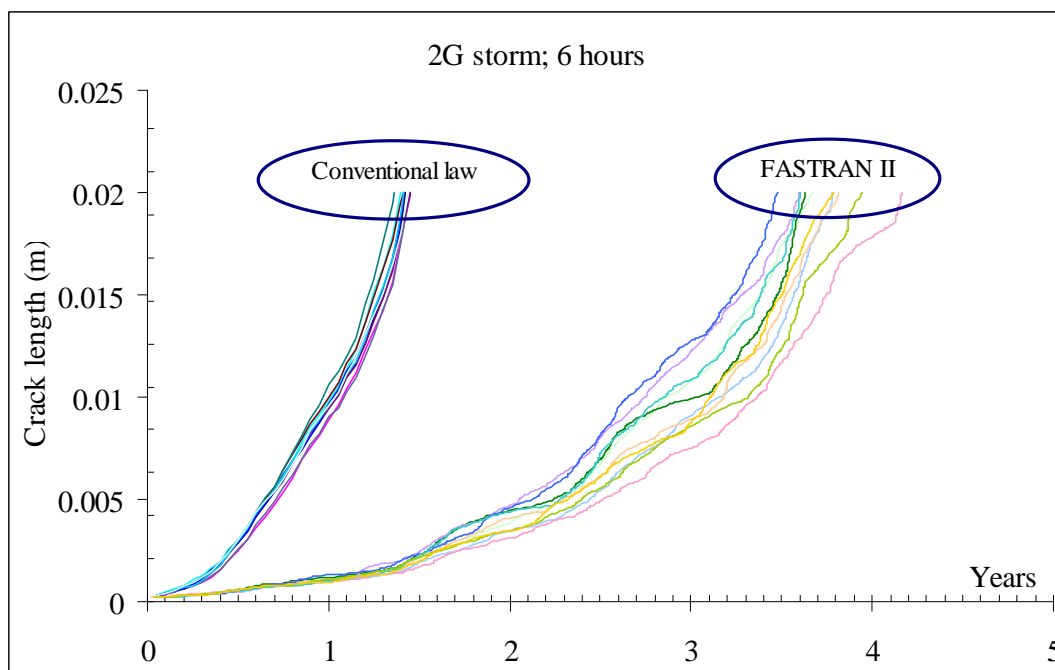
(a) Stress sequences derived by using 2G storm profiles with I_{OB}=6 hours.
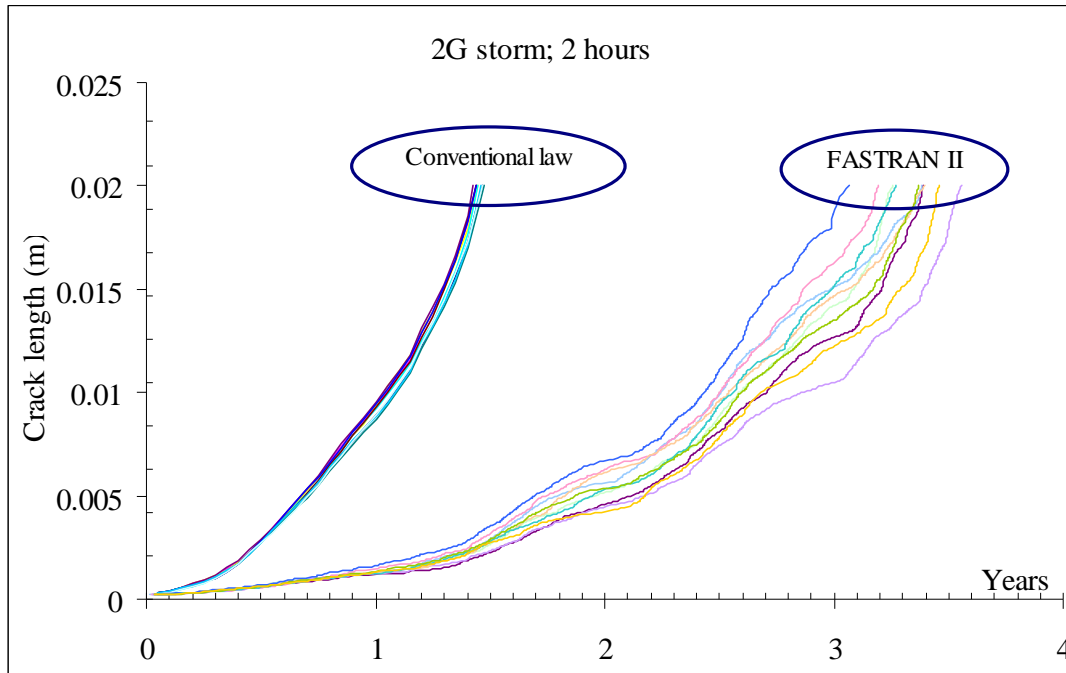
(b) Stress sequences derived by using 2G storm profiles with I_{OB}=2 hours.

Figure 5-7 Crack propagation lives in which stress sequences derived from 2G storm profile.
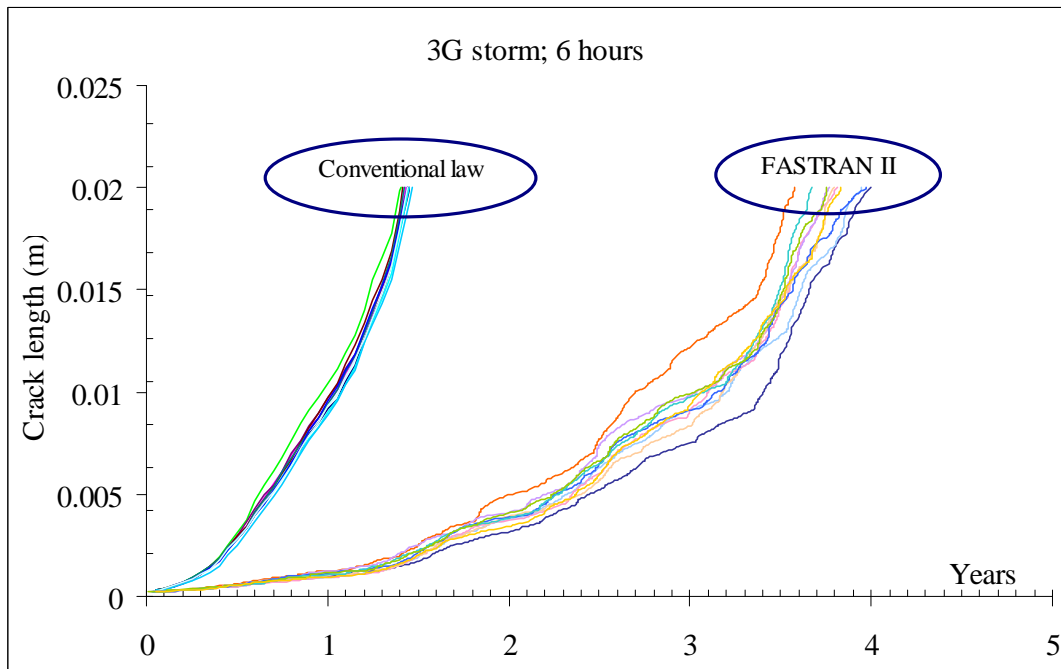
(a) Stress sequences derived by using 3G storm profiles with I_{OB}=6 hours.
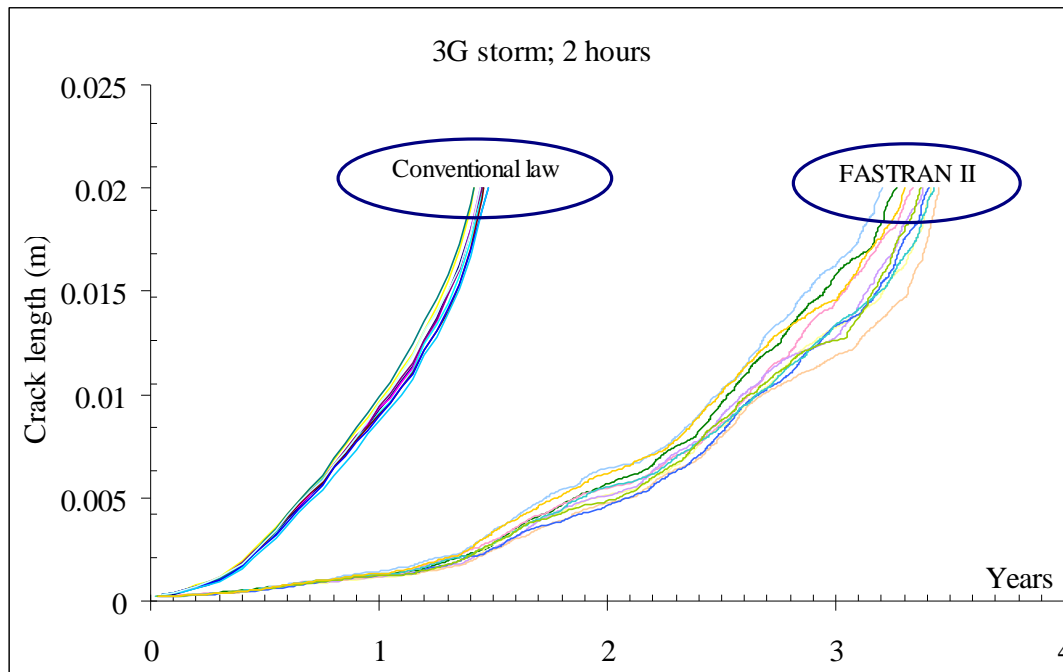
(b) Stress sequences derived by using 3G storm profiles with I_{OB}=2 hours.

Figure 5-8 Crack propagation lives in which stress sequences derived from 3G storm profile.
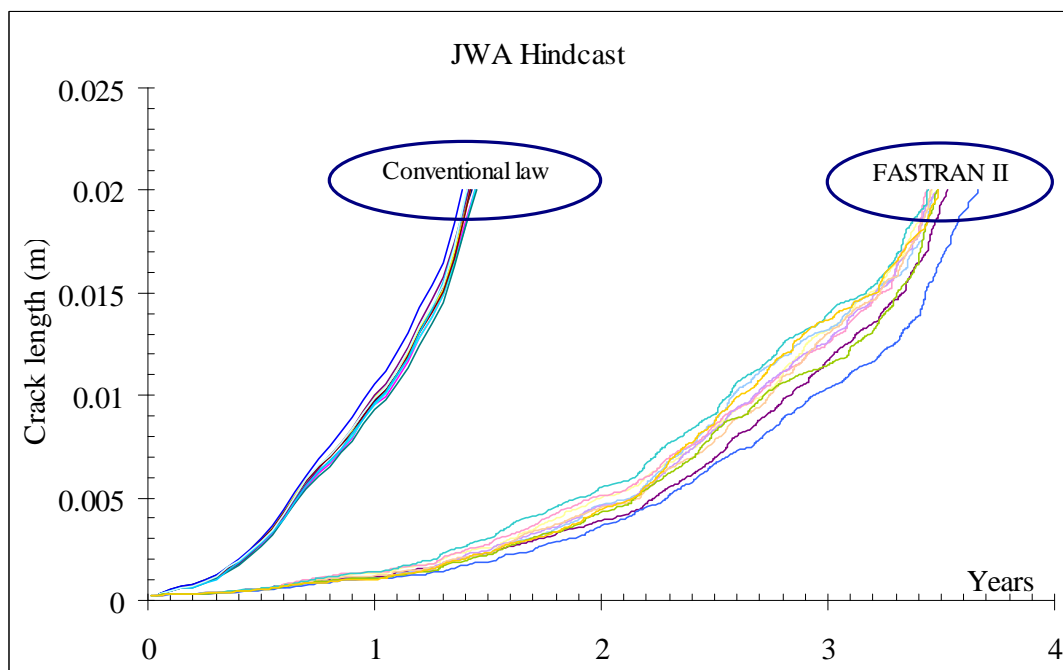
Figure 5-9 Crack propagation lives in which stress sequences derived from source of JWA hind-cast wave history.

From those tables and figures, it is found that:

(a) Fatigue damage calculated by using 2G and 3G storm profiles demonstrate good agreement with that of derived from source hind-cast data wave sequence. The difference fatigue damage between 2G and 3G storm profiles can be negligible.

(b) From the same stress sequences, FASTRAN II leads to longer calculated crack propagation life than the conventional law. The lives coefficient of variance for FASTRAN II results is significantly larger than that of the conventional law cases.

(c) The crack propagation lives of the source hind-cast wave histories is in the variation range of storm profiles (2G and/or 3G) simulation results regardless applied crack growth laws.

(d) In either the conventional laws and FASTRAN II analyses, the difference in crack propagation lives statistics for (2G or 3G) storm profiles with the same I_{OB} is negligible, and the crack propagation lives for I_{OB} =6 hours are larger than that of I_{OB}=2 hours. The difference in average crack propagation life is about 2% for the conventional laws, and 12% for FASTRAN II analyses.

In former research, Sumi et al (2008, 2013[27, 36]) carried out fatigue crack propagation analyses of a cracked base metal and a ship structure member in which the clustered loading cases based on 1G storm model. They employed two different crack propagation laws in their analyses. The first one is based on the conventional (Paris-Elber) law and the other is based on the strip yield model with the Re-tensile plastic zone generation (RPG) that calculated by using CP system (Sumi, 2008[27]) and FLARP (Toyosada, 2004[42-43]) program. They reported that crack propagation lives calculated by using conventional law becomes shorter than (about one third of) that calculated by CP system or FLARP. They considered that the difference in crack propagation life is in

consequence of the poor emulation capability by the conventional laws for retardation of crack propagation after the overload case. It is pondered that the difference results in (b) is caused by the same mechanism. In can be confirmed that the conventional law leads to over conservative estimates of fatigue crack propagation life.

The good agreement in fatigue damage and crack propagation life calculated from the storm models and source hind-cast data wave sequence reported in (a) and (c) shows that 2G and 3G storm profiles proposed in this work can emulate the changing nature of the stress sequence which is experienced by actual structural member of ocean going ships. The result (d) shows that the fatigue crack propagation life estimated by using 3G storm profile has almost the same accuracy with that based on 2G profile, although d is assumed to be 3.5 days regardless Ocean (North Pacific nor North Atlantic Oceans). It is also shown that larger I_{OB} leads to longer estimates propagation life. The difference in propagation life is considered because the smaller $H_{W,max|storm}$ for larger I_{OB} case as discussed in section 4.3.1.1.

This chapter can be summarized as following:

1) Fatigue crack propagation lives estimated by using proposed storm models with larger I_{OB} leads to longer (non-conservative) estimation due to smaller maximum H_W in storm profiles for larger I_{OB}.

2) Fatigue crack propagation lives estimated by using 2G and 3G storm models have almost the same accuracy. However, 3G storm model is recommended to reproduce wave induced loading sequence, because 3G storm model takes into account variation storm duration.

3) Additionally, the application of new generation storm model is also conducted by comparing two different wave models in fatigue assessment of Container ship, which sails in EU to USA trade route. The discussion of result is presented in Appendix 4.

4) It should be note that these numerical analysis is conducted in the condition in which the change in wave statistics without considering weather routing. Further investigation is needed to develop a 3G storm model, which can be applied to cases with weather routing.

6 CONCLUSIONS AND RECOMMENDATIONS

6.1 Conclusions

The following conclusions are made in relation to the developed and validated the advanced storm model.

- H_W's long-term probability distribution can be approximated by obeying Weibull distribution. Weibull parameters are fitting dependent with local wave scatter diagram. For GWS diagram, Weibull fitting is determined for all H_W range, while JWA hind-cast's scatter diagram is fitting from mid to high H_W ($H_W > H_{W,mean}$) data.

- The variation rough sea (storm) duration can be predicted following a normal distribution regardless maximum H_W in a storm.

- Fully automatic storm profile configuration is developed, and it is easy to configure storm profile for numerous sea areas and seasons.

- The advanced storm models are developed and it compares with the source hind-cast data. The advanced storm model (2G and 3G) developed in this thesis possess following capabilities:

  i) Can be coupled with seakeeping theory.

  ii) Long-term joint probability of H_W and T_W of the source data can be reproduced.

  iii) Stochastic characteristics of rough sea/ storm duration can be emulated (mean value for 2G storm model only and the mean value and its variance for 3G storm).

iv) The relation between the storm's maximum H_W and its occurrence probability (frequent distribution of storm class) recorded in the source hind-cast data can be reproduced.

v) Long-term probability of wave-induced stress, which is experienced by a ship on specific route, can be emulated.

vi) Equivalent short-sea sequence can be generated from the data with arbitrary observation period.

- 2G and 3G storm models for various oceans can be determined by assuming that the mean storm duration is the same as that of North Pacific Ocean (=3.5 days).

The following are found in relation with application of developed storm models to calculate fatigue crack propagation:

- The storm models (2G and 3G) developed in this thesis are demonstrated that their results have the same accuracy.

- Fatigue crack propagation lives estimated by using larger observation periods leads to longer (non-conservative) estimation.

6.2 Recommendations & Future works

The following recommendations are made in relation with storm models and observation period of source data:

- Because the longer observation period leads to smaller $H_{W,max|storm}$ (maximum wave height in a storm), it is recommended to choose shorter observation period when various observation periods are available from single source data.

- Although 2G and 3G storm models demonstrate the same accuracy when used to generate loading sequence, it is recommended to apply 3G storm model so that can generate loading sequence with emulated sea state as in real.

This thesis is conducted in the condition in which wave loading sequence is generated without considering weather routing. The sea state sequence experienced by a ship without weather routing may differ significantly from that routing case and it may deteriorate the preciseness of emulated wave loading sequence. Future work is needed in order to develop the advanced storm model in which can be applied to cases with weather routing.

REFERENCES

[1]   Boccoti P (2000): Wave mechanics for Ocean Engineering, Elsevier Oceanography series, Elsevier.

[2]   Baxevani A, Borgel C, Rychlik I (2008): Spatial model for variability of significant wave height in world oceans, International Journal of Offshore and Polar Engineering, 18 (1), pp.1-7.

[3]   Baxevani A, Caires S and Rychlik I (2009): Spatio-temporal statistical modelling of significant wave height. Environmetrics, Vol. 20, pp.14–31.

[4]   Cui W, Wang F, Huang X (2011), A unified fatigue life prediction method for marine structures, Marine Structures 24, pp.153-181.

[5]   Det Norske Veritas (2003/2010): Classification Note 30.7- Fatigue Assessment of Ship Structures, DNV.

[6]   Det Norske Veritas (2010): Recommendation Practice C205-Enviromental conditions and environmental loads, DnV.

[7]   European Centre for Medium-Range Weather Forecasts (ECMWF): www.ecmwf.int.

[8]   Evans M, Hastings N, Peacock B (2000): Statistical distributions, John Wiley & sons, Inc.

[9]   Fatilsen O M (1990): Sea loads on ships and offshore structures, Cambridge university press.

[10]   Forristall G Z (2008): How should we combined long and short term wave height distributions?, Proceeding of ASME 27th International Conference on OMAE.

[11] Fricke W, Cui W, Kierkegaard H, Kihl D, Koval M, Mikkola T, Parmentier G, Toyosada M, Yoon J H (2002): Comparative fatigue strength assessment of a structural detail in containership using various approach of classification societies, Marine Structures 15, pp.1-13

[12] Guedes Soares C, Scotto M G (2004): Application of the r largest-order statistics for long-term predictions of significant wave height, Coastal Engineering 51 (2004), pp.387-394.

[13] Hogben N, Dacunha N M, Olliver F (1985): Global wave statistics, British Maritime Technology Ltd.

[14] Huang X, Moan T, Cui W (2008), An Engineering model of fatigue crack growth under variable amplitude loading, International Journal of Fatigue 30, pp. 2- 10

[15] International Maritime organization (IMO) (2010): adoption of the international goal based ship construction standards for bulk carriers and oil tankers, resolution MSC.287 (87), IMO.

[16] International Association of Classification Society (IACS) (2001): Recommendation No.34 Standard wave data, IACS.

[17] Kawabe H (2002): Contribution of supposed wave condition on the long-term distribution of a wave-induced load, Journal of Marine Science and Technology, Vol. 6, pp. 135-147.

[18] Kawabe H, Syuuji O, Masayoshi O (2003): The study of storm loading simulation model for fatigue strength assessment of ship structural member: 1st report new storm loading simulation model which consistent with a wave frequency table, Journal of the Society of Naval Architects of Japan, 193, pp.39-47.

[19] Mao W, Fatigue assessment and extreme prediction of ship structures, PhD

dissertation, Chalmers University of Technology, Gotheburg, Sweden (2010).

[20] Mao W, Ringsberg J W, Rychlik I, Storhaug G (2010): Development of a fatigue model useful in ship routing design, Journal of Ship research, 54(4), pp.281-293.

[20b] Mao W, Prasetyo FA, Ringsberg JW, Osawa N (2013): A comparison of two wave models and their influence on fatigue damage in ship structure, proceeding of 32nd OMAE conference 2013.

[21] Matsuishi, M. & Endo, T. (1968) Fatigue of metals subjected to varying stress, Japan Soc. Mech. Engineering.

[22] Minoura M, Naito S (2004): A stochastic model for evaluation of seakeeping performance, proceeding of 14th ISOPE Conference.

[23] Minoura M, Naito S (2006): Stochastic sea climate simulation based on hindcast data, proceeding of 16th ISOPE conference.

[24] National data buoy center (NDBC), www.ndbc.nooa.com

[25] Newman Jr., J C (1981): A crack closure model for predicting fatigue crack growth under spectrum loading, ASTM STP 748, pp. 53-84.

[26] Newman Jr., J C (1992): FASTRAN II- a fatigue crack growth structural analysis program, NASA Technical Memorandum 104159.

[27] Okawa T, Sumi Y (2008): A computational approach for fatigue crack propagation in ship structures under random sequence of clustered loading, J Mar Scie Technol 13, pp.416-427.

[28] Osawa N, Hashimoto K, Sawamura J, Rokutanda A (2006): Construction of the storm model with consideration to the sea area and the season, proceeding of 2nd PAAMES and AMEC.

[29] Panel SR219 (1996): Annual report of panel 219, The Shipbuilding research Association of Japan, (in Japanese).

[30] Panel SR245 (2001): Annual report of panel 245, The Shipbuilding research Association of Japan, (in Japanese)

[31] Radaj D, Sonsino C M, Fricke W, Fatigue assessment of welded joints by local approaches, Woodland Publishing in Materials, 2nd edition, 2006.

[32] Rychlik, I. (1987) A New Definition of the Rainflow Cycle Counting Method, Int. J. Fatigue 9:2, 119-121.

[33] Storhaug G, Moe S, Lopes T A P (2007): Whipping measurements onboard a midsize container vessel operating in the North Atlantic, Marintec China proceeding (RINA, CMP, SNAME), International Symposium on Ship design and Construction, 28-29 November, Shanghai, China, pp.55-70.

[34] Suresh S, Fatigue of Materials, Cambridge Solid State Science series, 2nd Edition, 1998.

[35] Sumi Y, Inoue T (2011): Multi-scale modeling of fatigue crack propagation applied to random sequence of clustered loading, Marine Structures 24, pp.117-131.

[36] Sumi Y, Yajima H, Toyosada M, Yoshikawa T, Aihara S, Gotoh K, Ogawa Y, Matsumoto T, Hirota K, Hirasawa H, Toyoda M, Morikage Y (2013): Fracture control of extremely thick welded steel plates applied to the deck structure of large container ships, J Mar Sci Technol, DOI.10.1007/s00773-013-0222-5.

[37] Tomita Y, Hashimoto K, Osawa N, Terai K, Wang Y., Study on fatigue design loads for ships based on crack growth analysis, ASTM STP 1439.

[38] Tomita Y, Kawabe H, Fukuoka T (1992): Statistical characteristics of long-term

wave-induced load for fatigue strength analysis for ships, proceeding of 6th PRADS, vol. 2, pp. 2792-2805.

[39] Tomita Y, Matoba M, Kawabe H (1995): Fatigue crack growth behaviour under random loading model simulating real encountered wave condition, Marine Structure, Vol.8, pp.407-422.

[40] Toyosada M, Niwa T (1994): The significance of RPG load for fatigue crack propagation and the development of a compliance measuring system, International Journal of Fracture, 67, pp.217-230.

[41] Toyosada M, Niwa T, Sakai J (1997): Physical meaning of $\triangle$KRP and fatigue crack propagation in the residual stress distribution field, International Journal of Fatigue, 19, Supp. No.1, pp.S161-S166.

[42] Toyosada M, Gotoh K, Niwa T (2004): Fatigue crack propagation for a through thickness crack: a crack propagation law considering cyclic plasticity near crack tip, International Journal of Fatigue, 26(9), pp.983-992.

[43] Toyosada M, Gotoh K, Niwa T (2004): Fatigue life assessment for weld structures without initial defects: an algorithm for predicting fatigue crack growth from a sound site, International Journal of Fatigue, 26(9), pp.993-1002.

[44] Tromans P S, Vanderschuren L (1995), "Response Based Design Conditions in the North Sea: Application of a New Method", Proceeding of OTC 7683.

[45] Wan S, Shinkai A (1995): The statistical characteristics of global wave data and appraisal for long-term prediction of ship response, Trans. The Society of Naval Architects of Japan, Vol.90, (in Japanese).

[46] Warnsink W H, Report of Committee 1 on Environmental conditions, Proceeding of 2nd International Ship and Offshore Congress (1964).

[47]   Wheeler O E, Spectrum loading and crack growth, J Basic Eng, Trans ASME, D94,

1, 1972, 181-6.

[48]   World Maritime Organization (1998): Guide to wave analysis and forecasting,

World Maritime Organization.

APPENDIX 1   STRESS RESPONSE AMPLITUDE OPERATOR OF A BULK CARRIER'S STRUCTURAL MEMBER

Stress response amplitude operator (RAO) a bulk carrier's web stiffened cruciform weld joint at the bottom of lower stool determined for Japanese Ship research Panel 219 research project (SR219, 1996[29]) are used in this work. The stress RAO's curves are shown in Figure A1.1.
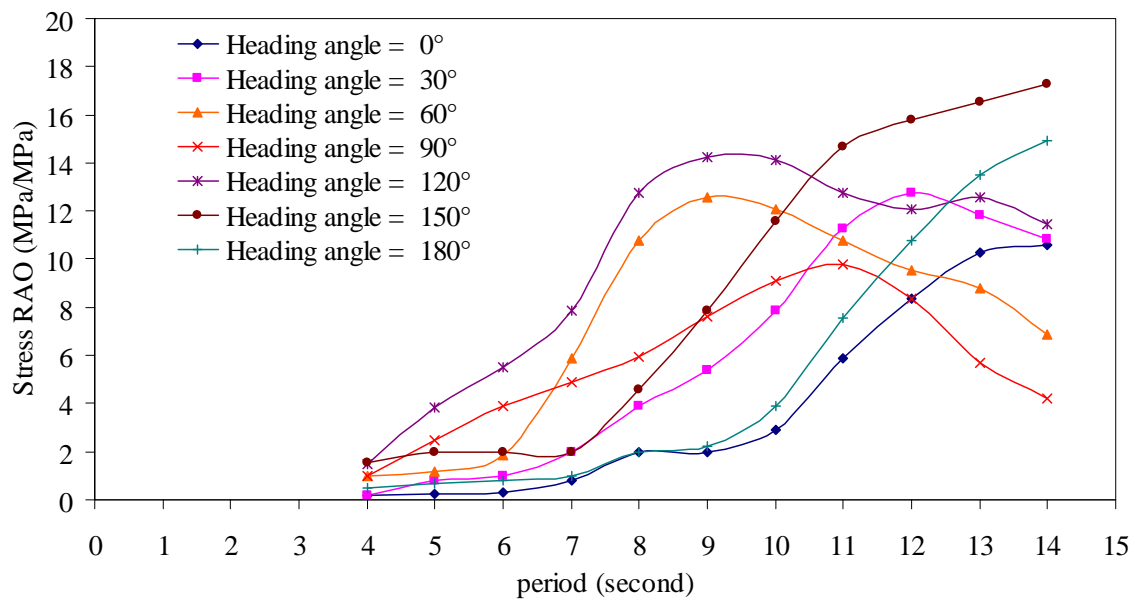
Figure A1.1 Stress response amplitude operator of a bulk carrier's web stiffened cruciform weld joint of Figure 5-1.

APPENDIX 2 SURFACE CRACK'S STRESS INTENSITY FACTOR

Stress Intensity factor, SIF of a surface crack is determined by using modified Raju-Newman formula (SR219, 1996[29]) given as below:

$$SIF = \left(S_m \cdot F_m + S_b \cdot F_b \right) \sqrt{b\pi}$$
(A2.1)
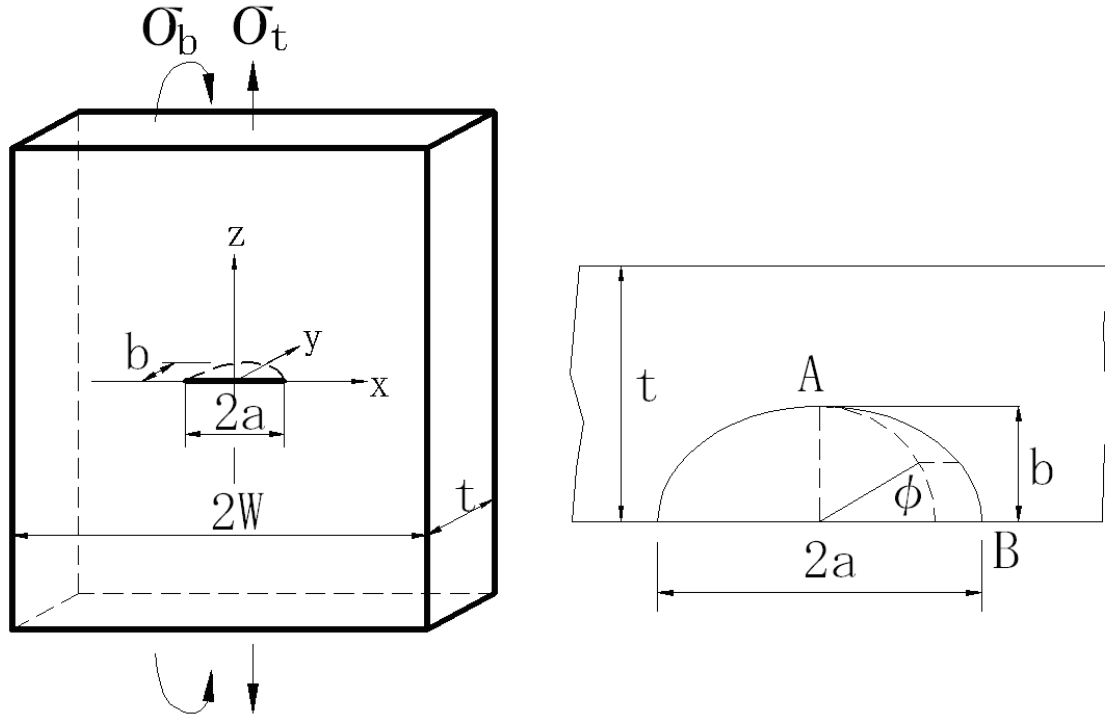
Figure A2.1 a surface crack dimension.

where:

$$F_m = \frac{F_0}{\Phi}; F_b = H \cdot \frac{F_0}{\Phi}$$
(A2.2)

$$F_0 = \left\{ M_1 + M_2 \left[\frac{b}{t} \right]^2 + M_3 \left[\frac{b}{t} \right]^2 \right\} f_\phi \cdot g \cdot f_w$$
(A2.3)

$$H = H_1 + (H_2 - H_1)\sin^p \phi; \; p = 0.2 + \frac{b}{a} + 0.6\left(\frac{b}{t}\right) \tag{A2.4}$$

$$H_1 = 1 - 0.34\frac{b}{t} - 0.11\frac{b}{a}\frac{b}{t}; \; H_2 = 1 + G_1\frac{b}{t} + G_2\left(\frac{b}{t}\right)^2 \tag{A2.5}$$

$$G_1 = -1.22 - 0.12\frac{b}{a}; \; G_2 = 0.55 - 1.05\left[\frac{b}{a}\right]^{0.75} + 0.47\left[\frac{b}{a}\right]^{1.5} \tag{A2.6}$$

$$f_\phi = \left\{\sin^2 \phi + \left[\frac{b}{a}\right]^2 \cos^2 \phi\right\}^{1/4}; \; f_w = \left[\sec\left\{\frac{a\pi}{W}\left[\frac{b}{t}\right]^{1/2}\right\}\right]^{1/2} \tag{A2.7}$$

for $0 < b/a \le 1$,

$$\Phi = \left\{1 + 1.464\left[\frac{b}{a}\right]^{1.65}\right\}^{1/2} \tag{A2.8}$$

$$M_1 = 1.13 - 0.09\left[\frac{b}{a}\right]; \; M_2 = -0.54 + \frac{0.89}{0.2 + b/a} \tag{A2.9}$$

$$M_3 = 0.5 - \frac{1}{0.65 + b/a} + 14\left(1.0 - \frac{b}{a}\right)^{24} \tag{A2.10}$$

$$g = 1 + \left\{0.1 + 0.35\left[\frac{b}{t}\right]^2\right\}(1 - \sin\phi)^2 \tag{A2.11}$$

for $1 < b/a \le 2$,

$$\Phi = \left\{1 + 1.464\left[\frac{a}{b}\right]^{1.65}\right\}^{1/2} \tag{A2.12}$$

$$M_1 = \left[\frac{a}{b}\right]^{1/2}\left(1 + 0.04\frac{a}{b}\right); \; M_2 = 0.2\cdot\left[\frac{a}{b}\right]^4 \tag{A2.13}$$

$$M_3 = -0.11\left[\frac{a}{b}\right]^4 \tag{A2.14}$$

$$g = 1 + \left\{ 0.1 + 0.35 \left[\frac{a}{b}\right]\left[\frac{b}{t}\right]^2 \right\} (1 - \sin\phi)^2 \qquad (A2.15)$$

Stress intensity factor for a surface crack at a weld joint is determined given as below:
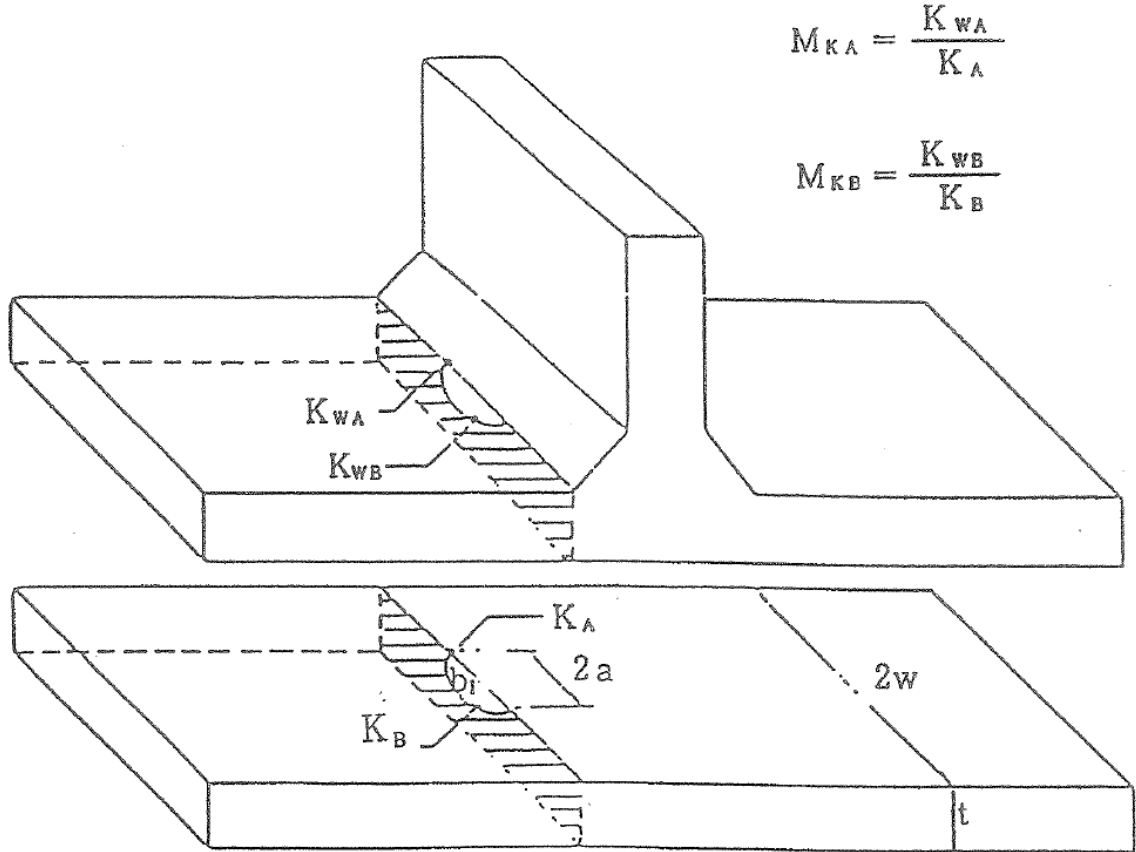
Figure A2.2 Stress intensity of a surface crack on typical weld joint.

$$\begin{aligned} K_{WA} &= \{M_k\}_A \cdot K_A \\ K_{WB} &= \{M_k\}_B \cdot K_B \end{aligned} \qquad (A2.16)$$

$$\{M_k\}_A = \{M_k\}_B + \{M_k\}_{(A-B)} \qquad (A2.17)$$

$$\{M_k\}_B = \alpha \left(\frac{b}{t}\right)^\beta \qquad (A2.18)$$

$$\{M_k\}_{(A-B)} = 1.15 \cdot \exp\left(-9.74 \times \frac{b}{t}\right) \qquad (A2.19)$$

K_{WA} and K_{WB} are SIF's of longest and deepest a surface crack at weld joint. K_A and K_B are SIF's of longes and deepest a surface crack for smooth plate.

Table A2.1 Definition of α and β.

Loading mode	L/t	L/t	α	β
Axial	≤ 2	$\leq 0.05\left[L/t\right]^{0.55}$	$0.51\left[L/t\right]^{0.27}$	-0.31
		$> 0.05\left[L/t\right]^{0.55}$	0.83	$-0.15\left[L/t\right]^{0.46}$
	> 2	≤ 0.073	0.615	-0.31
		> 0.073	0.83	0.20
Bending	≤ 1	$\leq 0.03\left[L/t\right]^{0.55}$	$0.45\left[L/t\right]^{0.21}$	-0.31
		$> 0.03\left[L/t\right]^{0.55}$	0.68	$-0.19\left[L/t\right]^{0.21}$
	> 1	≤ 0.03	0.45	-0.31
		> 0.03	0.68	-0.19

APPENDIX 3   PARAMETERS USED FOR FATIGUE DAMAGE CALCULATION

The following tables and figure are presented parameters used for fatigue damage calculation based on DnV CN.30.7 [5] given as:

$$D = \sum \frac{n_i}{N_i} < 1.0; N_i = \frac{\alpha}{S_a{}^M} \tag{A3.1}$$

$$FatLife = \frac{L_D}{D} \tag{A3.2}$$

Where;

L_D=ship's design life

n_i= number of stress cycles in *i*-th stress range block

N_i=number of stress cycles to failure at constant *i*-th stress range block

α, M are design S-N curve fatigue parameters, and these are given by DnV CN.30.7.
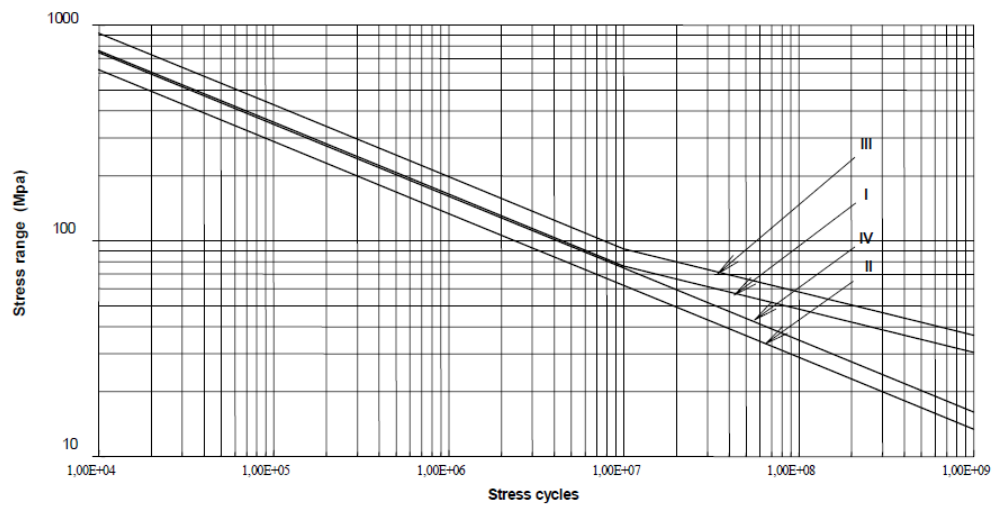
Figure A3.1 Design S-N curves (DnV CN.30.7, 2003[5]).

Table A3.1 S-N parameters; air or cathode protection (DnV CN.30.7, 2003[5]).

S-N curve	Material	$N \leq 10^7$		$N > 10^7$	
		$\log \hat{a}$	M	$\log \hat{a}$	M
I	Welded joint	12.65	3.0	16.42	5.0
III	Base material	12.89	3.0	16.81	5.0

Table A3.3 Alternative on-slope S-N parameters (DnV CN.30.7, 2003[5]).

S-N curve	Material	$\log \hat{a}$	M
II	Welded joint	12.38	3.0
IV	Base material	12.62	3.2

Table A3.2 S-N parameters; corrosive environment (DnV CN.30.7, 2003[5]).

S-N curve	Material	$\log \hat{a}$	M
II	Welded joint	12.38	3.0
IV	Base material	12.62	3.2

Table A3.4 Factor χ used for fatigue damage in correlation with corrosion protection of ship structure members (DnV CN.30.7, 2003[5]).

S-N Curve used for calculation of fatigue damage	Design life [years]	Ballast Tanks Effective Corrosion protection period (years)					Cargo Oil Tank
		5	10	15	20	25	
	20	2	1.7	1.3	1	-	1.7
I or III	25	2.1	1.8	1.5	1.3	1	1.7
	30	2.1	1.9	1.7	1.5	1.2	1.7

APPENDIX 4   FATIGUE ASSESSMENT OF SHIP STRUCTURE DUE TO DIFFERENT WAVE MODELS

Here, the applicability of 3G storm model is demonstrated by comparing with stochastic wave model in which is based on satellite and buoys data, so called as 'spatio-temporal wave model' (Baxevani, 2009[3]). This wave model generates H_W at position, p and time, t as $H_W(p, t)$ by means of log normal distribution. In the voyage route with position with t, $p(t)$, while for a fixed t, the field of logarithm of $H_W(p, t)$ is Gaussian with the changing of its covariance on the basis of $p(t)$ on the route. This means that $H_W(p, t)$ is a non stationary Gaussian process.

A4.1 Measured ship and its voyage
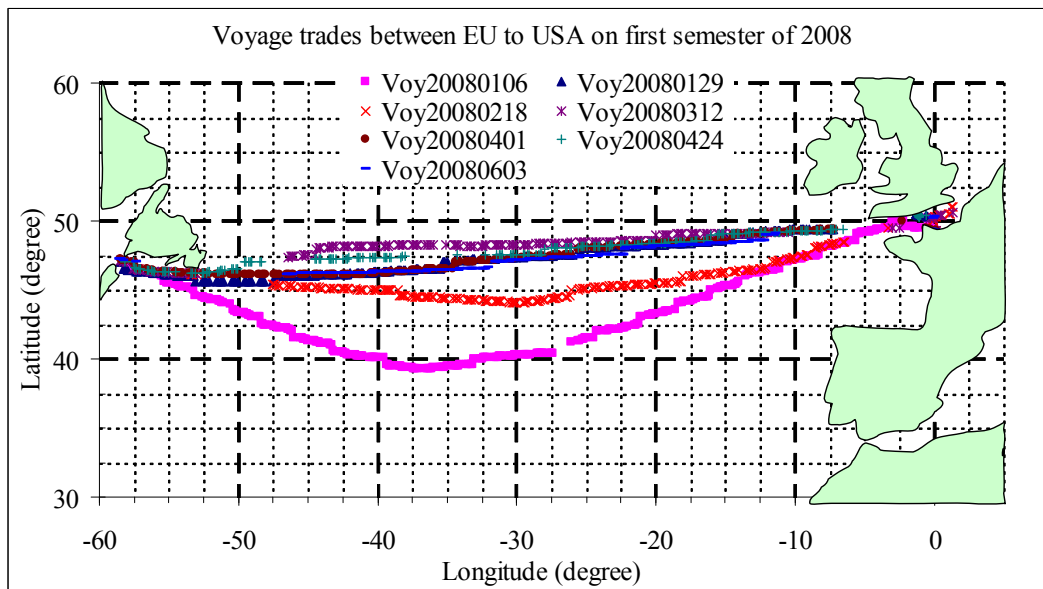
Figure A4-1 2800TEU's voyage from EU to USA on first semester of 2008 (the arrival date for each voyage is indicated in the legend) (Mao et al, 2010[19-20] and 2013[20b]).

Two wave models is utilized to simulate H_W along the route between EU to USA (see Figure A4-1) in which onboard measurement is conducted at 2800TEU's Containership by using the difference source. The seven ship's voyages presented in this figure are used for short-sea sequences, and the simulation result is compared with the H_W obtained from measurement using ship's wave radar. The ship used in this investigation, a 2800TEU containership, has been utilized by Mao et al (2010)[19-20]. The ship is equipped with ship's wave radar to measure waves along ship's sailing. It is also equipped with strain sensors and it located in the amidships section of the ship as shown in Figure A4-2.

Figure A4-2 The amidships section of typical Containership and strain gauge location on ship.

A4.2 Wave distribution

Hereafter, H_W generated based on 3G storm model is denoted as '3G-storm' and Spatio-temporal wave model is 'spatio-temporal'. 3G-storm's model parameters are identified from JWA hind-cast data along the measured route of Figure A4-1 when hind-cast data was collected in period between 2000 to 2010. In the same routes, spatio-temporal parameters are also prepared. H_W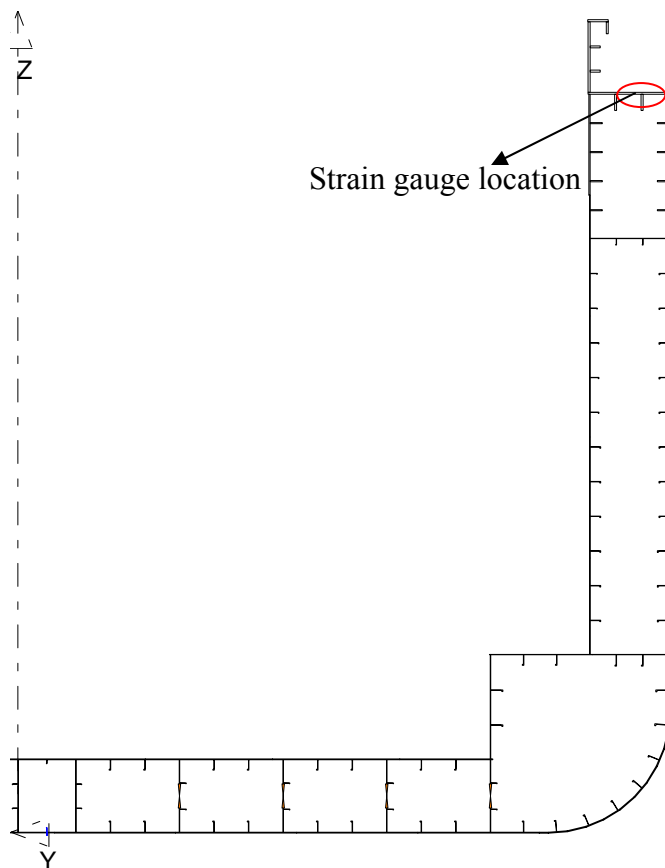 along the seven routes are generated by using 3G-storm and spatio-temporal, and its probability density function (pdf) are presented in Figure A4-3. The pdf of observed H_W in which measured along the same route and the wave distribution of DNV recommendation (DnV RP-C205, 2010[6]) are also plotted in this figure.

It is shown that two wave models and observed wave are significantly different with that of DnV recommendation, while shows similarity in the tails of large H_W (H_W >6m) for spatio-temporal and in low H_W (1m< H_W <2m) for 3G-storm. The generated wave model leads to higher H_W probability than DnV recommendation for the cases with H_W from 2m to 5m of spatio-temporal and 1m to 4m of 3G-storm. Compared with measured wave, two wave models are smaller H_W probability for H_W less than 1.5m while spatio-temporal gives larger H_W probability for the cases H_W 6m than 3G-storm and measured waves. It may be caused that waves was measured when the ships avoids large wave by utilizing installed weather routing tools. For 3G-storm, the reason is because the exceedance probability for the arbitrary H_W range is small. The characteristics shown in pdf of two wave models are almost similar.
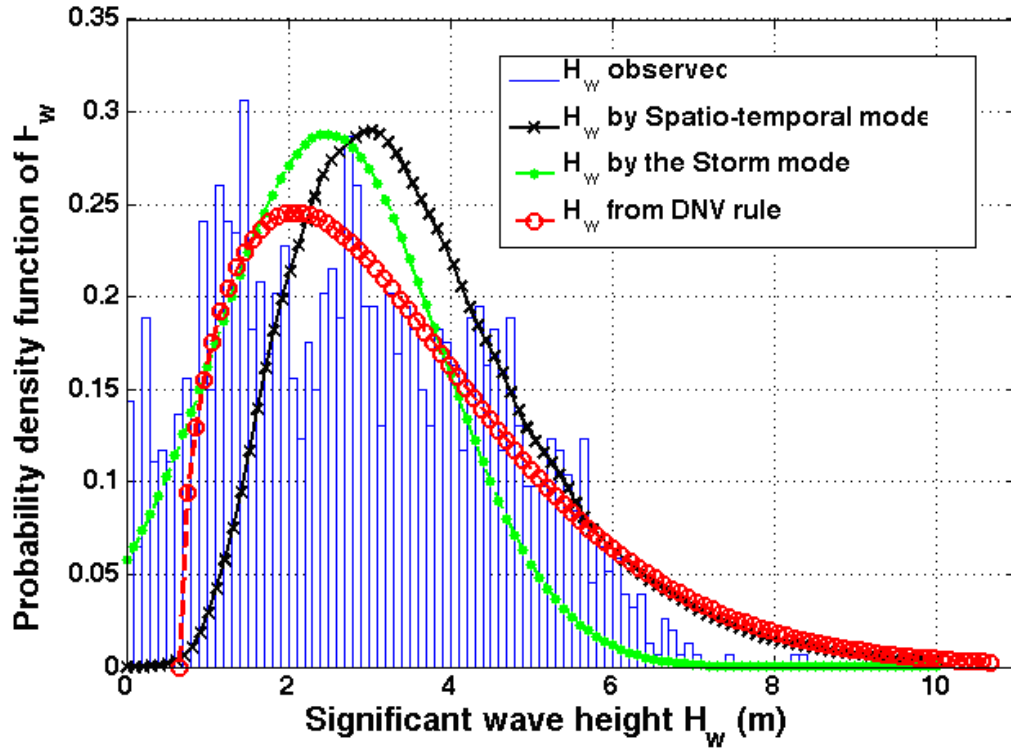
Figure A4-3 Probability density function (pdf) of H_W from onboard measurement, the spatio-temporal wave model and the storm model (Mao et al, 2013[20b]).

A4.3 Fatigue damage assessment

Since that the case study vessel also be equipped with strain sensor, the rain flow counting's (Endo and Matsuishi, 1968[21], Rychlik, 1987[32]) fatigue damage can be also computed from converted history of stress signal (S_i, i=1,2,...N). Fatigue damage of welded ship structure of Figure A4-2 is calculated based on Palmgreen-Miner law as described in Appendix 3 in a stationary sea state of time (T) given by Eq.A4.1 and the expected fatigue damage so called as narrow band approximation (Mao 2010) given as

$$D(T) = \frac{1}{\alpha} \sum\nolimits_{i=1}^{N} S_i^M \qquad (A4.1)$$

$$D_T = E\left[D(T) \approx \frac{T}{2\pi} \sqrt{\frac{\lambda_2}{\lambda_0}} \left(2\sqrt{2\lambda_0}\right)^m \Gamma\left(1 + \frac{m}{2}\right) \right] \tag{A4.2}$$

where, λ_0 and λ_2 are the zero and second order of spectral moment of stress spectrum $S_\sigma(\omega)$. α and M are design S-N curve's fatigue parameter given by class rules or recommendation. In this comparative study, $\alpha=10^{12.76}$ and M=3 are set (DnV RP-C205, 2010[6]).

Table A4-1 Fatigue damage estimated by using H_W's generated from spatio-temporal wave model and 3G storm model (Mao et al, 2013[20b])

Voyage	Rain flow fatigue damage	Spatio-temporal wave		3G storm model	
		E(D)	C.V(D)	*E*(D)	C.V(D)
Voy20080106	0.0080	0.0077	2.54	0.078	0.326
Voy20080129	0.0057	0.0075	2.29	0.0073	0.291
Voy20080218	0.0045	0.0067	1.65	0.0063	0.261
Voy20080312	0.0014	0.0032	2.05	0.0028	0.326
Voy20080401	0.0032	0.0041	2.32	0.0030	0.478
Voy20080424	0.0027	0.0019	1.96	0.0029	0.479
Voy20080603	0.0007	0.0010	1.7	0.0026	0.364
Total damage:	0.0262	0.0321	--	0.0325	--

Thereafter, the fatigue damage associated with wave, which is generated by using spatio-temporal wave model, is denoted as 'spatio-temporal'. If waves are generated by using 3G storm model, it is denoted as '3G-storm'. Fatigue damage is also calculated from the measured time series of strain (converted stress) by using rain flow counting method. Fatigue damage is calculated from the stress in which caused by vertical bending only. K_S is set at 2 according to fatigue guideline (DnV CN30.7, see Chapter 5). The numbers of wave simulations are conducted and the mean fatigue damage, *E*(D) and

coefficient of variance (C.V) of fatigue damage, C.V(D) is presented in Table A4-1. It shows that two wave models give about 25% overestimation comparing with that total rain flow damages, which is computed from the time series of recorded stress signals. In general, for each voyage, the difference of fatigue damage is negligible except for the voyage 20080603. The difference in total fatigue damage is due to the encountered of lower stress histories when ship sails with the weather routing tools in order to avoid larger storms.

A4.4 Fatigue crack propagation analysis

In the generation of wave, it consists of two components that is H_W and T_W, and called as sea state. Sea state (H_W and T_W) histories are simulated by using 3G storm model and spatio-temporal wave model. Once sea state obtained by using 3G storm model, the wave induced stress can be generated in the same manner as described in section 3.2.3. Further, once the probability distribution of H_W is given, which is estimated by spatio-temporal wave model at a given location and time, the energy spectrum of wave and stress response are computed by using ocean wave spectrum and RAO. Because the sea state generated based on spatio temporal wave is assumed to Gaussian distribution, hence, the wave induced stress is simulated by obtained stress spectral density for each sea state. The example of simulated stress histories is shown in Figure A4-4.
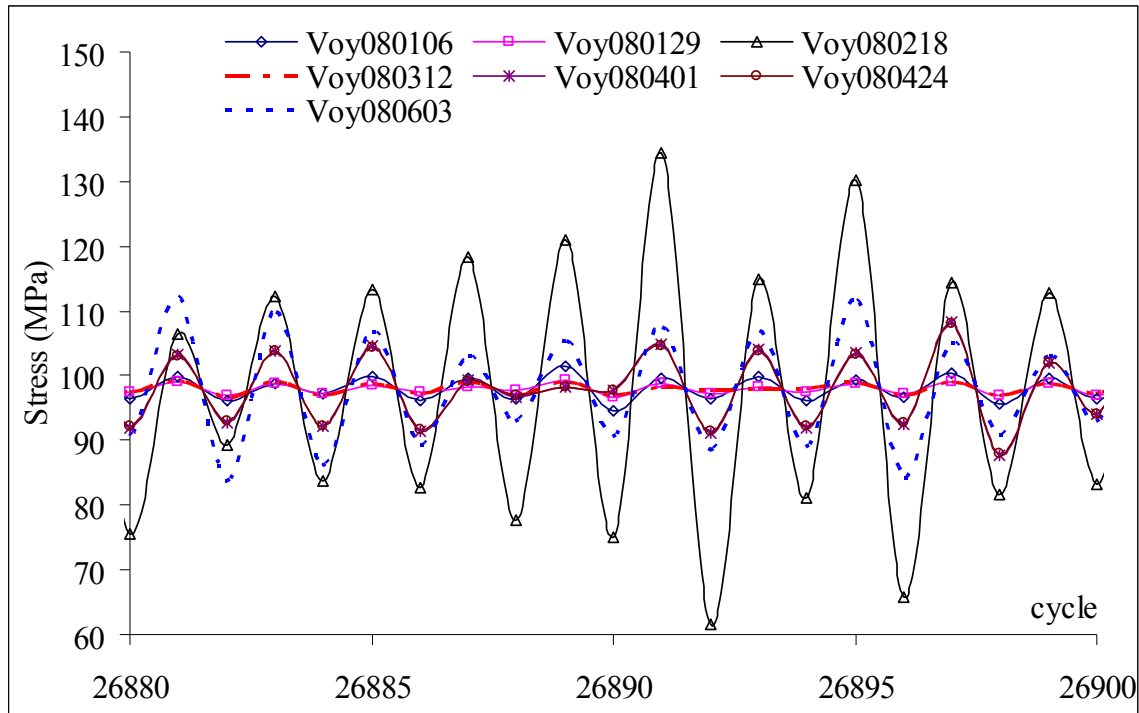
Figure A4-4 An example of simulated stress histories of 2800TEU's containership based on 3G storm model.
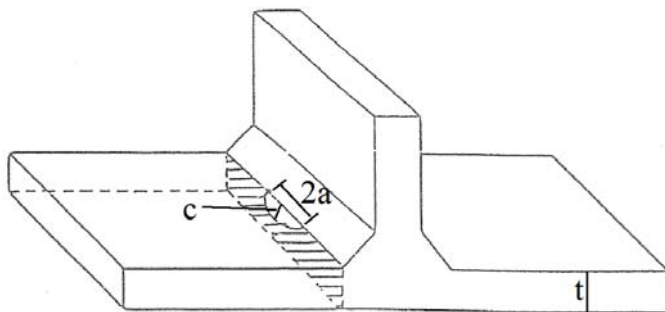
Figure A4-5 A semi-elliptical surface crack on weld toe fillet weld joint.

Fatigue crack propagation analyses of a semi-elliptical surface crack on weld toe of weld joint (see Figure A4-5) are conducted by using the wave induced stress histories in which simulated based on two (spatio-temporal and 3G storm) wave models. The crack growth is computed by FASTRAN II program (for the detail see Chapter 5). In this comparative, the initial surface crack length is 0.2 mm and the initial aspect ratio is 0.5. Propagation analyses are continued until the crack depth exceeds 8mm or the surface

length exceeds 10mm. The material parameters are given in Table 5-1. The wave induced

stress is simulated for 15 trials and the mean stress is set at 98.0MPa.

Table A4-2 Statistical crack propagation life in which stress histories derived by using

3G storm model and spatio-temporal wave model.

Voyage	3G storm model				Spatio-temporal wave model			
	Crack propagation life (x 10^6 cycles)							
	Shortest	Longest	$E(L_C)$	$SD(L_C)$	Shortest	Longest	$E(L_C)$	$SD(L_C)$
Voy20080106	782	8034	2590	1694	137	1768	568	498
Voy20080129	305	2244	1019	506	99	18807	1805	4794
Voy20080218	386	3030	1181	675	209	1856	679	542
Voy20080312	2269	37885	11658	8431	71	13120	2033	4429
Voy20080401	1285	17411	8320	4776	146	1494	438	385
Voy20080424	2769	30086	11537	9188	264	56415	8218	14740
Voy20080603	1848	30192	7901	7447	170	54144	18215	19633

Table A4-2 presents statistics data of computed crack propagation life. Let L_C be

calculated crack propagation life. The longest of L_C, shortest of L_C, mean of L_C, $E(L_C)$

and standard deviation of L_C, $SD(L_C)$ are given in this table. Figure A4-6 and Figure A4-

7 show the relationship between the crack growth rate and SIF range for the cases with

shortest propagation life as listed in Table A4-2 and its crack growth curves. From table

and figures, it is shown that 3G storm model leads to longer lives than that of spatio-

temporal model while fatigue damages computed from two wave models are almost

equal. The spatio-temporal wave model leads to rapid crack growth rate than 3G storm

model for the cases with same SIF range ($14MPa.m^{1/2} \leq SIF \leq 17MPa.m^{1/2}$) as shown in

Figure A4-6. The reasons are 3G storm model produces smaller large H_W ($H_W > 4m$) than

spatio-temporal model as seen in Figure A4-3. It is supposed that the retardation of crack

growth rate is caused by excessive load of the generated storm state in sea state histories

in which simulated by using 3G storm model. This demonstrates that the loading sequence of excessive load affects to crack propagation behavior.
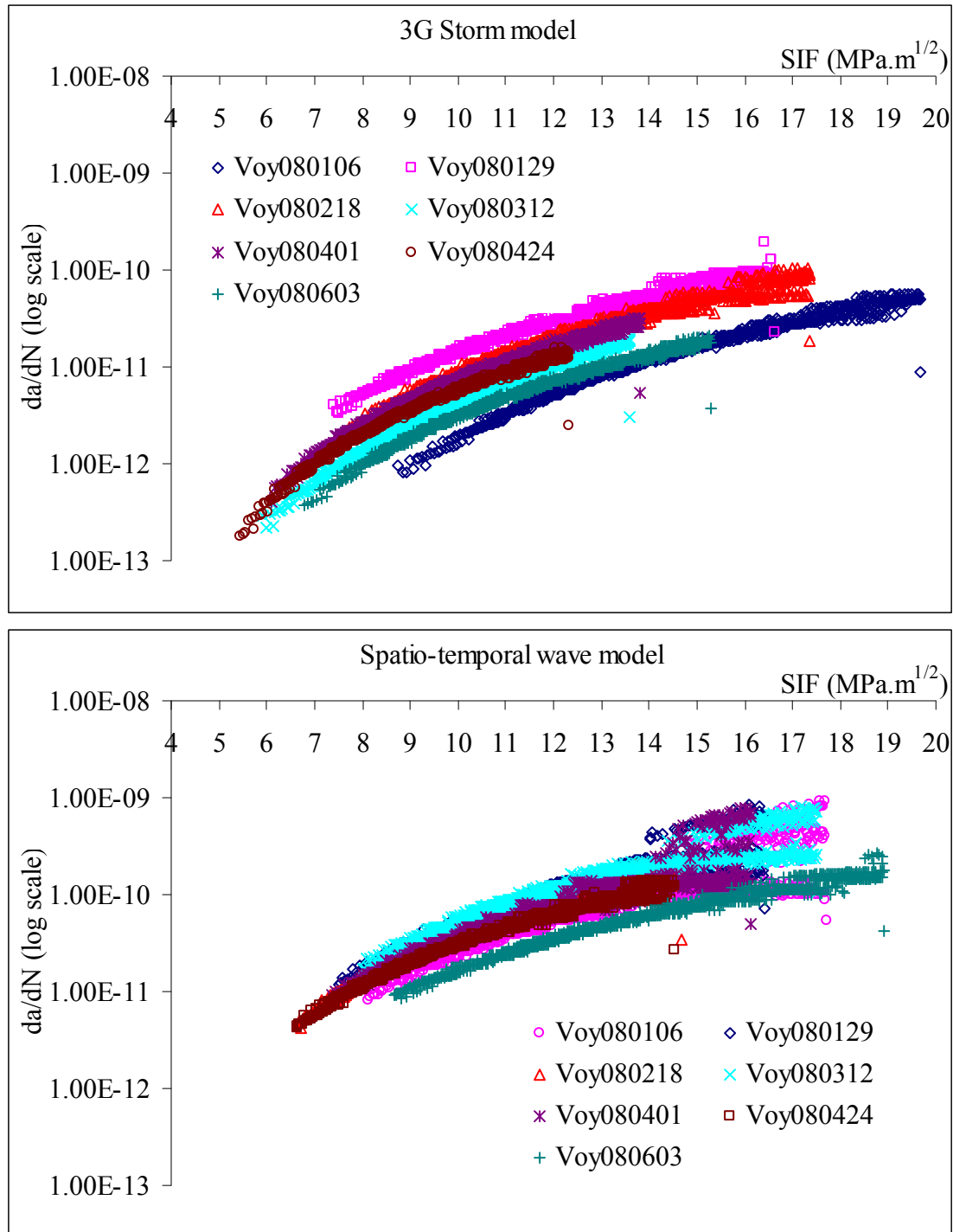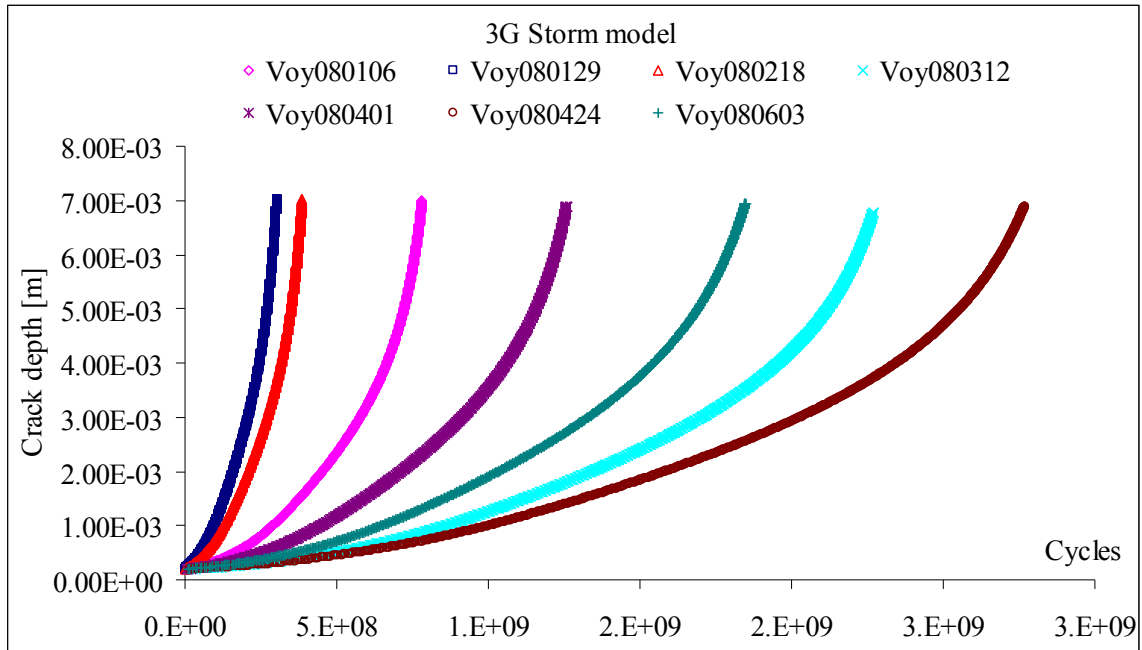

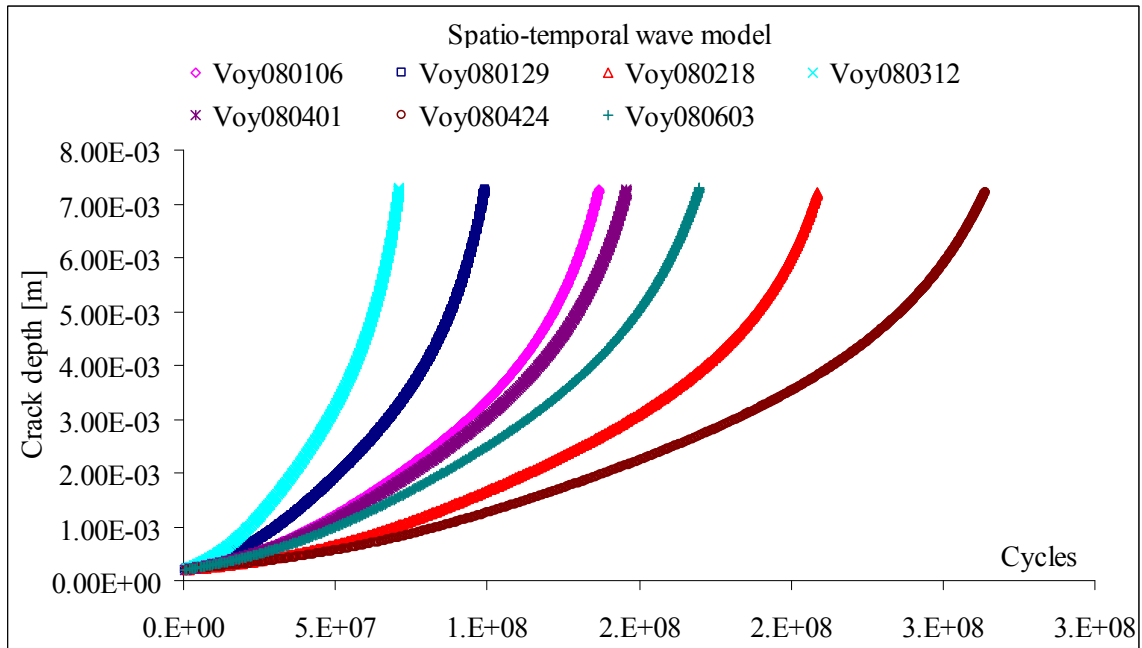Figure A4-6 The relation between crack growth rate and stress intensity factor performed by using 3G storm model (above) and Spatio-temporal wave model (below).

(a) 3G storm model

(b) Spatio-temporal wave model.

Figure A4-7 Crack growth in voyage of Figure A4-1 for the shortest crack propagation life in which stress history derived by using (a) 3G storm model and (b) Spatio-temporal wave model.

It can be summarized that 3G storm model and Spatio-temporal model have the same capability to produce significant wave height along specific ship voyages with other different wave model as well as when it is used to predict the accumulated fatigue damage and fatigue crack propagation lives. The loading sequence in which simulated in the optimizing voyage routes by using different wave models can clearly show the effect retardation and acceleration of crack growth.

LIST OF PAPERS

The Doctor dissertation includes the following papers:

1. Fredhi Agung Prasetyo, Naoki Osawa, Junji Sawamura (2011): Study on the effect of storm duration fluctuation on the accuracy of fatigue assessment of ship structural member, proceeding of 21st ISOPE conference, vol. IV, pp.921-928.

2. Fredhi Agung Prasetyo, Naoki Osawa, Junji Sawamura (2011): Study on Load History Generation Method based on "storm model" with consideration of fluctuation in storm duration, proceeding of the 25th Asian-Pacific Technical Exchange and Advisory Meeting on Marine Structure (TEAM) 2011.

3. Fredhi Agung Prasetyo, Naoki Osawa, Tomohei Kobayashi (2012), Study on Preciseness of Load History Generation based on Storm model for fatigue assessment of ship structures members, Proceeding of 22nd ISOPE conference, vol. IV, pp.709-715

4. Fredhi Agung Prasetyo, Naoki Osawa (2012): Study on the applicability of load history generation method based on storm model in North Atlantic route for fatigue assessment of ship structure members Proceeding of the 26th Asian-Pacific Technical Exchange and Advisory Meeting on Marine Structure (TEAM) 2012.

5. Wengang Mao, Fredhi Agung Prasetyo, Jonas W Ringsberg, Naoki Osawa (2013), A comparison of two wave models and their influence on fatigue damage in ship structure, Proceeding of 32nd OMAE conference 2013.

6. Fredhi Agung Prasetyo, Tomohei Kobayashi, Wengang Mao, Naoki Osawa, Jonas W Ringsberg (2013): Analysis of crack retardation effects and crack path in ship

structure members on different routes, proceeding of 13th International Conference on Fracture- ICF 13.

structure members on different routes, proceeding of 13th International Conference on Fracture- ICF 13.